

**STUDIES OF SYNTHESIS, KINETICS AND PARTICLE  
SIZE OF ZEOLITE X FROM NARATHIWAT KAOLIN**

**Mr. Saythong Thammavong**

**A Thesis Submitted in Partial Fulfillment of the Requirements for the**

**Degree of Master of Science in Chemistry**

**Suranaree University of Technology**

**Academic Year 2003**

**ISBN 974-533-267-4**

ศึกษาการสังเคราะห์ จลนพลศาสตร์ และขนาดอนุภาคของซีโอไลท์ X จาก  
ดินขาวราชิวาส

นายสายทอง ธรรมวงศ์

วิทยานิพนธ์นี้เป็นส่วนหนึ่งของการศึกษาตามหลักสูตรปริญญาวิทยาศาสตรมหาบัณฑิต

สาขาวิชาเคมี

มหาวิทยาลัยเทคโนโลยีสุรนารี

ปีการศึกษา 2546

ISBN 974-533-267-4

# **STUDIES OF SYNTHESIS, KINETICS AND PARTICLE SIZE OF ZEOLITE X FROM NARATHIWAT KAOLIN**

Suranaree University of Technology has approved this thesis submitted in partial fulfillment of the requirements for a Master's Degree

Thesis Examining Committee

.....

(Asst. Prof. Dr. Malee Tangsathitkulchai)

Chairperson

.....

(Asst. Prof. Dr. Kunwadee Rangriwatananon)

Member (Thesis Advisor)

.....

(Dr. Visit Vao-soongnern)

Member

.....

(Asst. Prof. Dr. Anan Tongraar)

Member

.....

(Assoc. Prof. Dr. Tawit Chitsomboon)

(Assoc. Prof. Dr. Prasart Suebka)

Vice Rector for Academic Affairs

Dean of the Institute of Science

สายทอง ชรรวมวงศ์: ศึกษาการสังเคราะห์ จลนพลศาสตร์ และขนาดอนุภาคของซีโอไลต์ X จาก ดิน  
 ขาวนาฬิกา (STUDIES OF SYNTHESIS, KINETICS AND  
 PARTICLE SIZE OF ZEOLITE X FROM NARATHIWAT  
 KAOLIN)

อาจารย์ที่ปรึกษา: ผู้ช่วยศาสตราจารย์ ดร. กุลวดี รั้งนิวัฒนานนท์, 93 หน้า ISBN 974-533-267-4

งานวิจัยนี้ได้ศึกษาการสังเคราะห์ จลนพลศาสตร์และขนาดอนุภาคของซีโอไลต์ X โดยใช้ ดิน  
 ขาว (เกาลิน) จากจังหวัดนราธิวาสเป็นสารตั้งต้น ได้พิจารณาปัจจัยต่างๆ ที่มีผลต่อการสังเคราะห์ ตรวจสอบ  
 สอดคล้องลักษณะของของแข็งที่ได้จากการเกิดปฏิกิริยาโดยเทคนิค XRD FT-IR SEM และเครื่องวัด  
 ขนาดอนุภาค พบว่าสภาวะที่เหมาะสมที่สุดในการสังเคราะห์ที่ให้ซีโอไลต์ X มีความบริสุทธิ์คือเผา  
 เกาลินที่อุณหภูมิ 900°C เป็นเวลานาน 1 ชั่วโมง สารละลาย Na<sub>2</sub>SO<sub>3</sub> เข้มข้น 10%w/v สารละลาย  
 NaOH เข้มข้น 7.5%w/v บ่มเป็นเวลานาน 3 วัน ที่ 30°C และทำปฏิกิริยาที่อุณหภูมิ 90±2°C เป็น  
 เวลา 24 ชั่วโมงภายใต้ความดันของตัวเอง ผลการทดลองแสดงให้เห็นว่าการกระจายของขนาด  
 อนุภาคของซีโอไลต์ X ขึ้นอยู่กับอุณหภูมิของการดำเนินปฏิกิริยา ปริมาณผลึกที่เกิดขึ้นและความเข้มข้น  
 ของสารละลายเบส

การศึกษาจลนพลศาสตร์ของการเกิดซีโอไลต์ X แสดงให้เห็นว่าอัตราการเกิดผลึกและอัตราการ  
 เกิดนิวเคลียสขึ้นอยู่กับความเข้มข้นของสารละลายเบส สารละลายซัลไฟต์ และอุณหภูมิของปฏิกิริยา  
 อันดับของการเกิดผลึกซีโอไลต์ X เมื่อพิจารณาความเข้มข้นของเบสมีค่าเท่ากับ 3 และเมื่อพิจารณากับ  
 ความเข้มข้นของซัลไฟต์มีค่าเท่ากับ -1/2 และอันดับของการเกิดนิวเคลียสมีค่าเท่ากับ 4.5 เมื่อพิจารณา  
 กับความเข้มข้นของเบสและมีค่าเท่ากับ -1 เมื่อพิจารณาความเข้มข้นของซัลไฟต์ พลังงานกระตุ้นของการ  
 เกิดผลึกและนิวเคลียสมีค่าเท่ากับ 12.5 กิโลแคลอรีต่อโมล และ 38.0 กิโลแคลอรีต่อโมลตามลำดับ  
 ตามแบบจำลองของอพรามีพบว่าเอ็กซ์โพเนนต์ n มีค่าเท่ากับ 4 เมื่อทำปฏิกิริยาที่อุณหภูมิ 80-90°C  
 และมีค่าเท่ากับ 2 เมื่อทำปฏิกิริยาที่อุณหภูมิ 100°C

สาขาวิชาเคมี

ปีการศึกษา 2546

ลายมือชื่อนักศึกษา.....

ลายมือชื่ออาจารย์ที่ปรึกษา.....

**SAYTHONG THAMMAVONG: STUDY OF SYNTHESIS, KINETICS AND  
PARTICLE SIZE OF ZEOLITE X FROM NARATHIWAT KAOLIN  
THESIS ADVISOR: ASST. PROF. KUNWADEE RANGSRIWATANANON, Ph.D.  
93 PP. ISBN 974-533-267-4**

In this research, the synthesis, kinetics and particle size of zeolite X by using Narathiwat kaolin as starting material have been studied. Many factors affecting the synthesis were considered. The solid phases of products were characterized by XRD, FT-IR, SEM, and particle analyzer. The optimum condition to get the pure phase of zeolite X was found to be metakaolinisation at 900°C for 1 h, Na<sub>2</sub>SiO<sub>3</sub> 10%w/v, NaOH 7.5%w/v, an ageing time for 3 days at 30°C and heating at 90±2°C for 24 h under autogeneous pressure. The results showed that the particle size distribution depended on reaction temperature, degree of crystallinity and alkaline concentration.

The kinetic studies of zeolite X revealed that the rates of crystallization and nucleation depend upon the alkaline and silicate concentration as well as reaction temperature. The order of crystalline zeolite X formation is 3 in NaOH and -1/2 in Na<sub>2</sub>SiO<sub>3</sub>. In addition, the order of nuclei formation is 4.5 and -1 with respect to NaOH and Na<sub>2</sub>SiO<sub>3</sub>, respectively. The activation energies of crystallization and nucleation are 12.5 kcal/mol and 38 kcal/mol, respectively. According to Avrami model, the exponent n value was found to be 4 with reaction temperature 80-90°C and 2 with reaction temperature 100°C.

School of Chemistry  
Academic Year 2003

Signature of Student.....  
Signature of Advisor.....

## Acknowledgements

I would like to express my sincere gratitude to my advisor, Assistant Professor Dr. Kunwadee Rangriwatananon, for her guidance and support throughout this research. I have been working under her invaluable supervision for more than three years and have had many unique research experiences which I will cherish throughout my life. I would like to thank Dr. Visit Vao-soongnern and Assistant Professor Dr. Anan Tongraar for being my thesis committee members.

I also would like to thank the Chairman of the School of Chemistry of Suranaree University of Technology, Assistant Professor Dr. Malee Tangsathitkulchai and all the lecturers for teaching and helping me during my study here. I want to express my appreciation to Mr. Aphiruk Chaisena and all graduate students of the School of Chemistry of Suranaree University of Technology for their invaluable professional guidance and friendly encouragement.

In addition, I wish to express my special thanks to the National University of Laos, the Government of the People's Republic of Laos and Asian Development Bank for offering the scholarship, which enable me to pursue my studies at Suranaree University of Technology, Thailand. My thanks also go to Dr. Channarong Intraraprasert, a lecturer at School of English, for his kind help as a proofreader.

Finally, I would like to thank my wife and children, Somphone Thammavong for their love, support, encouragement, and patience throughout the tedious process of producing a dissertation.

Saythong Thammavong

# Contents

	<b>Page</b>
Abstract in Thai.....	I
Abstract in English.....	II
Acknowledgements.....	III
Contents.....	IV
List of Figures.....	VII
List of Tables.....	XII
List of Abbreviation.....	XIII
<b>Chapter</b>	
<b>I Introduction.....</b>	<b>1</b>
1.1 General description of zeolite.....	1
1.2 Convention of zeolite synthesis.....	3
1.3 Properties of zeolite X.....	5
1.4 Applications of zeolite X .....	6
1.5 Description of kaolinite.....	6
1.6 Theory of Avrami .....	8
1.7 Characterization techniques.....	10
1.7.1 Powder x-ray diffraction.....	10
1.7.2 Fourier transform infrared spectroscopy.....	11
1.7.3 Scanning electron microscope.....	12
1.8 Literature reviews.....	13

## Contents (Continued)

	<b>Page</b>
1.9 Research objectives.....	15
<b>II Materials, Instrumentation and Methods.....</b>	<b>17</b>
2.1 Material lists.....	17
2.1.1 Chemicals and materials.....	17
2.1.2 Apparatus.....	17
2.2 Instrumentation.....	18
2.2.1 Powder x-ray diffraction.....	18
2.2.2 Fourier transform infrared spectroscopy.....	19
2.2.3 Scanning electron microscopy.....	19
2.2.4 Particle analyzer.....	19
2.3 Experimental methods.....	20
2.3.1 Raw material.....	20
2.3.2 Metakaolin preparations.....	21
2.3.3 The zeolite X synthesis methods.....	21
2.3.4 Kinetics study of zeolite X formation.....	21
<b>III Results and Discussion.....</b>	<b>23</b>
3.1 Characterization of kaolin and metakaolin.....	23
3.2 Transformation of kaolin into zeolite X.....	24
3.3 Factors affecting the synthesis of zeolite X.....	28
3.3.1 Effect of the calcination .....	28
3.3.2 Effect of the ageing time.....	33
3.3.3 Effect of the alkaline concentration.....	34

## Contents (Continued)

	<b>Page</b>
3.3.4 Effect of the reaction temperature.....	35
3.3.5 Effect of the addition of sodium silicate.....	38
3.4 Kinetics study results.....	41
3.4.1 Determination of Avrami's exponent.....	41
3.4.2 Determination of activation energies of nucleation and crystallization of zeolite X.....	46
3.4.3 Determination of reaction order with respect to NaOH and Na <sub>2</sub> SiO <sub>3</sub> concentrations.....	50
3.5 Particle size distributions.....	53
3.6 Chemical composition diagram.....	59
<b>IV Conclusion</b> .....	<b>61</b>
References.....	63
Appendices.....	67
Appendix A Simulated XRD powder patterns for zeolites.....	67
Appendix B XRD powder patterns of the solid products.....	79
Curriculum Vitae.....	93

## List of Figures

Figure	Page
1.1 Framework structures of zeolite X.....	5
1.2 Structural models of kaolinite (according to Bish).....	7
3.1 XRD patterns of Narathiwat kaolin and its metakaolin at 700°C, 800°C, and 900°C .....	24
3.2 The evolution of IR spectra during the synthesis of zeolite X from metakaolin: The positions of the absorption bands are labeled. The bands evolution directions from metakaolin to zeolite X spectra are indicated by arrows. The synthesis condition was 7.5%w/v NaOH, 10%w/v Na <sub>2</sub> SiO <sub>3</sub> , at 90°C reaction temperature.....	27
3.3 SEM micrographs of solid phases obtained in the synthesis of zeolite X from Narathiwat kaolin activated at 900°C with 10% Na <sub>2</sub> SiO <sub>3</sub> , 7.5% NaOH, aged 3 days, and reaction temperature 100°C (a) 21 h, (b) 24 h.....	28
3.4 The simulated XRD powder pattern of zeolite X (Treacy, M. M. J. and Higgins, J. B., 1996).....	30
3.5 Powder XRD patterns of solid phase samples obtained during the synthesis of zeolite X from kaolin activated at 700°C, 800°C and 900°C .....	31
3.6 Percentages of crystallinity of zeolite X obtained from the reaction conditions with metakaolin activated at 700°C, 800°C, and 900°C, 7.5%w/v NaOH, 10%w/v Na <sub>2</sub> SiO <sub>3</sub> , aged 3 days and reaction temperature at 90°C .....	32

## List of Figures (Continued)

Figure	Page
3.7 Percentages of crystallinity of zeolite X obtained from the reactions of kaolin activated at 900°C, 7.5% NaOH, 7.5% Na <sub>2</sub> SiO <sub>3</sub> , with aged 1, 3, and 5 days at the reaction temperature 90°C .....	33
3.8 Percentages of crystallinity of zeolite X obtained from the kaolin activated at 900°C, 7.5%w/v Na <sub>2</sub> SiO <sub>3</sub> , with NaOH concentrations of 5%, 7.5%, and 10%w/v, aged 3 days at the reaction temperature 90°C .....	35
3.9 Percentages of crystallinity of zeolite X obtained from kaolin activated at 900°C, 7.5% NaOH, 10% Na <sub>2</sub> SiO <sub>3</sub> , aged 3 days, with the reaction temperature 80°C, 90°C, and 100°C .....	36
3.10 XRD powder patterns of the solid phases obtained in the synthesis of kaolin activated at 900°C, 10% Na <sub>2</sub> SiO <sub>3</sub> , 7.5% NaOH with reaction temperatures (a) 90°C, (b) 100°C .(*) denoted the characteristic of zeolite Na-P <sub>1</sub> .....	37
3.11 Percentages of crystallinity of zeolite X obtained from the reaction of kaolin activated at 900°C, 7.5% NaOH, with the addition of 5%, 10% and 15% Na <sub>2</sub> SiO <sub>3</sub> and, aged 3 days at the reaction temperature 90°C .....	39
3.12 XRD powder pattern of solid phase obtained in the synthesis of Narathiwat kaolin activated at 900°C with 7.5% NaOH, aged 3 days, without addition of Na <sub>2</sub> SiO <sub>3</sub> , and reaction temperature 90°C .....	39

## List of Figures (Continued)

Figure	Page
3.13 XRD powder patterns of the solid phases obtained in the synthesis of kaolin activated at 900°C, 7.5% NaOH, aged 3 days and reaction temperature 90°C, (a) 2.5% Na <sub>2</sub> SiO <sub>3</sub> , (b) 15% Na <sub>2</sub> SiO <sub>3</sub> , (*) denoted the characteristic peaks of zeolite NaA.....	40
3.14 The plots of ln(-ln(1-α)) versus ln t plots from XRD results under the experimental conditions of the metakaolin activated at 900°C, 7.5% NaOH, 10% Na <sub>2</sub> SiO <sub>3</sub> , aged 3 days, and at different reaction temperatures(80°C, 90°C and 100°C).....	43
3.15 The plots of ln(-ln(1-α)) versus ln t from XRD results under the experimental conditions of the metakaolin activated at 900°C, 10% Na <sub>2</sub> SiO <sub>3</sub> , aged 3 days, reaction temperature at 90°C and with various NaOH concentrations (5%, 7.5%, 10%).....	43
3.16 The plots of ln(-ln(1-α)) versus ln t from XRD results with the experimental Conditions of the metakaolin activated at 900°C, 7.5% NaOH, aged 3 days, reaction temperature at 90°C, and with various Na <sub>2</sub> SiO <sub>3</sub> concentrations (7.5%, 10%, 15%).....	44
3.17 Plots of conversion factors, α, against time for the thermal experiment obtained from Narathiwat kaolin activated at 900°C with 10% Na <sub>2</sub> SiO <sub>3</sub> , 7.5% NaOH, aged 3days at reaction temperatures 80°C, 90°C and 100°C .....	48
3.18 The plots of ln k versus 1/T obtained from the synthesis of zeolite X from Narathiwat kaolin activated at 900°C with 10% Na <sub>2</sub> SiO <sub>3</sub> , 7.5% NaOH, aged 3 days and at reaction temperatures 80°C, 90°C, 100°C .....	48

## List of Figures (Continued)

Figure	Page
3.19 The plots of $\ln t_0$ versus $1/T$ obtained from the synthesis of zeolite X from Narathiwat kaolin activated at $900^\circ\text{C}$ with 10% $\text{Na}_2\text{SiO}_3$ , 7.5% NaOH, aged 3 days and at reaction temperatures $80^\circ\text{C}$ , $90^\circ\text{C}$ , $100^\circ\text{C}$ .....	49
3.20 The plots of $\log(1/t_0)$ against $\log[\text{NaOH}]$ obtained from the various NaOH concentrations of 5%, 7.5% and 10%w/v at reaction temperature $90^\circ\text{C}$ .....	51
3.21 The plots of $\log(d\alpha/dt)$ against $\log[\text{NaOH}]$ obtained from the various NaOH concentrations of 5%, 7.5% and 10%w/v at reaction temperature $90^\circ\text{C}$ .....	51
3.22 The plots of $\log(1/t_0)$ against $\log[\text{Na}_2\text{SiO}_3]$ obtained from the $\text{Na}_2\text{SiO}_3$ with concentrations of 7.5%, 10% and 15%w/v at reaction temperature $90^\circ\text{C}$ .....	52
3.23 The plots of $\log(d\alpha/dt)$ against $\log[\text{Na}_2\text{SiO}_3]$ obtained from the $\text{Na}_2\text{SiO}_3$ with concentrations of 7.5%, 10% and 15%w/v at reaction temperature $90^\circ\text{C}$ .....	52
3.24 Particle size distributions for zeolite X from metakaolin activated at $900^\circ\text{C}$ (a) 7.5% NaOH, 10%w/v $\text{Na}_2\text{SiO}_3$ , aged 3 days, reaction temperature at $90^\circ\text{C}$ with various times (b) 7.5% NaOH, 7.5%w/v $\text{Na}_2\text{SiO}_3$ , reaction temperature at $90^\circ\text{C}$ with various ageing times (c) 7.5% NaOH, 10%w/v $\text{Na}_2\text{SiO}_3$ , aged 3days with various reaction temperatures (d) 7.5%w/v $\text{Na}_2\text{SiO}_3$ aged 3 days, reaction temperature at $90^\circ\text{C}$ with various NaOH concentrations.....	55

## List of Figures (Continued)

<b>Figure</b>	<b>Page</b>
3.25 Zeolite X crystal growth with metakaolin activated at 900°C, 7.5% NaOH, 10% Na <sub>2</sub> SiO <sub>3</sub> , aged 3 days at different reaction temperatures on the syntheses (a) 80°C, (b) 90°C, (c) 100°C .....	56
3.26 Zeolite X crystal growth with metakaolin activated at 900°C, 7.5% NaOH, 10% Na <sub>2</sub> SiO <sub>3</sub> , reaction temperature 90°C at different ageing times of reaction mixture on the synthesis (a) aged 1 day, (b) aged 3 days,(c) aged 5 days.....	57
3.27 Zeolite X crystal growth with metakaolin activated at 900°C, 10% Na <sub>2</sub> SiO <sub>3</sub> , aged 3 days at different NaOH concentrations on the syntheses (a) 7.5% NaOH, (b) 10% NaOH.....	58
3.28 Ternary chemical composition diagram SiO <sub>2</sub> -Al <sub>2</sub> O <sub>3</sub> -Na <sub>2</sub> O defining specific crystallization domains from Narathiwat kaolin activated at 900°C and the reaction temperature at 90°C (▲) zeolite X, (■) zeolite NaA, (●) sodalite, (◆) zeolite X+A.....	60

## List of Tables

<b>Tables</b>	<b>Page</b>
1.1 Exponents, n, of the Avrami's equation for different nucleations and growth mechanisms.....	9
2.1 The chemical compositions and Si/Al ratio of kaolin sample from Narathiwat province determined by XRF.....	20
3.1 Infrared absorption bands for kaolin, metakaolin activated at 900°C, and zeolite X.....	26
3.2 The analytical results of the Avrami's exponents for the crystallization of zeolite X from Narathiwat kaolin activated at 900°C with various conditions.....	45
3.3 Results of apparent activation energies of crystallization and nucleation.....	49
3.4 The mean particle size at the highest % crystallinity at each condition.....	54
3.5 The particle size distribution coefficients obtained from the plot of mean particle size versus % crystallinity.....	58

## List of Abbreviation

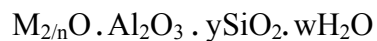
XRD	X-ray Diffraction
XRF	X-ray fluorescence
IR	Infrared
SEM	Scanning electron microscope
MK	metakaolin
°C	Degree Celsius
Å	Angstrom
g	gram
µm	micrometer
h	hour
kV	kilovolt
mA	milliampere
cps	count per second
cm <sup>-1</sup>	per centimeter
w/v	weight by volume
FAU	Faujasite
α	alpha
β	beta

# Chapter I

## Introduction

### 1.1 General description of zeolite

Zeolites are crystalline aluminosilicates of group IA and IIA elements such as sodium, potassium, magnesium and calcium (Breck, D.W., 1974). Chemically, they are represented by the empirical formula:



where y is 2 to 10, n is the cation (M) valence, and w represents the water contained in the voids of the zeolite. Structurally, zeolites are complex, crystalline inorganic polymer based on an infinitely extending three-dimensional, four connected framework of SiO<sub>4</sub> and AlO<sub>4</sub> tetrahedra linked to each other by sharing of oxygen ions. Each AlO<sub>4</sub> tetrahedron in the framework bears a net negative charge, which is balanced by a cation. The framework structure contains channels or interconnected voids that are occupied by the cation and water molecules. The cations are mobile and ordinarily undergo ion exchange.

The structural formula of a zeolite is based on the crystallographic unit cell, the smallest unit of structure, represented by:



where n is the valence of metal cation M, w is the number of water molecules per unit cell, x and y are numbers of total tetrahedra per unit cell, and y/x usually

has values of 1-5, in the case of high silica zeolites  $y/x$  is 10 to 100. The primary structural units of zeolite, the  $\text{SiO}_4$  and  $\text{AlO}_4$  tetrahedra, are assembled into secondary building units which may be simple polyhedra such as cubes, hexagonal prisms, or octahedral. The final structure framework consists of assemblages of secondary units. The structure can be divided into two categories: one that provides a system of uniform channels and the other that provides internal pores system comprising of interconnected cage-like void (Bekkum, V.H., Jansen, J. C., and Flanigen, E. M., 1991).

Generally, zeolite can be classified into small, large and ultralarge pore materials. Small pore structure has aperture consisting of six, eight or nine tetrahedra (6-8-9 membered rings), medium pore frameworks have 10-membered ring, large pore zeolite has 12-membered ring, and ultralarge structures have 14-18 or 20 membered rings. Pore diameters in known zeolite are approximately between 0.3 and 1.5 nm (Meier, W. M., and Olson, D. H., 1996). Zeolites are also classified according to their framework symmetries with an identification code of three letters used by the International Zeolite Association (IZA). Zeolite X and Y belong to the Faujasite (FAU) group which has equidimensional channels intersecting perpendicular to each other (see Figure 1.1).

There are more than 40 known natural zeolites and almost 200 synthetic ones with about 50 novels, distinct framework structures of zeolite. They exhibit pore size of 0.3-0.8 nm and pore volumes of 0.10-0.35 cc/g. The physical and chemical properties of zeolites are based upon fragmentary structural information. The molecular structure of zeolite can be related to these properties as follows (Breck, D.W., 1974).

1. High degree of hydration and the behavior of water in zeolite
2. Low density and large void volume when dehydrated
3. Stability of crystal structure of many zeolites when dehydrated and when as much as 50 vol% of the dehydrated crystal are void
4. Cation exchange properties
5. Uniform molecular size channels in the dehydrated crystals
6. Various physical properties such as electrical conductivity
7. Adsorption of gases and vapors
8. Catalytic properties.

These properties make zeolite excellent compounds, especially for industry where they have many applications, for example, in petroleum refining, hydro-cracking catalysis and hydro-isomerization. Other applications are using in the detergent formulation and in sequestering agent as the substitution for phosphate, using in wastewater treatment, animal feed supplements, and soil improvements (Bekkum, V.H., Jansen, J. C., and Flanigen, E., M.1991).

## **1.2 Convention of zeolite synthesis**

Zeolites are generally synthesized from sodium aluminosilicate gels prepared from various silica and alumina sources. Kaolinite has been reported as an ideal, combined source for silica and alumina for the synthesis of low silica zeolites as early as 1964 (Breck, D.W., 1974). Zeolite synthesis involves the hydrothermal crystallization of active hydrated aluminosilicate gels or sols in a basic environment. A gel is defined as a hydrous metal aluminosilicate, which is prepared from aqueous solution, reactive solids, colloidal sols, or reactive aluminosilicates such as the residue

structure of metakaolin (derived from kaolin clay by dehydroxylation) and glasses. The gels are crystallized in a hydrothermal system at temperatures varying generally from room temperature to about 175°C. In some cases, higher temperatures up to 300°C are used. The pressure is the autogenous pressure approximately equivalent to the saturated vapor pressure of water at the temperature designated. The duration required for crystallization varies from a few hours to several days (Barrer, R. M., 1982).

Suitable silica sources are hydrated silicates, precipitated silica powders, and colloidal silica sol, etc. The alumina source may be aluminum salts, aluminum oxides, and aluminum hydroxide or metal aluminates, etc. Alkali hydroxides, alkaline earth hydroxides, organic bases or their combinations supply the necessary alkalinity. In general, the composition of reaction mixtures, nature of reactants, reaction temperature, alkalinity (pH) and crystallization time as well as pretreatments can affect the type of zeolite form and its properties. The ease of which the zeolites crystallize is attributed to the high reactivity of the gel, the concentration of the alkali hydroxide, and the high surface activity due to the small particle size of the solid phases concerned.

Some methods have been developed to produce small zeolite crystals, such as reducing the temperature of crystallization, ageing of aluminosilicate gels prior to the crystallization, increasing the alkalinity of the aluminosilicate mixture and adding the organic cations (Fegan, S. G., and Lowe, P. J., 1986). Moreover, in order to produce small crystals with a narrow crystal size distribution, colloidal zeolites are also crystallized from clear homogeneous solution with a high alkalinity in the absence of heterogeneous gel phases. Synthesis conditions yielding discrete colloidal crystals

from a clear solution have been originally described by Schoeman, et al. (1995). Examples are colloidal zeolite Y and zeolite A, hydroxysodalite particles. The size of crystals are in a range of 20-200 nm.

### 1.3 Properties of zeolite X

Zeolite X is an aluminum-rich synthetic analogue of the naturally occurring mineral Faujasite (Figure 1.1) with the general formula  $\text{Na}_2\text{O} \cdot \text{Al}_2\text{O}_3 \cdot n\text{SiO}_2 \cdot w\text{H}_2\text{O}$  when the value of  $n$  is 2-3; they are designated as zeolite X and those with higher values as zeolite Y. The large cavities (super cage,  $\alpha$  cage, diameter = 13 Å), and sodalite cage cavities ( $\beta$  cage, diameter = 6.6 Å) with windows of 7.4 Å. are interlocked to be a three dimensional network (Zhu, L., and Seff, K., 1999).

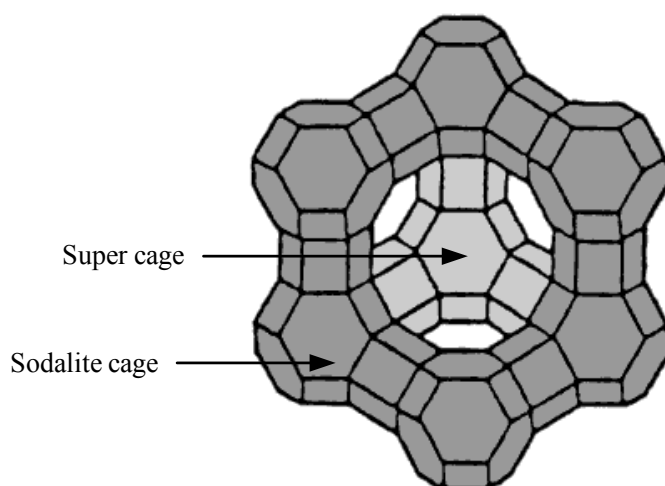


**Figure 1.1** Framework structure of zeolite X

The oxygen atoms lie approximately midway between each pair of Si and Al atoms, but are displaced from those points to give near-tetrahedral angles about Si and

Al (S6R's). The oxygen atoms are shared by sodalite units and super cages and may be viewed as entrances to the sodalite cavities. Each unit cell has eight sodalite units and eight super cages, 16 D6R's, 16, 12-rings, and 32 S6R's (Zhu, L., and Seff, K., 2000).

#### **1.4 Applications of zeolite X**

Zeolite X has a wide range of industrial applications, partly because of its large pore size and void volume. Its sorptive and catalytic properties depend also on its exchangeable cations: its size, its charge, its chemical nature, and its placement within the zeolite (Zhu, L., and Seff, K., 2000). Three main properties of zeolite are technologically important: they are selective and strong absorbents; they are selective ion exchanger and they are catalytically active. Other interesting properties associated with zeolites are their high thermal stability and their metal-oxygen tetrahedral that are exposed to the surface accessible for modification. Currently, they are useful for commercial applications such as being catalyst for hydrocarbon cracking, detergent builders, ion exchanger for removal of heavy metals, and absorbent for separation and purification processes (Bekum, V.H., Jansen, J. C., and Flanigen, E. M., 1991).

#### **1.5 Description of kaolinite**

Kaolinite, a clay mineral used as a combined source of alumina and silica, is a convenient starting material for the synthesis of zeolite. It is one of the most common minerals on earth. Kaolin can be found in many parts of the world. Kaolinite has a structure formula:  $\text{Al}_4[\text{Si}_4\text{O}_{10}](\text{OH})_8$  and theoretical composition of 46.54%  $\text{SiO}_2$ , 39.50%  $\text{Al}_2\text{O}_3$ , and 13.98%  $\text{H}_2\text{O}$ . Kaolinite is a layer aluminosilicate with a 1:1

uncharged dioctahedral layered structure. Each layer consists of a sheet of  $\text{SiO}_4$  tetrahedra forming six-membered silicate rings connected via common oxygen atoms to a sheet of  $\text{AlO}_6$  octahedra building four membered aluminates rings (Figure 1.2). The colors of kaolin are white, pink or gray depending on their compositions (Bougeard, D., Geidel, E., and Smirnov, K. S., 2000). The mineral kaolinite is found in kaolin clay.

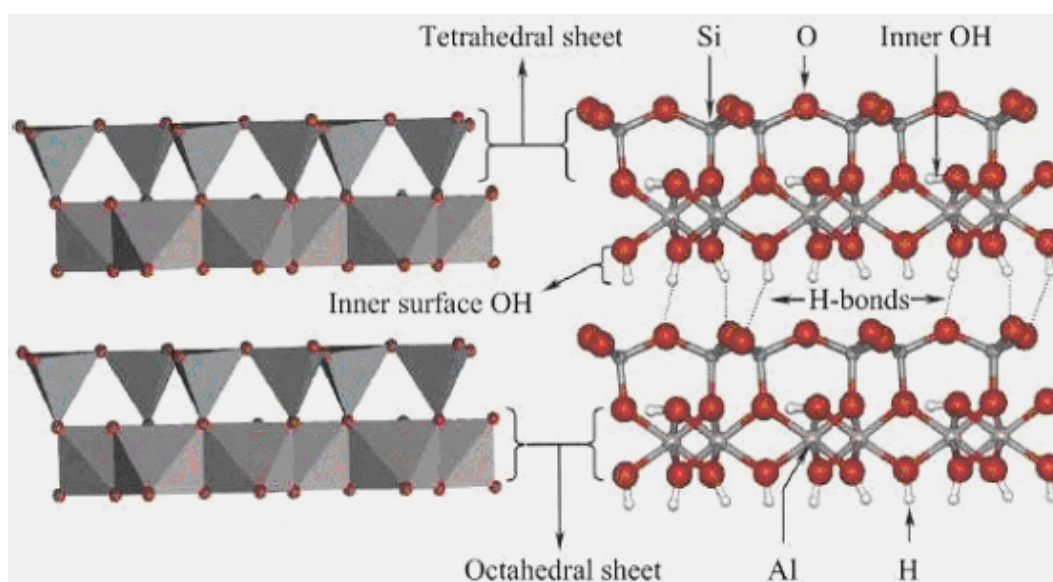


**Figure 1.2** Structural models of kaolinite (according to Bish).

Kaolin has long been mainly used in the ceramic industry, especially in fine porcelains because it can be easily moulded, has fine structure, and is white when fired. It is very soft with hardness of 2-2.5 (Grim, R. E. 1968, Velde, B. 1992).

Kaolin has been found in many regions of the world. In Thailand, it is found mainly in Lampang, Narathiwat, and Ranong provinces. In the past, kaolin was mainly used in ceramic industry. However, new applications of kaolin have been

continuously discovered. Typical kaolin contains traces amount of iron, titanium, calcium, magnesium, etc., which are originally present in natural kaolinite. Therefore, zeolite prepared from natural kaolin is always contaminated with these elements. These elements may have some influences on the zeolite properties such as brightness, hardness, catalytic activity, or electrical properties, etc. Nevertheless, kaolin is still a popular choice to be used as starting material for the synthesis of zeolite. Presently, many researchers are working actively on various aspects of the synthesis of zeolite from kaolin.

## **1.6 Theory of Avrami**

A general theory of crystallization kinetics was developed by Avrami in 1940. The theory describes that crystallization processes consist of nucleation and crystal growth.

1. Some nucleation and growth processes are:
  - Spontaneous nucleation: During cooling molten material to a fixed temperature, nuclei appear randomly throughout the volume.
  - Time dependence of nucleation: Nuclei can appear instantaneously on cooling or during crystallization in the non-uniformed phase.
  - Nature of growth process: Growth can proceed in one, two or three dimensions resulting in needles, discs or spheres. Growth stops when neighboring crystals merge.
  - Time dependence of growth: Linear dimension of growing crystals increases in proportional to time.

- Density of growing units: The transformed phase is not totally crystalline and assumed that the density of the growing crystals is constant.
2. The Avrami's exponent and the rate constant can be determined from the Avrami's equation

$$-\ln(1 - \alpha) = kt^n \quad (1.1)$$

where,  $\alpha$ , is the conversion factor, ranging from 0 to 1,  $k = d\alpha/dt$  is the rate constant and the exponent,  $n$ , is the parameter which describes reaction mechanism.

3. The Avrami's exponent value depends on the dimensionality of the growth process, and on the kinetic order of the nucleation. In general case, where three dimensional growth is combined with the first order nucleation, the Avrami's exponent,  $n=3+1=4$ . The Avrami's exponents for different nucleation and growth mechanisms are shown in Table 1.1

**Table 1.1** Exponents,  $n$ , of the Avrami's equation for different nucleation and growth mechanisms.

n	Nucleation and growth mechanism
3+1=4	3 dimensional growth + random nucleation
3+0=3	3 dimensional growth + instantaneous nucleation
2+1=3	Disc like growth + random nucleation
2+0=2	Disc like growth + instantaneous nucleation
1+1=2	Rod-like growth + random nucleation
1+0=1	Rod-like growth + instantaneous nucleation

To study the kinetics of crystal formation, the Avrami's equation can provide a good empirical fit to the kinetic curves. It can be used for the calculation of the rate constant and Avrami's exponent. According to Avrami's equation as shown in equation (1.1), taking logarithms of this equation, gives

$$\ln(-\ln(1-\alpha)) = n \ln t + \ln k \quad (1.2).$$

Thus, when plotting of  $\ln(-\ln(1-\alpha))$  versus  $\ln t$ , the slope of the regression lines,  $n$ , is related to the mechanism of reaction.

The rate constant  $k$  can be expressed using the Arrhenius' equation as

$$k = A \exp\left(-\frac{E_a}{RT}\right) \quad ..(1.3)$$

where  $E_a$  represents the activation energy,  $A$  is a constant,  $R$  is gas constant and  $T$  is the absolute temperature. Similarly, the time used in the nucleation process can be expressed as

$$\frac{1}{t_0} = B \exp\left(-\frac{E_n}{RT}\right) \quad (1.4)$$

where  $t_0$  is called inductive period.  $E_n$  represents activation energy for nucleation, and  $B$  is a constant.

## 1.7 Characterization techniques

### 1.7.1 Powder x-ray diffraction

X-ray is an electromagnetic radiation with wavelength about 1 Å ( $10^{-10}$  m), which is about the same size as atomic distance in solid; thus, it can be used to probe the crystalline structure at the atomic level. X-ray diffraction has been used in two main areas, for the fingerprint characterization of crystalline materials and for the

determination of their structures. Each crystalline solid has its unique characteristic x-ray powder pattern, which may be used as a “fingerprint” for its identification. Once the material has been identified, x-ray crystallography may be used to determine its structure, i.e. how the atoms packed together in the crystalline state and what the inter-atomic distance and angle are. These unique properties made x-ray diffraction one of the most important characterization tool used in solid state chemistry and material science.

An important equation for x-ray diffraction is Bragg’s equation which shows the relationship between x-ray wavelength ( $\lambda$ ) with lattice point distance (d) and incident diffraction angle ( $\theta$ ).

$$n \lambda = 2d \sin \theta \quad (1.5)$$

The different crystal planes in the crystal will diffract x-ray at different angles according to the Bragg’s equation. Therefore, by rotating the sample plane with respect to the incident x-ray, the diffracted angles can be recorded by a detector and the diffraction pattern is obtained. The identification of the sample structure can be done by comparing the spectrum with the patterns stored in the database.

### **1.7.2 Fourier transform infrared spectroscopy**

The region of the infrared spectrum that is of great interest to most of the chemists is the wavelength range 2.5 to 15  $\mu\text{m}$ . In practice, units proportional to frequency, (wave number in units of  $\text{cm}^{-1}$ ) rather than wavelength, are commonly used and the region 2 to 15  $\mu\text{m}$  corresponds to approximately 4000 to 400  $\text{cm}^{-1}$ .

The atoms in a molecule are constantly oscillating around average positions. Bond lengths and bond angles are continuously changing due to this vibration. A molecule absorbs infrared radiation when the vibration of the atoms in the molecule

produces an oscillating electric field with the same frequency as the frequency of incident IR radiation when they are in resonance. Each molecule has its own characteristic spectrum. The bands that appear depend on the types of bonds and the structure of the molecule.

Fourier transform infrared (FT-IR) spectroscopy measures dominantly vibrations of functional groups and highly polar bonds. Thus, these chemical fingerprints are made up of the vibration features of all the sample components. FT-IR spectrometer records the interaction of IR radiation with experimental samples, measuring the frequencies at which the sample absorbs the radiation and the intensities of the absorptions. Determining this frequency allows the identification of the sample's chemical makeup, since chemical functional groups are known to absorb light at specific frequencies. FT-IR experiments can generally be classified into the following two categories: (a) qualitative analysis, where the aim is to identify the sample and (b) quantitative analysis, where the intensities of the absorptions are related to the concentration of the component.

### **1.7.3 Scanning electron microscope**

Scanning electron microscope (SEM) is a type of microscope that uses electrons rather than light to form an image. There are many advantages to use SEM instead of a light microscope. SEM has a large depth of field, which allows a large amount of sample to be in focus at one time. SEM also produces images of high resolution, which means that small spaced features can be examined at a high magnification. Preparation of samples is relatively easy since most SEM instruments only require the sample to be conductive. The combination of higher magnification,

larger depth of focus, greater resolution, and ease of sample observation, make SEM one of the most heavily used instruments in present-day researches.

By using the wave-particle duality, SEM creates the magnified images by using electrons instead of light waves. The SEM shows very detailed 3-dimensional images at much higher magnification than is possible with a light microscope. The images created without light waves are rendered black and white. By the nature of an electron beam, the vacuum is required during the operation; therefore, the sample has to be prepared carefully to withstand the vacuum inside the microscope. The samples must be a conductive material in order to be able to interact with an electron. SEM samples are coated with a very thin layer of gold by a machine called a sputter coater. The sample is placed inside the microscope's vacuum column through an airtight door.

After the air is pumped out of the column, an electron gun emits a beam of high energy electrons. This beam travels downward through a series of magnetic lenses designed to focus the electrons to a very fine spot. Near the bottom, a set of scanning coils moves the focused beam back and forth across the specimen, row by row. As the electrons beam hits each spot on the sample, secondary electrons and back scattered electron are knocked loose from its surface. A detector counts these electrons and sends the signals to an amplifier. The final image is built up from the number of electrons emitted from each spot on the sample. By this way, the morphology of the sample can be seen directly from the micrograph.

## **1.8 Literature reviews**

Modification of clay minerals by converting them to zeolites was reported as early as 1935 according to Breck (Breck, D.W., 1974). Clay minerals have been used as a combined source of  $\text{Al}_2\text{O}_3$  and  $\text{SiO}_2$  for the syntheses of zeolites. Kaolinite

( $\text{Al}_2\text{O}_3 \cdot 2\text{SiO}_2 \cdot 2\text{H}_2\text{O}$ ) with a Si/Al ratio of 1, is the principal mineral in china clay and ideally suitable for the synthesis of zeolite A which also has a Si/Al ratio of 1. Other low silica zeolites like X and Y have been conveniently prepared from kaolin (Barreer, R. M., 1978). The reactions involved are: (1) calcination of kaolin at 550-900°C to give a dehydroxylated x-ray amorphous, reactive product called metakaolin and (2) hydrothermal treatment of metakaolin with aqueous NaOH to give zeolite A.

The synthesis of zeolite X from kaolin has been reported as early as 1964 (Howell, P.H., 1964). Later, various aspects of the synthesis have been reported from several researchers. The fluoride medium synthesis of zeolites including NaX from kaolinite has also been recently reported (Chandrasekhar, S., 1993). The synthesis of low silica zeolites from kaolin essentially consists of two steps (1) thermal preactivation of kaolin to get a dehydroxylated x-ray amorphous, reactive product called metakaolin, and (2) hydrothermal treatment of metakaolin with aqueous alkali to give zeolite A. Generally, a Si/Al ratio  $>1$  in the reaction mixture is advisable for the crystallization of zeolite X and this has been achieved by either adding silica externally or by removing some aluminium from metakaolin by acid leaching or in the presence of certain Al complexing agent (Kuhl, G. H. et al., 1971).

Chandrasekhar, S. et al. (1999) studied the synthesis of zeolite X from Kerala kaolin. They found that the optimum conditions to get pure phase zeolite X with good crystallinity from kaolin were found to be metakaolinizations of the clay at 900°C for 1 h, ageing of reactants at room temperature for 24 h and heating  $87 \pm 2^\circ\text{C}$  for 15 h under autogenous pressure.

Gualtieri, A. et al. (1997) studied the kinetics of zeolite Na-A from natural kaolinite activation at 800°C with 4M NaOH concentration at reaction temperature

70-100°C, by time resolved synchrotron powder diffraction techniques. They found that the formation of zeolite NaA was depended on the calcinations of starting material but not the number of defects of the starting material. Also, the n values obtained from Avrami method decreased when reaction temperature increased and the ranges of n were between 5 and 7.

Kacirek, H. et al. (1976) studied the kinetics of zeolite X from aluminate and silicate solutions with various Si/Al ratios (1.53-2.54). They found that the activation energies of the crystallization were about 11.8-15.6 kcal/mol.

As mentioned earlier, the introduction and the literature reviews have been guided by the principal that the synthesis of zeolite X from kaolin depends on calcinations of starting material, base concentration, temperature and duration of the synthesis. Kaolin is one of the convenient starting material for the synthesis of zeolite because of its structure and its chemical composition is suitable for the synthesis of zeolite (Rocha, J., 1999). Kaolinite has been found in many parts of Thailand, especially in Lampang, Ranong and Narathiwat provinces. However, there are some limited numbers of reports on the synthesis of zeolite X from Thai kaolin and the detail of kaolinite transformation to crystalline zeolite has not been investigated. Furthermore, it is wellknown that Thai kaolin is mainly used in ceramic industry, thus, it is useful to utilize Thai kaolin as a starting to produce new materials which are expensive and applicable to many industrial organizations such as in environmental sectors, detergent industry and catalyst industry.

## **1.9 Research objectives**

The main objectives of this study are:

1. How to synthesize zeolite X with high percentage of crystallinity by using Narathiwat kaolin as a starting material.
2. Study the factors affecting the synthesis of zeolite X.
3. Study the kinetics of zeolite X formation.
4. Determination of the particle size of zeolite X during the reaction at various concentrations of NaOH, ageing times and temperatures.
5. Determination of a reaction composition diagram.

## **Chapter II**

### **Materials, Instrumentation and Methods**

#### **2.1 Material lists**

##### **2.1.1 Chemicals and materials**

- (a) Kaolin from Narathiwat Province obtained from Thai Clay Mineral Ltd.
- (b) Sodium hydroxide anhydrous pellets (NaOH), Analytical reagent, Carlo Erba
- (c) Sodium silicate ( $\text{Na}_2\text{SiO}_3$ ) powder, Riedel Hen AG
- (d) Distilled water
- (e) pH paper

##### **2.1.2 Apparatus**

- (a) Plastic bottles (Polypropylene) for zeolite synthesis
- (b) Shaker, SWB 505 shaking water bath
- (c) Desiccators
- (d) Air oven for synthesis and drying
- (e) Muffle furnace for calcinations of kaolin
- (f) Thermometer
- (g) Glass microfiber filters, Whatman GF/C diameter 47 mm
- (h) Vacuum filtration apparatus

## 2.2 Instrumentation

### 2.2.1 Powder x-ray diffraction

XRD is a popular technique used for the analysis of structural properties and identification of mineral in solid state and material science. A Bruker D5005 Powder x-ray diffractometer with Ni-filtered Cu  $K\alpha$  radiation was used to record diffraction spectra. Prior to the measurement, each sample was prepared by using a standard method for powder sample.

#### Sample preparation procedure for XRD

1. Dry the sample in the oven at 120°C.
2. Grind about 1 g of each solid sample to get powder as homogeneous as possible, and then load into the polymethylmethacrylate (PMMA) sample holder.
3. Tap the powder gently and evenly to uniformly cover the holder cavity.
4. Gently press the powder sample into the cavity using a glass slide.
5. Gently lift off glass slide to reveal the sample surface.

Each diffraction spectrum was recorded with condition:  $2\theta$  angle between 5° and 45°, Cu-target, 35 kV, 35 mA, and scan speed of 0.3 degree/0.02 second. Typically, the data were expressed in the plot between intensity of diffraction peaks and  $2\theta$  angles. The positions of diffraction peaks were compared with the reference database and the compounds could be identified. The percentage of crystallinity was obtained by the area of 13 strong diffraction peaks of the sample compared with the patterns of the product with the highest intensity in the studied experiment.

$$\text{Percent of crystallinity} = \frac{\text{Total area of 13 strong peaks of the sample}}{\text{Total area of 13 peaks of the one with the highest intensity}} \times 100\% \quad (2.1)$$

### **2.2.2 Fourier transform infrared spectroscopy**

FT-IR spectrophotometer with model Perkin-Elmer spectrum GX was used to analyze the samples and the infrared spectra were recorded in the mid IR region ( $4000\text{-}370\text{ cm}^{-1}$ ) with the KBr pellet technique. The solid sample and KBr were dried at  $120^{\circ}\text{C}$  for 1h before using. Approximately 0.5 mg of each sample was mixed with 300 mg dried KBr powder and ground to very fine powder with a mortar and pestle. The ground powder was pressed into a transparent disk using a hydraulic pressing machine with an equivalent weight of about 10 tons for 1 min. The spectra were obtained using an average of 4 scans with  $4\text{ cm}^{-1}$  resolution. To compare several spectra together, the normalization was done using one fixed point at  $2500\text{ cm}^{-1}$ .

### **2.2.3 Scanning electron microscope**

Morphology of the solid sample could be seen through the use of SEM. The crystal shape and size of the crystalline solid phase could be identified from the micrograph. The observation was done using scanning electron microscope model JSM6400. To prepare for the observation, the solid sample was placed on a brass stub sample holder using a double stick carbon tape. Then, the sample was dried using infrared light for five minutes. After that, the sample was coated with a layer of gold approximately  $20\text{-}25\text{ \AA}$  thick using a Balzer sputtering coater. The micrographs were recorded with 12 kV, 8000x magnification.

### **2.2.4 Particle analyzer**

The particle size distribution was determined by a laser scattering particle size distribution analyzer (Malvern Mastersizer S series). For this purpose, the wet method of particle size distribution analysis was used. Water was used as the medium for dispersion of the zeolite. The solution was ultrasonicated for 45 min in order to break

down the flocculates before the run was performed. As claimed by the manufacturer, the instrument is accurate to within 5% of the middle value. All samples were run twice to ensure the accuracy of the measurements.

## 2.3 Experimental methods

### 2.3.1 Raw material

Kaolin samples collected from Narathiwat Province were determined for the chemical composition by x-ray fluorescence as given in Table 2.1. The main compositions of kaolin samples are oxides of Si and Al. The Si/Al ratio is found to be 1.13. The kaolin contains mineral impurities of iron, titanium, calcium, magnesium, etc. (Janjira, W., 2002).

**Table 2.1** The chemical compositions of kaolin sample from Narathiwat Province determined by XRF.

Chemical content	(weight %)
SiO <sub>2</sub>	46.72
Al <sub>2</sub> O <sub>3</sub>	35.75
Fe <sub>2</sub> O <sub>3</sub>	0.70
TiO <sub>2</sub>	0.64
MnO <sub>2</sub>	0.01
CaO	0.03
MgO	0.05
K <sub>2</sub> O	0.43

### 2.3.2 Metakaolin preparations

Kaolin samples from Narathiwat Province were ground in agate mortar and sieved with a mesh number 106 micron aperture sieve. The kaolin samples were calcined in the muffle furnace at different temperatures (700°C, 800°C, 900°C) with a uniform gradation giving a soaking period for 1 h. After the calcination processes, the kaolin samples were transformed to metakaolin. The metakaolin samples from each calcination were used as materials for the syntheses of zeolite X.

### 2.3.3 The zeolite X synthesis methods

1. 1g each of metakaolin from various calcination (700°C, 800°C, 900°C) was mixed with NaOH of various concentrations (5%, 7.5% and 10%w/v) and with sodium silicate ( $\text{Na}_2\text{SiO}_3$ ) of various concentrations 2.5%, 5%, 7.5%, 10%, and 15%w/v.
2. The synthesis mixtures from (1) were put in sealed polypropylene bottles and shaken in water bath at 30°C for 1, 3, and 5 days. This step is called ageing of the reaction mixture.
3. After ageing period, the reaction mixtures were heated in air oven kept at 80°C, 90°C, and 100±2°C. Then the samples were withdrawn at regular intervals i.e., 3, 6, 9, 12, 15, 18, 21, 24, 30, and 36 h. The products were filtered, washed with distilled water and dried in air oven at 120°C for 6 h.
4. The solid products were characterized by XRD, FT-IR, SEM, and particle analyzer.

### 2.3.4 Kinetic study of zeolite X formation

The percentages of crystallinity of zeolite X were determined from x-ray diffraction patterns of solid phase products at various reaction times under different

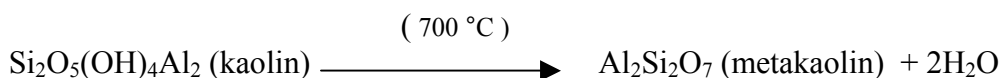
experiment conditions. The crystalline percentage was defined as the ratio of the total peak area of the sample to the product with the highest intensity. The correlation between the percentage of crystallinity and reaction time with different concentrations of NaOH and Na<sub>2</sub>SiO<sub>3</sub> at different temperatures provides the information on the kinetic study. The rates of the crystallinity were taken from the slope of this correlation.

## Chapter III

### Results and Discussion

#### 3.1 Characterization of kaolin and metakaolin

The heat treatment of kaolin extrudates transforms them into metakaolin extrudates. Kaolin is a dioctahedral 1:1 layer silicate mineral with formula  $\text{Si}_2\text{O}_5(\text{OH})_4\text{Al}_2$ . Dehydration by thermal treatment converts kaolin to metakaolin, which is semicrystalline and much more reactive than the starting material:



Metakaolin is believed to be a defect phase in which the tetrahedral silica layers of the original clay structure are largely retained adjacent to  $\text{AlO}_4$  tetrahedral units derived from the original octahedral layer of the kaolin. Maximum reactivity for metakaolin can be obtained by calcinations of the kaolin at  $700^\circ\text{C}$  to  $750^\circ\text{C}$ , producing a maximum concentration of 4 and 5 coordinate aluminum and minimum concentration of 6 coordinate aluminum. Higher temperature treatment leads to mullite and cristobalite (Rocha, J., and Klinowski, J., 1990).

Figure 3.1 shows the XRD patterns of the kaolin sample and metakaolin at different temperatures of calcinations. It was found that the temperature needed to calcine kaolin into metakaolin completely was at least  $700^\circ\text{C}$ . All traces of the crystal

kaolinite diffraction peaks are removed. These changes are completely consistent with the previous literature on the kaolin-metakaolin transformation (Rocha, J. et al., 1990). Metakaolin is x-ray amorphous. The remaining peak in the diffraction pattern is due to a quartz impurity. This peak declined at a higher temperature.

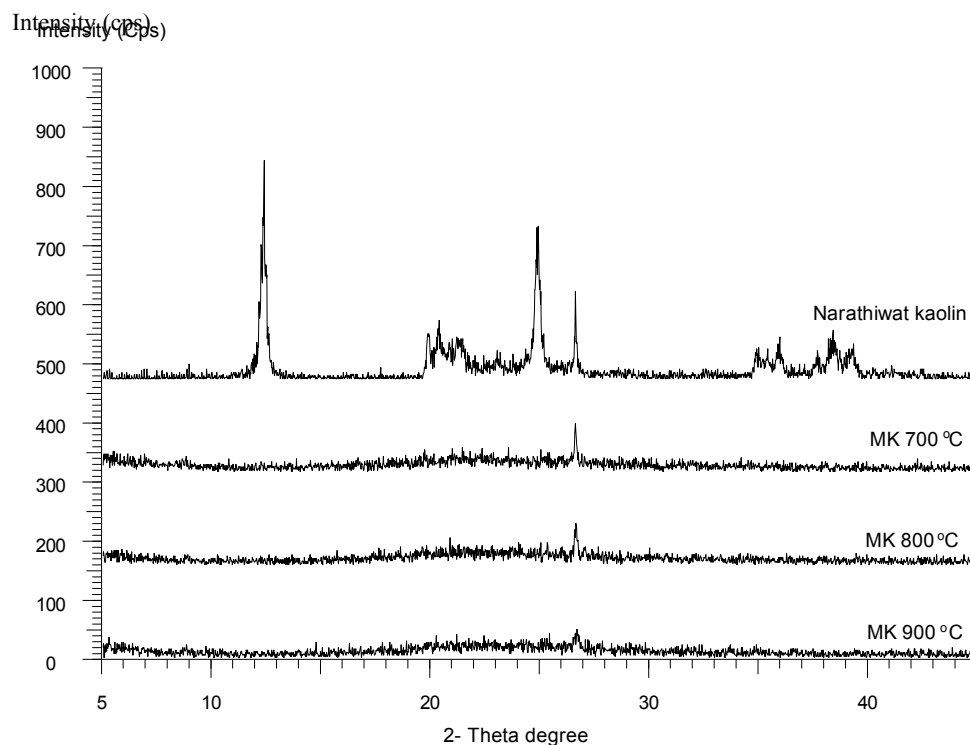


**Figure 3.1** XRD patterns of Narathiwat kaolin and its metakaolin at 700°C, 800°C, and 900°C.

### 3.2 Transformation of kaolin into zeolite X

The transformation of kaolin to metakaolin and then to zeolite X can be clearly seen from IR spectra in the region 1400-400  $\text{cm}^{-1}$ . The kaolin starting material gives at least 10 well-defined IR bands in this region due to Si-O, Si-O-Al, and Al-OH vibrations (see Table 3.1). The conversion to metakaolin totally removes these

bands, leaving a broad intense asymmetric band at  $1091\text{ cm}^{-1}$  as the major feature. The disappearance of  $912\text{ cm}^{-1}$  band indicates the loss of Al-OH units, while the changes in the Si-O stretching bands and the disappearance of the Al-O-Si bands at  $791$  and  $754\text{ cm}^{-1}$  are consistent with the distortion of the tetrahedral and octahedral layers (Deepak, A., 1997)

In a similar manner to the XRD measurement, the IR spectra of solid products can be used to obtain the crystallinity of zeolite X. The direction of evolution of IR absorption bands during the synthesis of zeolite X from metakaolinite is shown in Figure 3.2. The IR bands assignment of the zeolite X (after the reaction process taken 24 h) in this work and zeolite X from references are demonstrated in Table 3.1.

In the IR spectra (Figure 3.2) of the samples measured as a function of zeolite X crystallization, the broad band of the metakaolin located at  $805\text{ cm}^{-1}$  assigned to the Al-O bond in  $\text{Al}_2\text{O}_3$  is not observed. The vibrational band of metakaolin at  $1091\text{ cm}^{-1}$  assigned to the stretching of Si-O bond in  $\text{SiO}_2$  (Demortier, A. et al., 1999) is shifted towards  $983\text{ cm}^{-1}$  after 24 h, i.e., towards the frequency of the antisymmetric stretching of T-O bond ( T = Si or Al) in aluminum silicates with zeolite or sodalite structure. The band position of zeolite X at  $567\text{ cm}^{-1}$  is attributed to double six rings (D6R) related to a Faujasite structure (Breck, D.W., 1974, and Barrer, R.M., 1982). The bands of zeolite X (in this work) at  $567\text{ cm}^{-1}$  and  $458\text{ cm}^{-1}$  are closely similar to the references (Flanigen, E.M. et al., 1971). However, the bands at  $983\text{ cm}^{-1}$  and  $761\text{ cm}^{-1}$  are about  $15\text{ cm}^{-1}$  more than Flanigen's work. The big differences in frequency can be attributed to the higher silica content of the zeolite X. The frequency shift of infrared stretch bands with the substitution of tetrahedral Al for Si aluminosilicate frameworks has been reported by many authors. Since the mass of Al and Si are

almost the same, the decrease in frequency with increasing Al concentration is related to variation in bond length and bond order. The longer bond length of Al-O and decreased electro negativity of Al result in a decrease in force constant (Milkey, R.G., 1960 and Flanigen, E.M., et al., 1971).

**Table 3.1** Infrared absorption bands for kaolin, metakaolin activated at 900°C, and zeolite X.

IR absorption bands (cm <sup>-1</sup> )				
Kaolinite (assignment)	Metakaolin 900°C	Zeolite X ( in this work)	Zeolite X (Chandrasekhar,S.1993)	Zeolite X (Flanigen,E.M)
1115(Si-O)	1091s	-	-	1060
1033(Si-O)	805m	983s	980s	971s
1007(Si-O)	-	761m	750m	746m
912(Al-OH)	-	-	690wsh	690wsh
791(Si-O-Al)	465m	685m	670m	668m
754(Si-O-Al)	-	567ms	565ms	560ms
696(Si-O)	-	458ms	460ms	458ms
536(Si-O-Al)	-	-	-	406w
475(Si-O)				
428(Si-O)				

S: strong, m: medium, sh: shoulder, w: weak.

Assignment of zeolite vibrations following (Flanigen, E.M. 1971): internal TO<sub>4</sub> tetrahedra: asymm.stretch 973; symm.stretches 690, 668; bending 458; external linkages: D6R 560; pore opening 406; symm.stretch 746; assymm. stretch 1060.

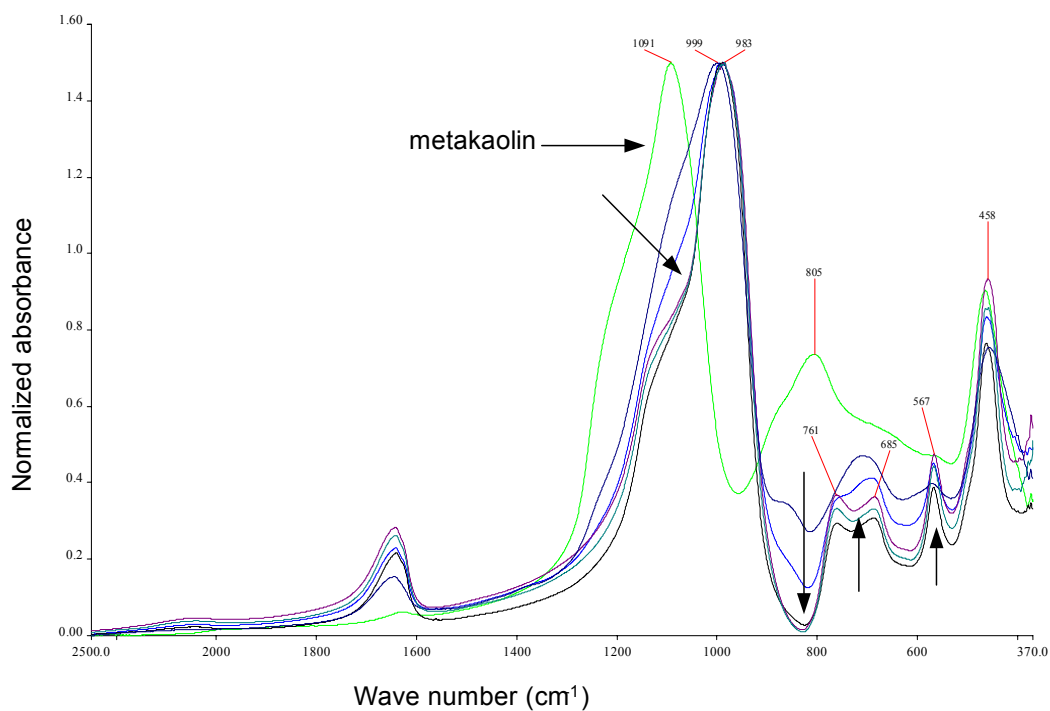


**Figure 3.2** The evolution of IR spectra during the synthesis of zeolite X from metakaolin: The positions of the absorption bands are labeled. The bands evolution directions, from metakaolin to zeolite X spectra are indicated by arrows. The synthesis condition was 7.5%w/v NaOH, 10%w/v Na<sub>2</sub>SiO<sub>3</sub>, with 90°C reaction temperature.

Figure 3.3 shows the SEM micrographs of solid phase products obtained from the reaction reaching 21 h (a) and 24 h (b). The result shows that the crystals of zeolite X clearly appear in octahedral shape and the growth process occurs on the octahedral face.

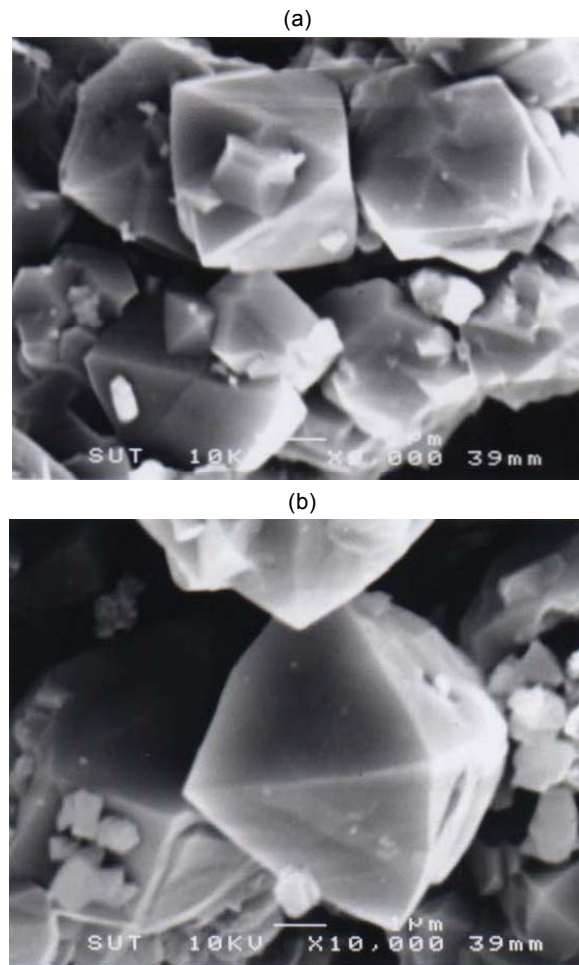


**Figure 3.3** SEM micrographs of solid phases obtained in the synthesis of zeolite X from Narathiwat kaolin activated at 900°C with 10% Na<sub>2</sub>SiO<sub>3</sub>, 7.5% NaOH, aged 3 days, and reaction temperature 100°C (a) 21 h, (b) 24 h.

### **3.3 Factors affecting the synthesis of zeolite X**

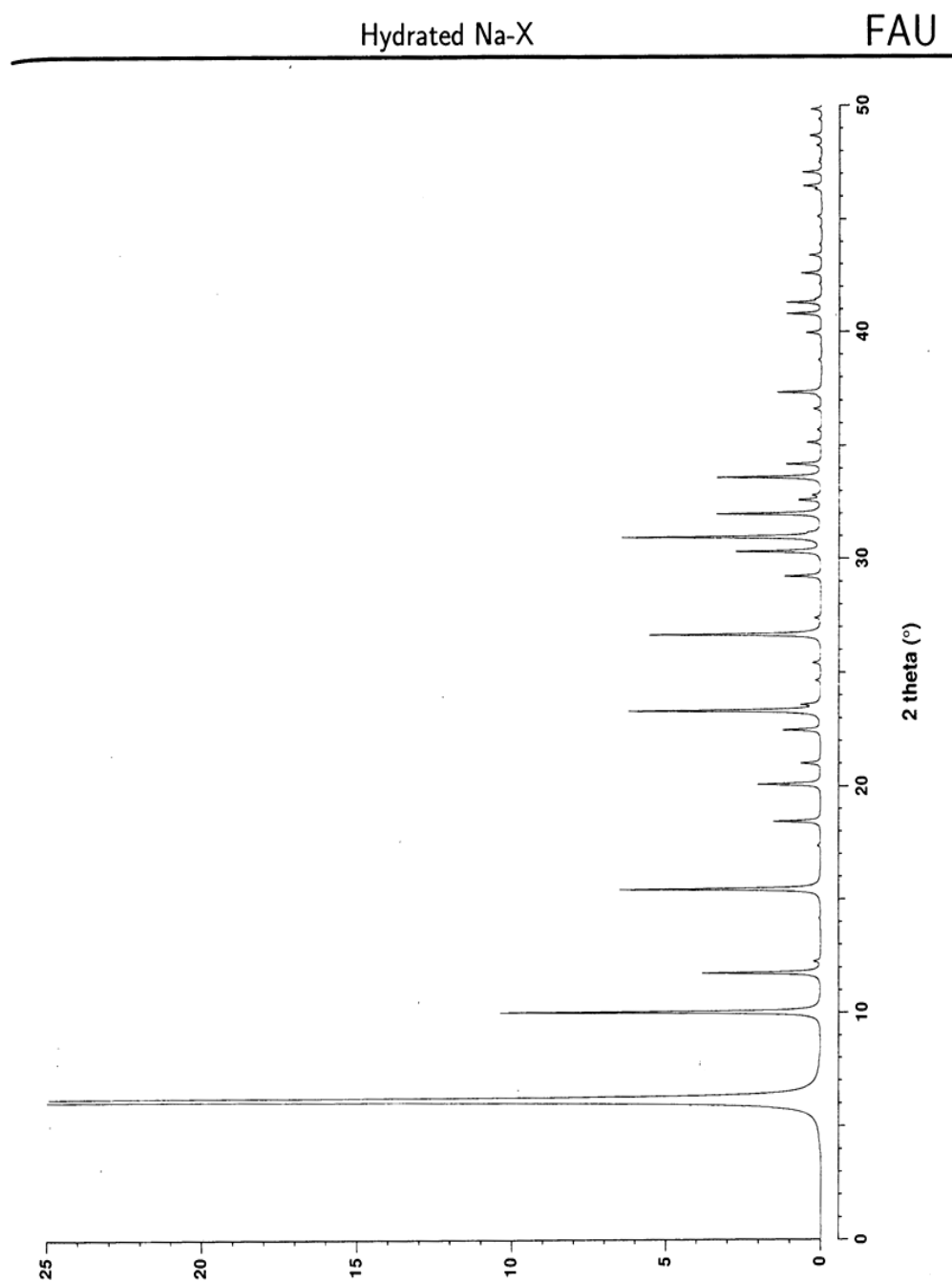
#### **3.3.1 Effect of the calcination**

The study of the synthesis of zeolite X from a Kerala kaolin (Chandrasekar, S., 1998) found that the metakaolin prepared at 400°C, 500°C and 600°C the final products as hydroxyl sodalite. With an increase in the metakaolinisation temperature to 700°C or more, zeolite X is obtained. Janjira, W. (2002) shows that Narathiwat

kaolin activated at 700°C is the most suitable to synthesize zeolite Na-A with the highest % crystallinity content.

The aim of this study is to find out what metakaolinisation temperature brings the most suitable structure of metakaolin for synthesizing zeolite X under the assigned experimental conditions. In this experiment, the temperatures of 700°C, 800°C and 900°C were considered in the study of the effect of calcination temperatures on the synthesis. The Narathiwat kaolin samples were activated at the temperatures of 700°C, 800°C, 900°C for 1 h and the calcined kaolin samples were used for the synthesis of zeolite X with the condition of 7.5%w/vNaOH, 10%w/vNa<sub>2</sub>SiO<sub>3</sub>, reaction temperature 90°C, and various reaction times. The XRD patterns of solid phase products during the reaction with kaolin calcined at 700°C, 800°C, and 900°C, are shown in Figure 3.5. It was found that the  $2\theta$  positions and intensities of the peaks are consistent with the simulated XRD pattern of zeolite X (Treacy, M.M.J., and Higgins, J.B., 1996) in Figure 3.4 and the peaks intensities gradually increase with the reaction time until 24 h when the change in intensity is rarely observed. It appears that the increase in intensity of zeolite X from the metakaolin at 900°C is swifter than the others. This indicates that the evolution of zeolite X peaks under the condition of using metakaolin at 900°C is the fastest.

As a consequence, the metakaolin at 900°C provides the best condition for further synthesis of zeolite X. This result is discrepant to the result obtained from zeolite Na-A synthesis (Janjira, W., 2002). It may be possible that the metakaolin at 700°C contains more active species for forming nuclei of zeolite Na-A while the metakaolin at 900°C has more active species for building the nuclei of zeolite X.



Zeolites 16:323-802, 1996 451

**Figure 3.4** The simulated XRD powder pattern of zeolite X (Treacy, M. M. J., and Higgins, J. B., 1996)

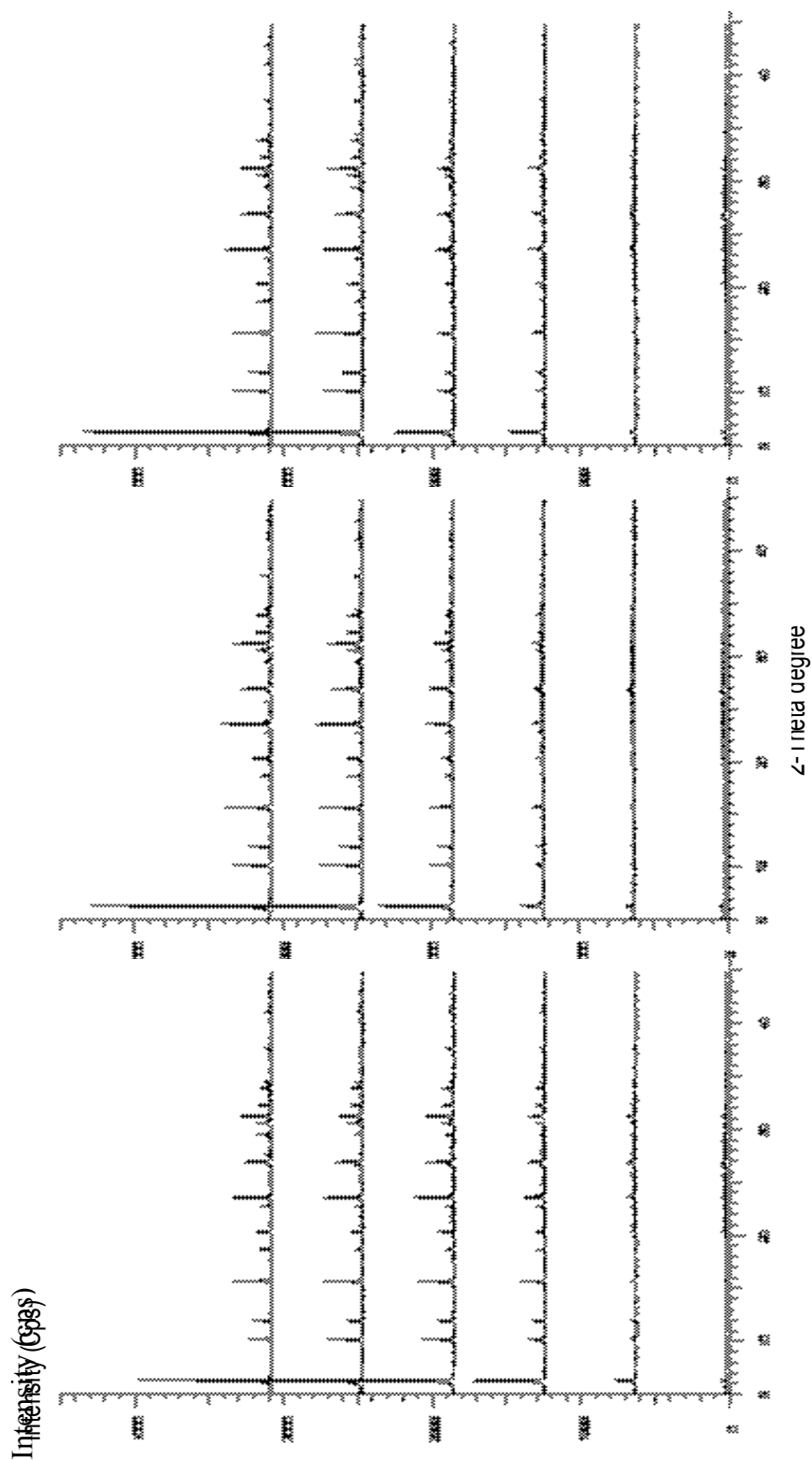


**Figure 3.5** Powder XRD patterns of solid phase samples obtained during the synthesis of zeolite X from kaolin activated at 700°C, 800°C and 900°C.

The percentages of crystallinity calculated from Figure 3.5 by equation (2.1) as a function of reaction time are shown in Figure 3.6. It showed that after the induction period, the initial appearances of crystalline zeolite X in the metakaolin at 900°C started at 6 h, and then followed by the 800°C sample at 9 h and the 700°C sample at 12 h. The growth rate tends to increase with the calcinations temperature. The product produced from metakaolin at 900°C grew at the fastest rate till the reaction time reached 24 h, at which the maximum yield was observed for all the metakaolin samples. After 24 h, all yields in 900°C, 800°C and 700°C are quite constant within the range of observing. Because the reaction with metakaolin at 900°C brings the highest yield, the rate of crystallization is faster than the others. Therefore, the calcined kaolin at 900°C was selected for the further experiments.

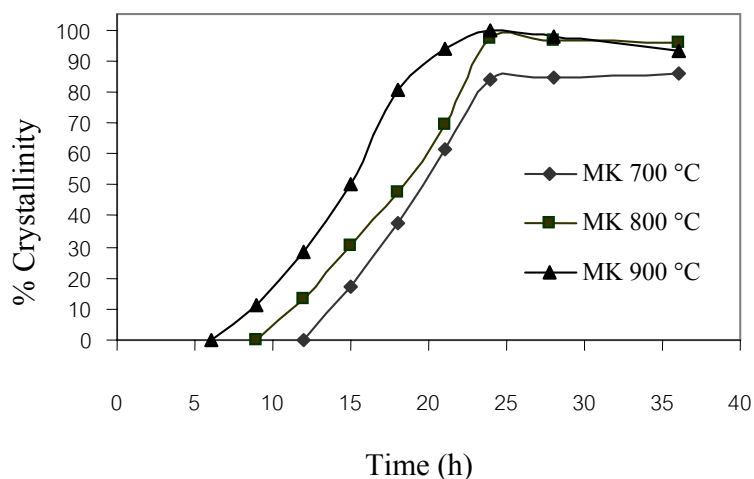


**Figure 3.6** Percentages of crystallinity of zeolite X obtained from the reaction conditions with metakaolin activated at 700°C, 800°C, and 900°C, 7.5%w/v NaOH, 10%w/v Na<sub>2</sub>SiO<sub>3</sub>, aged 3 days and reaction temperature at 90°C.

### 3.3.2 Effect of the ageing time

In the hydrothermal synthesis of zeolite X at low temperatures (80-100°C), a consideration of ageing reactants before heating it at the reaction temperature is also important. To study this effect on the synthesis, the time of ageing for 1, 3 and 5 days were selected. The reaction mixtures (7.5% NaOH, 7.5% Na<sub>2</sub>SiO<sub>3</sub>, metakaolin at 900°C) were aged at 30°C for those periods before leaving them at the reaction temperature 90°C. The plots of the percentages of crystallinity of the solid products, which depend on the time of ageing, as a function of the reaction time deduced from the XRD technique, are shown in Figure 3.7. The percentage of solid phase in each condition was higher than 90%. The rates of reaction increase with the ageing time of the reaction mixture. The result is consistent with the result from Katovic', A. et al. (1989). This implies that an increase of the ageing time enhances the formation of germ nuclei, probably by an increase of dissolution of solid amorphous.

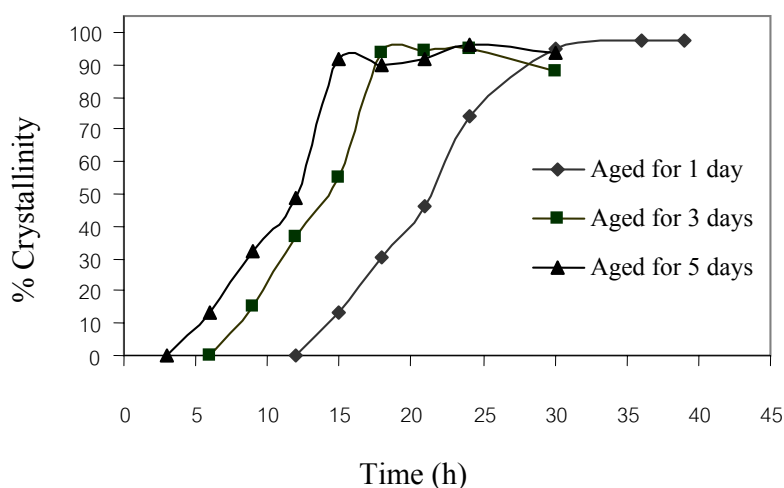


**Figure 3.7** Percentages of crystallinity of zeolite X obtained from the reactions of kaolin activated at 900°C, 7.5% NaOH, 7.5% Na<sub>2</sub>SiO<sub>3</sub>, with aged 1, 3, and 5 days at the reaction temperature 90°C.

### 3.3.3 Effect of the alkaline concentration

The effects of NaOH concentration on the synthesis of zeolite X were investigated. The kaolin activated at 900°C was chosen to be the starting material. The synthesis conditions were carried out with NaOH concentrations of 5%, 7.5% and 10%w/v at reaction temperature 90°C. XRD technique was used to characterize and determine the crystallinity at various reaction times (3-48 h). The plots of the percentage of crystallinity of solid products with the reaction time are shown in Figure 3.8. In general, the reaction rate increases with increasing alkaline concentration. The rate of zeolite X formation is fastest at 10% NaOH and slowest at 5% NaOH. The percentages of crystallinity were high in the range 85-87% at 10% NaOH and 88-94% at 7.5% NaOH with the reaction time about 18 h. At the concentration of 5% NaOH, the induction period was very long and zeolite X began to appear around 24 h. Moreover, the percentage of the crystallinity obtained was about 30% at the reaction time more than 48 h. This indicates that the dissolution of solid amorphous increases with an increase in the concentration of alkali, resulting in enhancing the formation of nuclei and increasing the rate of crystallization. For a further study of zeolite X synthesis, the NaOH concentration of 7.5% seems to be the suitable condition, because it gives the highest yield within the assigned reaction time.

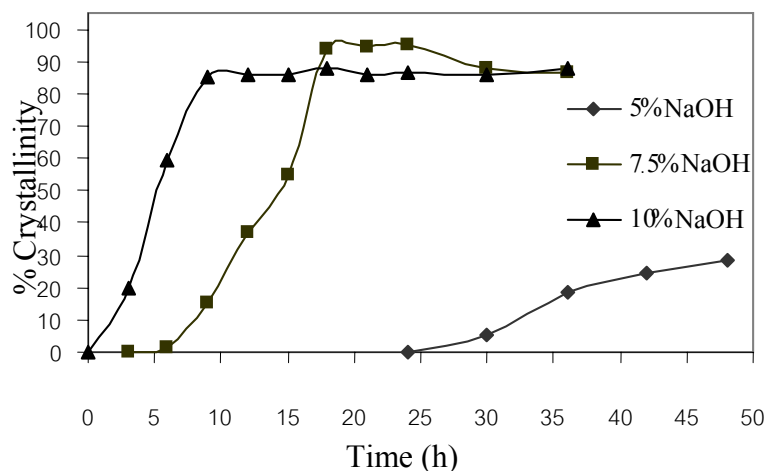


**Figure 3.8** Percentages of crystallinity of zeolite X obtained from the kaolin activated at 900°C, 7.5%w/v Na<sub>2</sub>SiO<sub>3</sub>, with NaOH concentrations of 5%, 7.5%, and 10%w/v, aged 3 days at the reaction temperature of 90°C

### 3.3.4 Effect of the reaction temperature

In this section, the effect of hydrothermal synthesis temperature on zeolite X formation was examined. Figure 3.9 shows the crystallization curves of zeolite X synthesized at different reaction temperatures from a substrate of kaolin activated at 900°C, 7.5% NaOH, 10% Na<sub>2</sub>SiO<sub>3</sub> and aged for 3 days, with the reaction temperatures of 80°C, 90°C, and 100°C. It was observed in the induction period and shortening the overall crystallization period. The result suggests that the rate of zeolite X occurrence has been accelerated with an increase of the reaction temperature. For the zeolite X samples obtained at the reaction temperature 80°C, the maximum crystallinity of the zeolite phase reached only 72% even after 36 h. Whereas, highly crystalline zeolite X crystal was obtained in 24 h at 90°C. Figure

3.10 shows the x-ray diffraction patterns of zeolite X samples obtained at different crystallization periods. The peak intensities developed progressively as the crystallization period increased. The characteristic XRD peaks of the zeolite X began to appear after 12 h at 90°C and fully crystalline zeolite X sample was obtained after 24 h. No other crystalline phase appeared in the XRD pattern of this sample even after the prolonged crystallization period up to 36 h (Figure 3.10 a). Significantly, at the reaction temperature 100°C and the ageing time of 1 day, a new phase mixed with zeolite X product was observed (Figure 3.10 b). The XRD patterns showed the phase which was identified to be zeolite Na-P1. This caused the crystallization percentage of zeolite X to decrease after 24-36 h. Besides, the zeolite Na-P<sub>1</sub>, an aluminosilicate amorphous should be involved in reducing the percentage of the yield (Takahashi. H. et al., 1976).

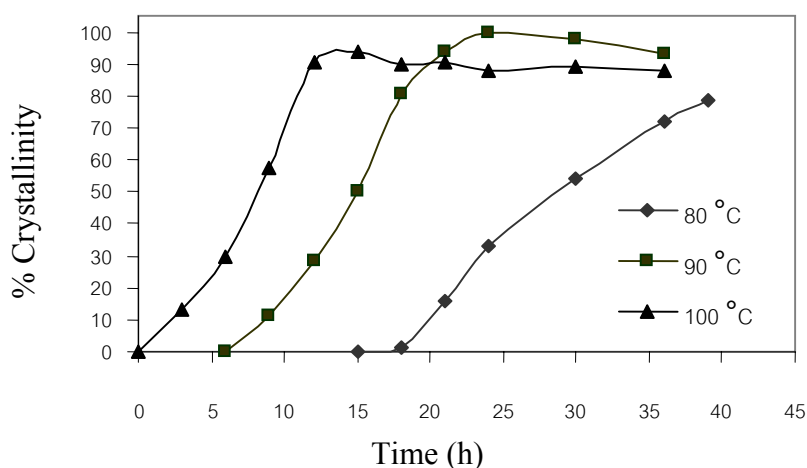


**Figure 3.9** Percentages of crystallinity of zeolite X obtained from kaolin activated at 900°C, 7.5% NaOH, 10% Na<sub>2</sub>SiO<sub>3</sub>, aged 3 days, with the reaction temperature 80°C, 90°C, and 100°C.

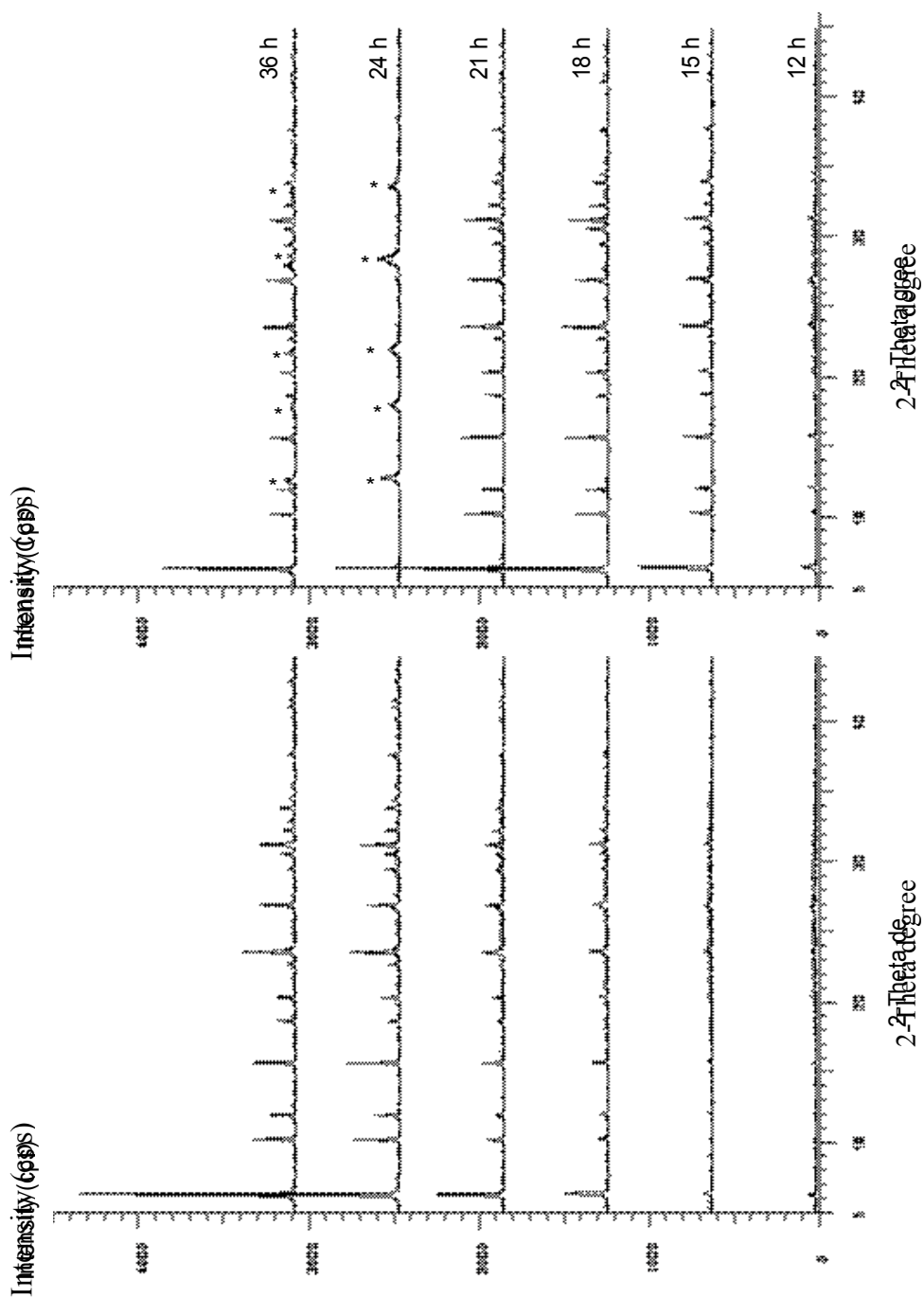


**Figure 3.10** XRD powder patterns of the solid phases obtained in the synthesis of kaolin activated at 900°C, 10% Na<sub>2</sub>SiO<sub>3</sub>, 7.5% NaOH with reaction temperatures (a) 90°C, (b) 100°C. (\*) denoted the characteristic of zeolite Na-P<sub>1</sub>.

### 3.3.5 Effect of the addition of sodium silicate

In order to form zeolites with greater  $\text{SiO}_2/\text{Al}_2\text{O}_3$  ratios than 2, an example of zeolite X was synthesized from the reactant composition of  $4\text{Na}_2\text{O}\cdot\text{Al}_2\text{O}_3\cdot 4\text{SiO}_2\cdot 160\text{H}_2\text{O}$  (Howell, P. A., and Acara, N. A., 1964). Therefore, an extra silica must be added in a case of starting material like clays with the Si/Al ratio equal 2. Another way to produce zeolites with high Si/Al ratio is to leach alumina from clays by acid treatment (Howell, P.A., 1968).

As mentioned above, the addition of silica to a starting material with low ratio of Si/Al is necessary for the synthesis of zeolite X. In this work, sodium silicate was chosen as an additional silica source and the appropriate amount of  $\text{Na}_2\text{SiO}_3$  added in the reaction process was determined. The synthesis of zeolite X was carried out with various concentrations of  $\text{Na}_2\text{SiO}_3$  ( 2.5%, 5%, 7.5%, 10%, and 15%w/v), 7.5% NaOH, kaolin activated at  $900^\circ\text{C}$  and reaction temperature  $90^\circ\text{C}$ . As usual, the XRD technique was used to characterize and to determine the crystallinity of zeolite X. The plots of the percentages of crystallinity of the solid products with the reaction time from experimental conditions are shown in Figure 3.11. It was found that the lower silicate concentration is in the reaction, the faster reaction is observed. The highest percentage of crystallinity was obtained with 10%  $\text{Na}_2\text{SiO}_3$  and at 24 h. In the reaction process without the addition of  $\text{Na}_2\text{SiO}_3$ , the product occurred with only pure zeolite NaA as shown in Figure 3.12. With the addition of 2.5%  $\text{Na}_2\text{SiO}_3$  (Figure 3.13a) and 15%w/v (Figure 3.13 b), the solid product phase contained not only zeolite X but also a trace amount of zeolite NaA. The result reveals that it is impossible to

produce zeolite X from kaolin without any addition of silica in the reaction. In order to get a pure phase of zeolite X, the amount of needed silica is also important.

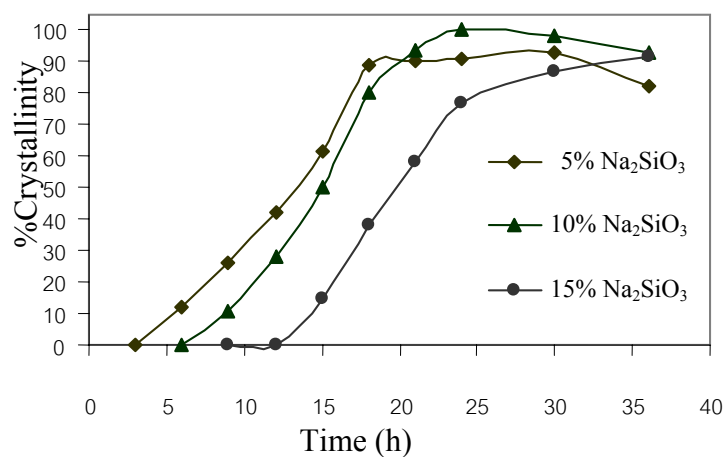


**Figure 3.11** Percentages of crystallinity of zeolite X obtained from the reactions of kaolin activated at 900°C, 7.5% NaOH, with the addition of 5%, 10% and 15% Na<sub>2</sub>SiO<sub>3</sub>, aged 3 days at the reaction temperature 90°C.

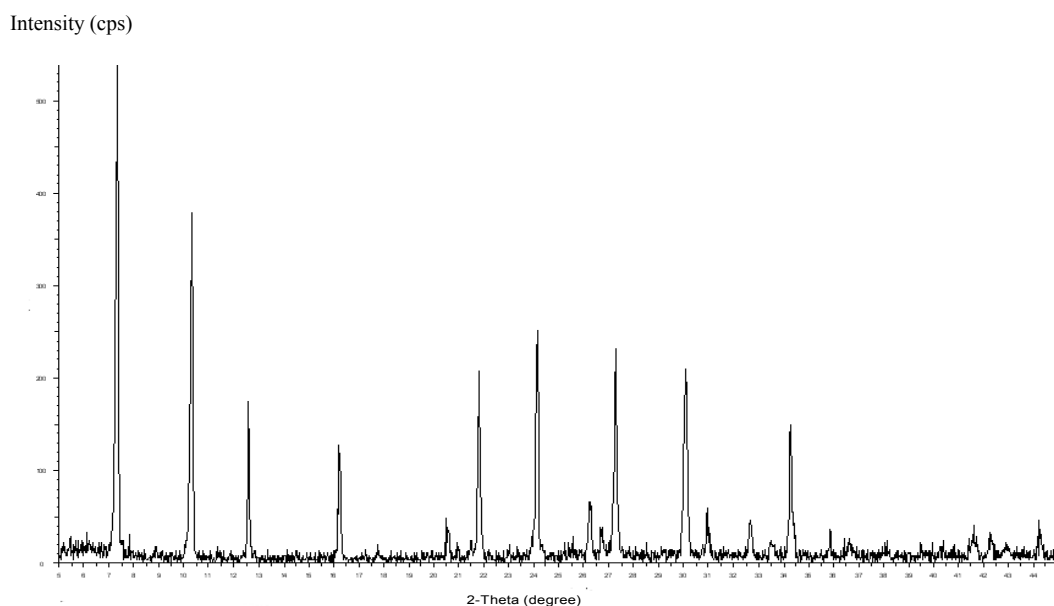


**Figure 3.12** XRD powder pattern of solid phase obtained in the synthesis of Narathiwat kaolin activated at 900°C with 7.5% NaOH, aged 3 days, without addition of Na<sub>2</sub>SiO<sub>3</sub>, and reaction temperature 90°C.

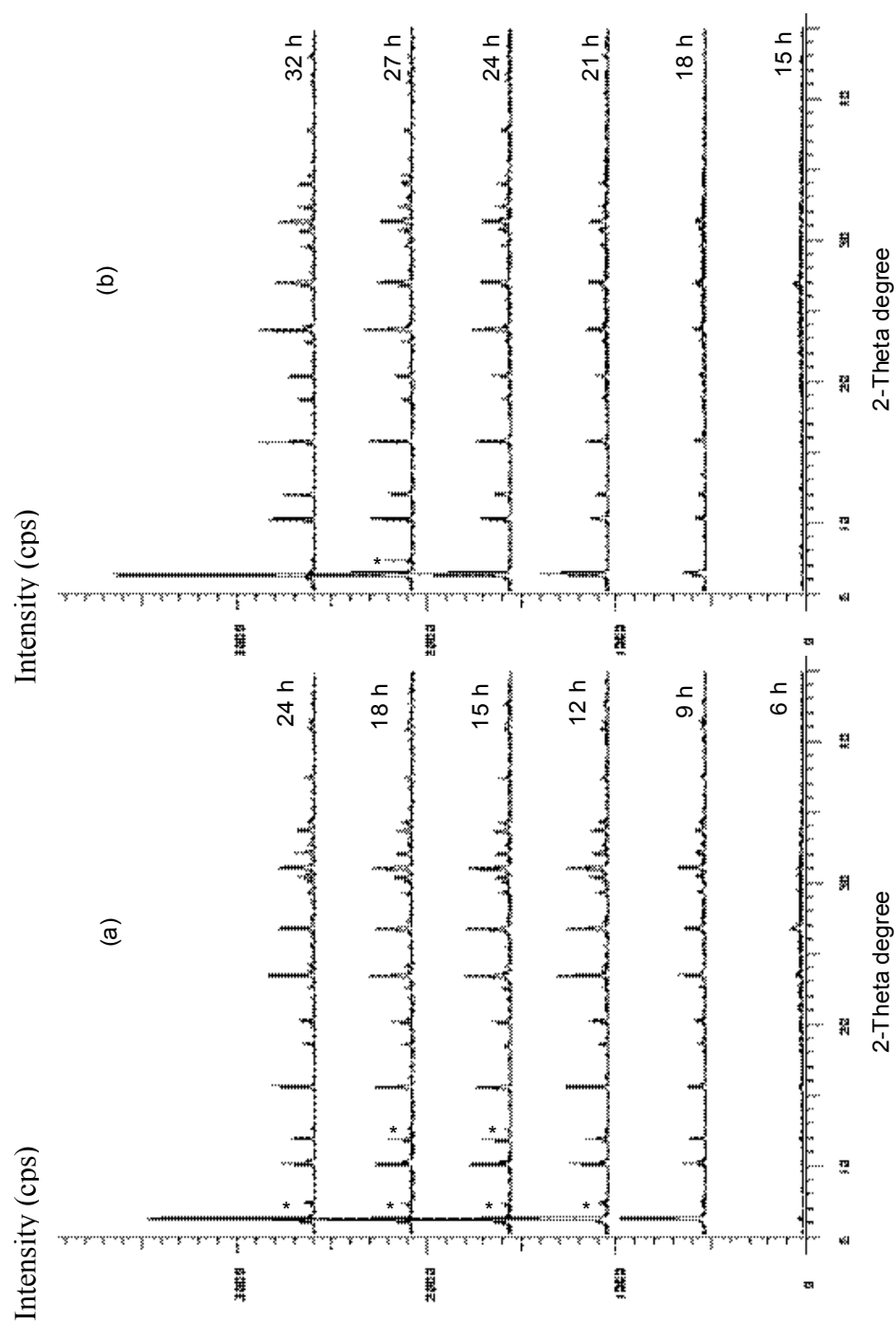


**Figure 3.13** XRD powder patterns of the solid phases obtained in the synthesis of kaolin activated at 900°C, 7.5% NaOH, aged 3 days and reaction temperature 90°C, (a) 2.5% Na<sub>2</sub>SiO<sub>3</sub>, (b) 15% Na<sub>2</sub>SiO<sub>3</sub>, (\*) denoted the characteristic peaks of zeolite NaA

### 3.4 Kinetic study results

Studies on the kinetics of zeolite crystallization have received extensive attention from many investigators. Most kinetic studies deal with the influence of the reaction variables such as temperature, alkalinity, and composition of the original medium on the evolution of the crystallized component (Barrer, R. M., 1982). Nucleation and crystal growth are generally not separated, but are described by a single kinetic equation. The yields versus time curves are indeed very useful for the modeling of zeolite synthesis (Thompson, R. W., and Dyer, A., 1985). However, the mechanism of zeolite crystallization referring to kinetics, such as the autocatalysis of crystallization process, alkalinity effect on the rate of crystallization and the seeding effect, have been insufficiently studied. In this part, we attempt to fit the data on the nucleation growth model of Avrami and calculate the activation energy from Arrhenius equation. In addition, the order of reaction with respect to alkaline and silicate concentration was also determined.

#### 3.4.1 Determination of Avrami's exponent (n)

The theoretical basis for the description of the isothermal crystallization involving both nucleation and growth was formulated by Avrami (Grizzetti, R., and Artioli, G., 2002). In its basic form, the theory describes the time dependence of the fractional extent of crystallization. The resulting equation is usually written in the following form:

$$\alpha = 1 - \exp(-kt^n) \quad (3.1)$$

Where  $\alpha$  is the volume fraction of the crystallized phase at time  $t$ ;  $n$  and  $k$  are constants with respect to time;  $n$  is a parameter related to the mechanism of the

process. The rate constant  $k$  is related to the absolute temperature  $T$  by an Arrhenius equation

$$k = A \exp\left(-\frac{E_a}{RT}\right) \quad (3.2)$$

where  $E_a$  is the activation energy,  $R$  the gas constant and  $A$  the frequency factor. In many cases (Gualtieri, A. et al., 1997 and Artioli, G. et al., 2002), the Avrami equation provides a good empirical fit of the overall kinetics of crystallization curves. Therefore, in this work, the Avrami model was employed to analyze the formation of zeolite X under various conditions of the synthesis. The kinetic parameters ( $k$ ,  $n$ ) were determined from equation (3.3) which is obtained by taking double logarithm on both sides of equation (3.1).

$$\ln \ln\left(\frac{1}{1-\alpha}\right) = \ln k + n \ln t \quad (3.3)$$

As mentioned previously, if the left side of equation (3.3),  $\ln \ln [1/(1-\alpha)]$ , is plotted against  $\ln t$ , the value of  $n$  is denoted by the slope of the straight line. The exponent  $n$  value is expected to vary between 1 and 4, depending on the dimensionality of the growth process, and on the kinetic order of nucleation (Henderson, D, W., 1979).

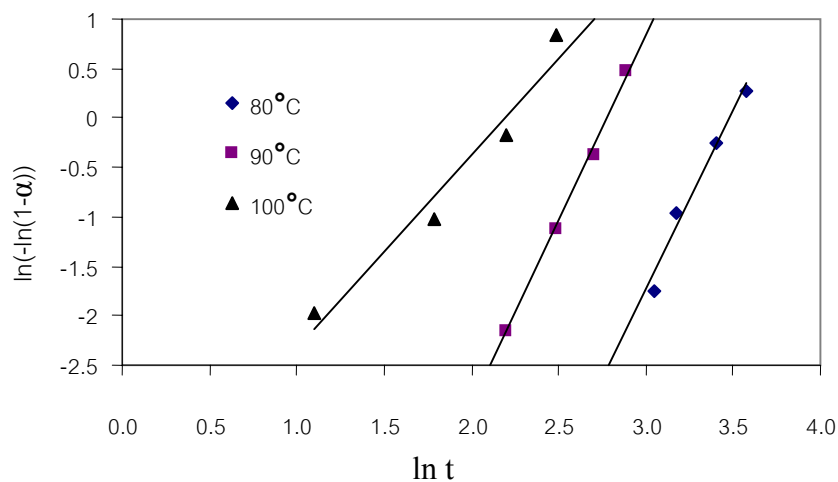


**Figure 3.14** The plots of  $\ln(-\ln(1-\alpha))$  versus  $\ln t$  from XRD results under the experimental condition of the metakaolin activated at  $900^{\circ}\text{C}$ , 7.5% NaOH, 10%  $\text{Na}_2\text{SiO}_3$ , aged 3 days, and at different reaction temperatures ( $80^{\circ}\text{C}$ ,  $90^{\circ}\text{C}$  and  $100^{\circ}\text{C}$ ).

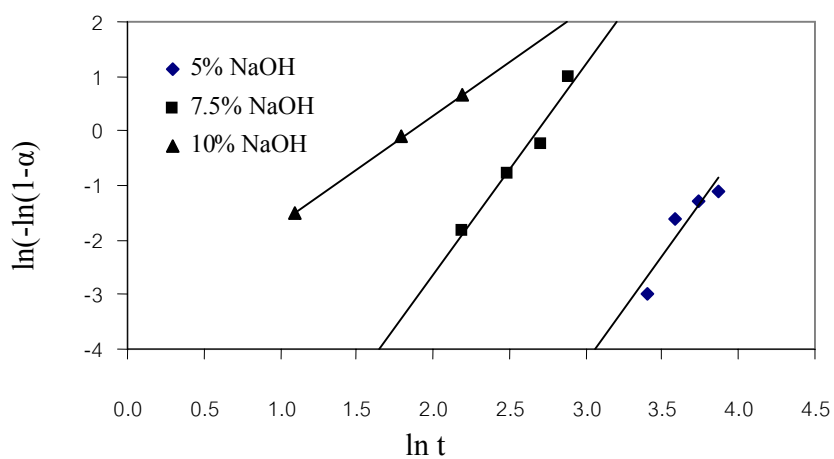


**Figure 3.15** The plots of  $\ln(-\ln(1-\alpha))$  versus  $\ln t$  from XRD results under the experimental conditions of the metakaolin activated at  $900^{\circ}\text{C}$ , 10%  $\text{Na}_2\text{SiO}_3$ , aged 3 days, reaction temperature  $90^{\circ}\text{C}$  and with various NaOH concentrations (5%, 7.5%, 10%).

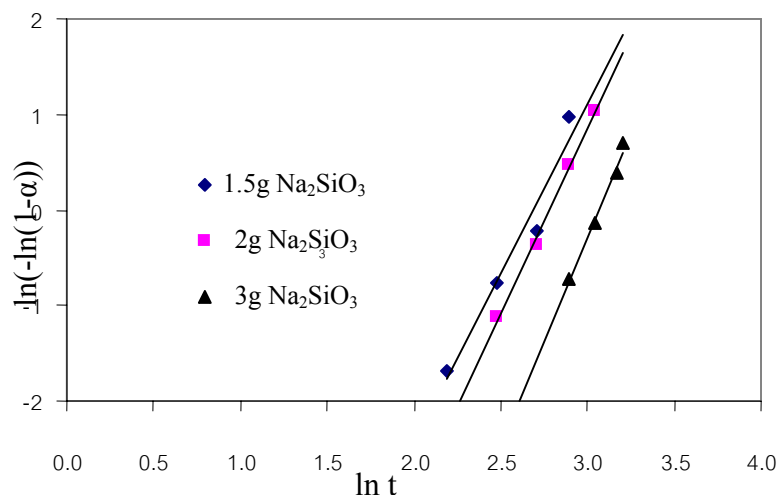


**Figure 3.16** The plots of  $\ln(-\ln(1-\alpha))$  versus  $\ln t$  from XRD results with the experimental conditions of the metakaolin activated at  $900^{\circ}\text{C}$ , 7.5% NaOH, aged 3 days, reaction temperature  $90^{\circ}\text{C}$ , and with various  $\text{Na}_2\text{SiO}_3$  concentrations (7.5%, 10%, 15%).

The plots of  $\ln \ln [1/(1-\alpha)]$  against  $\ln t$  under various experimental conditions were displayed in Figures 3.14-3.16. From the plots, most of the data points tended to follow the Avrami model at the beginning of the plot. Some deviations were seen late in the reaction with the lower slope value or indicated lower  $n$  value. This deviation implied that there were more than one mechanism of the crystal formation. The results of Avrami exponent ( $n$ ) for the series of crystallization under varying conditions were given in Table 3.2. It was found that the  $n$  values vary from 2 to about 4 with the decrease in temperature from  $100^{\circ}\text{C}$  to  $80^{\circ}\text{C}$  and with the decrease in alkaline concentration from 10%w/v to 5%w/v. The values of  $n$  are rarely dependent

on sodium silicate concentration. Within the experimental error, these values are approximately 4.

The same trend of the  $n$  value depending on the temperature and alkaline concentration was also observed in the synthesis of zeolite NaA (Barrer, R. M., 1982). Based on the Avrami model, the observed values of  $n$  varying with the synthesis conditions may be interpreted as follows. At a higher reaction temperature (100°C), or at a higher alkaline concentration in reaction with the value of  $n = 2$ , the nuclei of zeolite X can appear instantaneously; that means the time dependence of nucleation is zero order and the growth proceeds in two dimensions. When the temperature or NaOH concentration decreases, the  $n$  value increases to about 4. This indicates that three dimensional growth is combined with the first order nucleation. With the value of  $n$  between 3 and 4, three dimensional and two dimensional growth combined with the first order nucleation simultaneously occurred; otherwise, the zero order and the first order of nucleation combined with three dimensional growth are working simultaneously during the crystallization. The Avrami's equation essentially describes the solid state reaction. However, the Avrami's equation is not always able to describe the rate process for several reasons such as solution mediated processes (Gualtieri, A. et al., 1997).

**Table 3.2** The analytical results of the Avrami's exponents for the crystallization of zeolite X from Narathiwat kaolin activated at 900°C with various conditions.

	Temperature (°C)			NaOH concentration(w/v)			Na <sub>2</sub> SiO <sub>3</sub> concentration(w/v)		
	80	90	100	5%	7.5%	10%	7.5%	10%	15%
n	3.6	3.7	2	3.9	3.85	2	3.6	3.9	4.4
R	0.985	0.998	0.977	0.93	0.98	0.99	0.977	0.996	0.99

### 3.4.2 Determination of activation energies of nucleation and crystallization of zeolite X

The activation energies of nucleation and crystallization from the thermodynamic point of view can be used to determine the minimum energy needed for the crystallization. The activation energy could vary depending on the process and mechanism.

The relationship between the crystallization time and the temperature for the formation of zeolite X from aluminosilicate gel, gave the activation energy of crystallization 15 kcal/mol (Breck, W. M., and Flanigen, E. M., 1968). Guatieri, A. et al. (1997) synthesized zeolite Na-A from natural kaolinite activated at 800°C at temperatures between 70-110°C and obtained the activation energy of crystallization 8.7 kcal/mol. Kacirek, H., and Lechert, H. (1976) reported the activation energies of formation of zeolite X with various ratios of Si/Al as given in Table 3.3.

It has been shown that the  $k$  in equation (3.1) is related to activation energy ( $E_a$ ) by Arrhenius equation in equation (3.2). To determine  $E_a$ , the rate constant is utilized in Arrhenius equation. Taking the logarithms on equation (3.2) gives

$$\ln k = -\frac{E_a}{RT} + \ln A \quad (3.4)$$

where  $k = d\alpha/dt$  is the rate constant obtained from the hydrothermal operating at 80°C-100°C. The value of  $k$  was obtained from the slope of the plot between  $\alpha$  (in the range of 0.1-0.85) and crystallization time shown in Figure 3.17. Then the plot of  $\ln k$  versus  $1/T$  was performed to calculate the apparent activation energy of the process. This linear plot was displayed in Figure 3.15 and the values of activation energies were given in Table 3.3.

In Table 3.3, the activation energy of nucleation of zeolite X in this work has also been reported. The value of activation energy of nucleation can be calculated in a similar manner to the activation energy of crystallization. The measured induction periods ( $t_0$ ) for each experiment at various temperatures (80°C, 90°C and 100°C) were employed in an Arrhenius' equation. The plot of  $\ln(t_0)$  versus  $1/T$  was shown in Figure 3.19. The value of the activation energy of the nucleation process ( $E_n$ ) was calculated from the slope of this plot. This method was successfully applied by Joshi et al. (1990) in the kinetic analysis of the formation of zeolite LTL. The result in Table 3.3 indicates that the value of activation energy of crystallization of zeolite X from Narathiwat metakaolin is in good agreement with most of the reports in literature. This implies that the crystal growth has been controlled by a chemical process, because  $E_a$  is quite too large to be controlled by diffusion. The obtained value of  $E_n$  is approximately 3 times as much as the value of activation energy of crystallization. This means that the process of building nuclei of zeolite X takes a lot of time before going to the growth process.

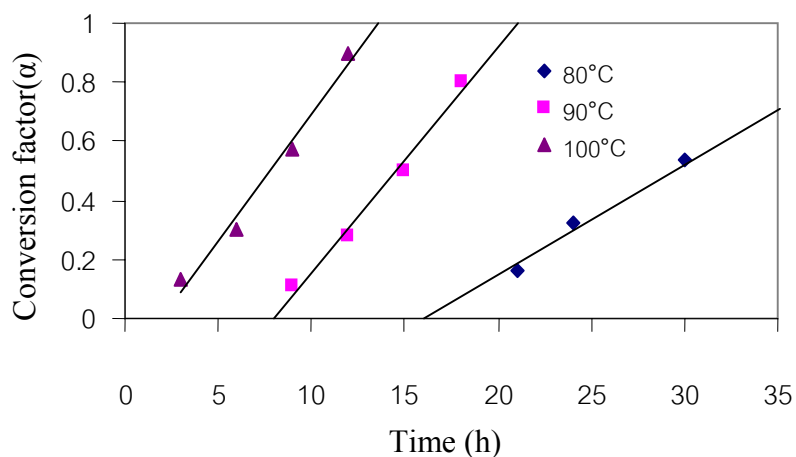


**Figure 3.17** Plots of conversion factors,  $\alpha$ , against time for the thermal experiments obtained from Narathiwat kaolin activated at 900°C with 10%  $\text{Na}_2\text{SiO}_3$ , 7.5% NaOH, aged 3 days at reaction temperatures 80°C, 90°C and 100°C.

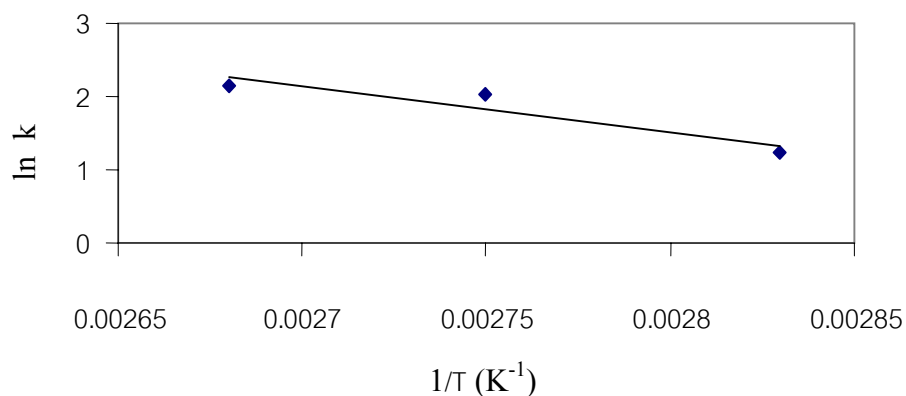


**Figure 3.18** The plots of  $\ln k$  versus  $1/T$  obtained from the synthesis of zeolite X from Narathiwat kaolin activated at 900°C with 10%  $\text{Na}_2\text{SiO}_3$ , 7.5% NaOH, aged 3 days and at reaction temperatures 80°C, 90°C, 100°C.

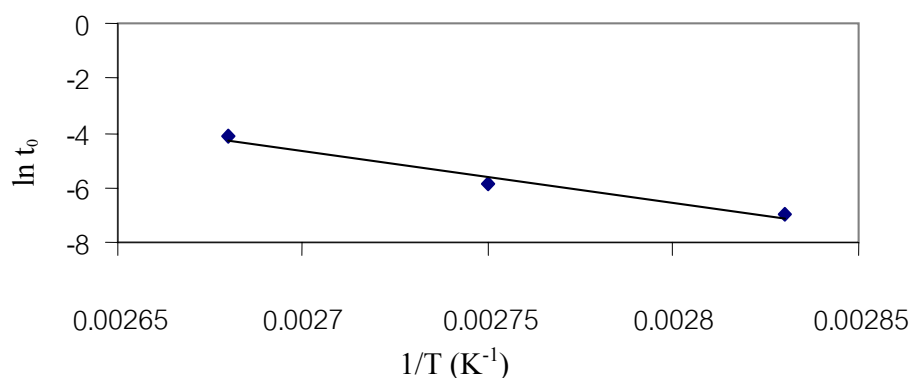


**Figure 3.19** The plots of  $\ln t_0$  versus  $1/T$  obtained from the synthesis of zeolite X from Narathiwat kaolin activated at  $900^\circ\text{C}$  with 10%  $\text{Na}_2\text{SiO}_3$ , 7.5%  $\text{NaOH}$ , aged 3 days and at reaction temperatures  $80^\circ\text{C}$ ,  $90^\circ\text{C}$ ,  $100^\circ\text{C}$ .

**Table 3.3** Results of apparent activation energies of crystallization and nucleation.

	Precursor	Si/Al	$E_a$ (kcal/mol)
Kacirek, H., and Lechert, H., (1976)	Gel	1.53	11.8
		1.78	12.3
		2.20	14.1
		2.54	15.6
Breck, W. M. Flanigen, E. M., (1968)	Gel	Na-X	15
Guatieri, A. et al., (1997)	metakaolin	Na-A	8.7
This work	metakaolin	Na-X	$E_a = 12.5$ $E_n = 38$

### 3.4.3 Determination of the reaction order with respect to NaOH and Na<sub>2</sub>SiO<sub>3</sub> concentrations

This section concerns with the preliminary kinetic study of the influences of alkaline and silicate concentration on the rate of zeolite X formation. The resulting values of the reaction orders may provide some kinetic information for anyone interested in mechanism of zeolite crystallization depending on the concentration of alkali. The order of reaction regarding to NaOH and Na<sub>2</sub>SiO<sub>3</sub> was related to rate equations as in equations (3.5) and (3.6)

$$Rn = \frac{1}{t_0} = k' [NaOH]^x \quad (3.5)$$

$$Rc = \frac{d\alpha}{dt} = k'' [NaOH]^y \quad (3.6)$$

where  $Rn$  is the nucleation rate taken as the reciprocal of the time which crystals start to take shape;  $Rc$  is the rate of crystallization taken as the slope on the crystallization curve ( $\alpha$  range within 0.1-0.85).  $k'$  and  $k''$  are rate constants including the constant concentration of aluminates and silicate;  $x$  and  $y$  are reaction order with respect to NaOH for nucleation and crystallization, respectively. The linear plots of  $\log Rn$  or  $\log Rc$  versus  $\log[NaOH]$  or  $\log[Na_2SiO_3]$  are shown in Figures 3.20 to 3.23. The values of  $x$  and  $y$  were deduced from the slopes of these plots. The same method was also employed to calculate the reaction order of nucleation and crystallization with respect to the added Na<sub>2</sub>SiO<sub>3</sub> concentration. The obtained  $x$  and  $y$  are about 4.5 and 3 in NaOH and about -1 and -1/2 with Na<sub>2</sub>SiO<sub>3</sub> added. This reveals that the reaction order of both processes which are depending on the concentration of alkali and sodium silicate seems to have the same trend.

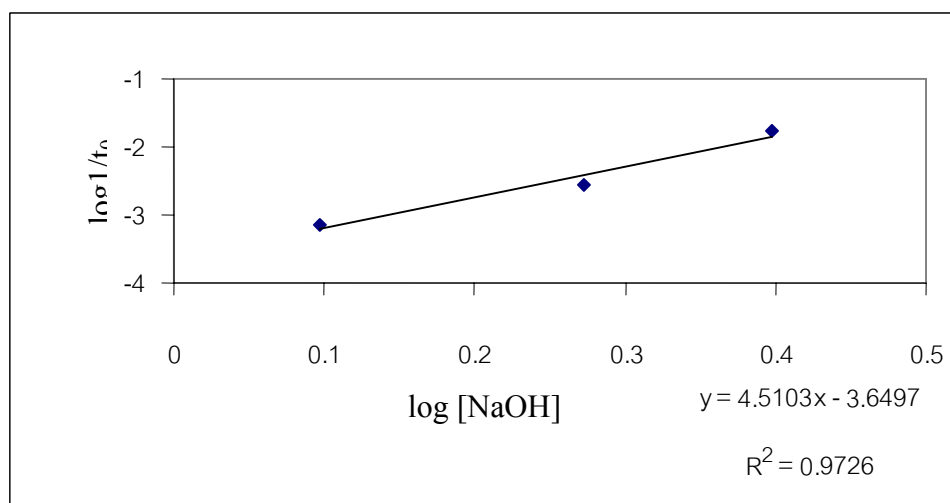


**Figure 3.20** The plots of  $\log(1/t_0)$  against  $\log[\text{NaOH}]$  obtained from various NaOH concentrations of 5%, 7.5% and 10%w/v at reaction temperature 90°C.

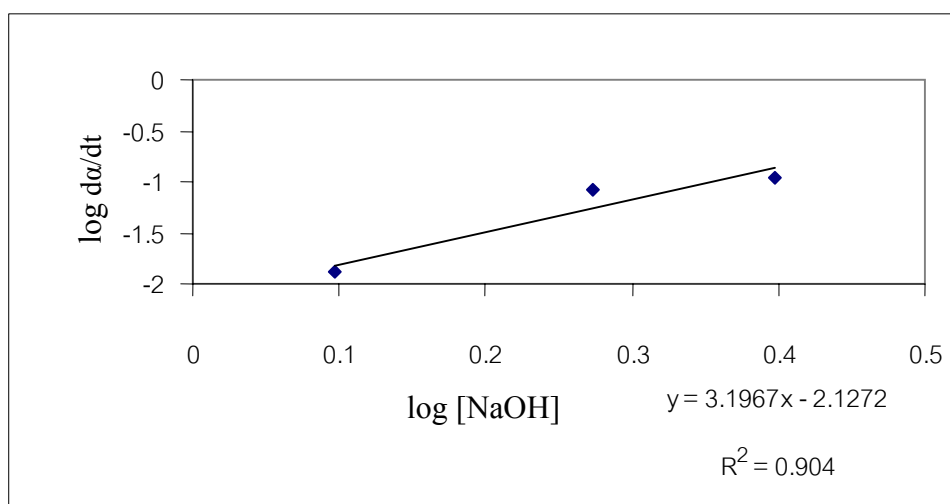


**Figure 3.21** The plots of  $\log(d\alpha/dt)$  against  $\log[\text{NaOH}]$  obtained from the various NaOH concentrations of 5%, 7.5% and 10%w/v at reaction temperature 90°C.

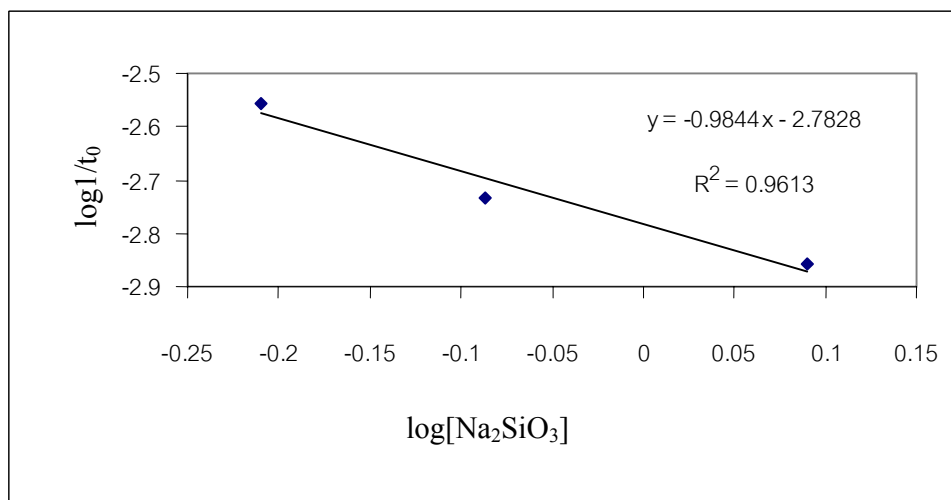


**Figure 3.22** The plots of  $\log (1/t_0)$  against  $\log[\text{Na}_2\text{SiO}_3]$  obtained from the  $\text{Na}_2\text{SiO}_3$  with concentrations of 7.5%, 10% and 15%w/v at reaction temperature  $90^\circ\text{C}$ .

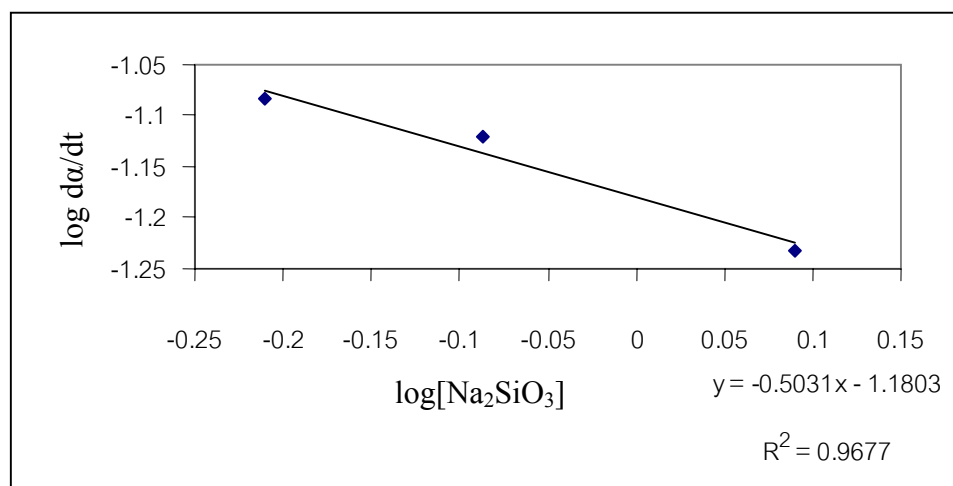


**Figure 3.23** The plots of  $\log (d\alpha/dt)$  against  $\log[\text{Na}_2\text{SiO}_3]$  obtained from the  $\text{Na}_2\text{SiO}_3$  with concentrations of 7.5%, 10% and 15%w/v at reaction temperature  $90^\circ\text{C}$ .

### 3.5 Particle size distributions

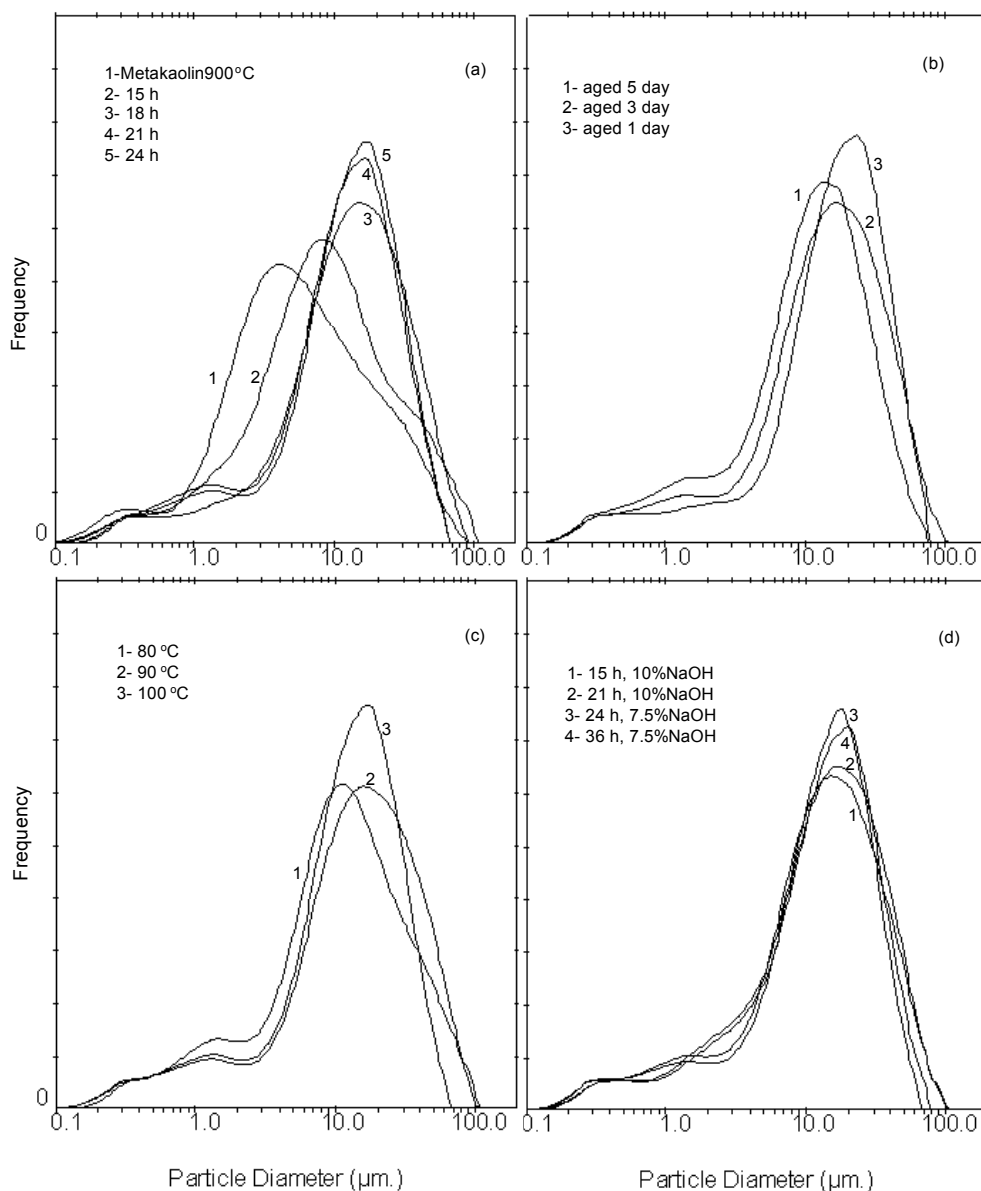
The particle size distributions and the mean particle size of products under various conditions were determined with a laser scattering particle size analyzer. The means particle sizes of all the products from this work vary in a range of 8-17  $\mu\text{m}$ . The effects of some parameters on the particle size, such as the reaction time, ageing time and reaction temperature were analyzed. Many plots which related the particle size distributions and mean particle size with these affecting parameters were shown in Figures 3.24-3.27.

Figure 3.24, as can be seen from the particle size distribution, illustrates that there is a very direct correlation between mode of the particle size distribution and reaction time under the best condition for zeolite X synthesis (Figure 3.24 a), while Figures 3.24 b-d show the particle size distributions of the products with the highest % crystallinity at every condition. In Figure 3.24 a the mean particle size of metakaolin in this experiment is about 5  $\mu\text{m}$ , after the reaction time of 24 h, the mean particle size of the product is up to 12.8  $\mu\text{m}$ . This result is caused by an increase in the amount of crystallinity when the reaction runs longer. The mean particle sizes obtained from the curves in Figure 3.24 were collected in the Table 3.4.

**Table 3.4** The mean particle size at the highest % crystallinity at each condition.

Affecting parameters	Mean particle size ( $\mu\text{m}$ )
Ageing time of reaction at 30°C	
1 day	15.38
3 days	13.38
5 days	11.09
Concentration of NaOH (w/v)	
5%	-
7.5%	14.38
10%	14.02
Reaction temperature	
80°C	10.19
90°C	13.23
100°C	14.30

To find out the other factors, besides the amount of crystallinity which affect the particle size, the plots of the mean particle size and the percentage of crystallinity under various conditions were performed. The results were shown in Figures 3.25-3.27. The slope of such plot was defined as a coefficient. The coefficient value of each conditions were given in Table 3.5. These results indicate that the mean crystal size of zeolite X increases with an increase in the NaOH concentration and the reaction temperature but with a decrease in the ageing time.



**Figure 3.24** Particle size distributions for zeolite X from metakaolin activated at 900°C (a) 7.5% NaOH, 10%w/v  $\text{Na}_2\text{SiO}_3$ , aged 3 days, reaction temperature at 90°C with various times (b) 7.5% NaOH, 7.5%w/v  $\text{Na}_2\text{SiO}_3$ , reaction temperature at 90°C with various ageing times (c) 7.5% NaOH, 10%w/v  $\text{Na}_2\text{SiO}_3$ , aged 3 days with various reaction temperatures (d) 7.5%w/v  $\text{Na}_2\text{SiO}_3$  aged 3days, reaction temperature at 90°C with various NaOH concentrations.

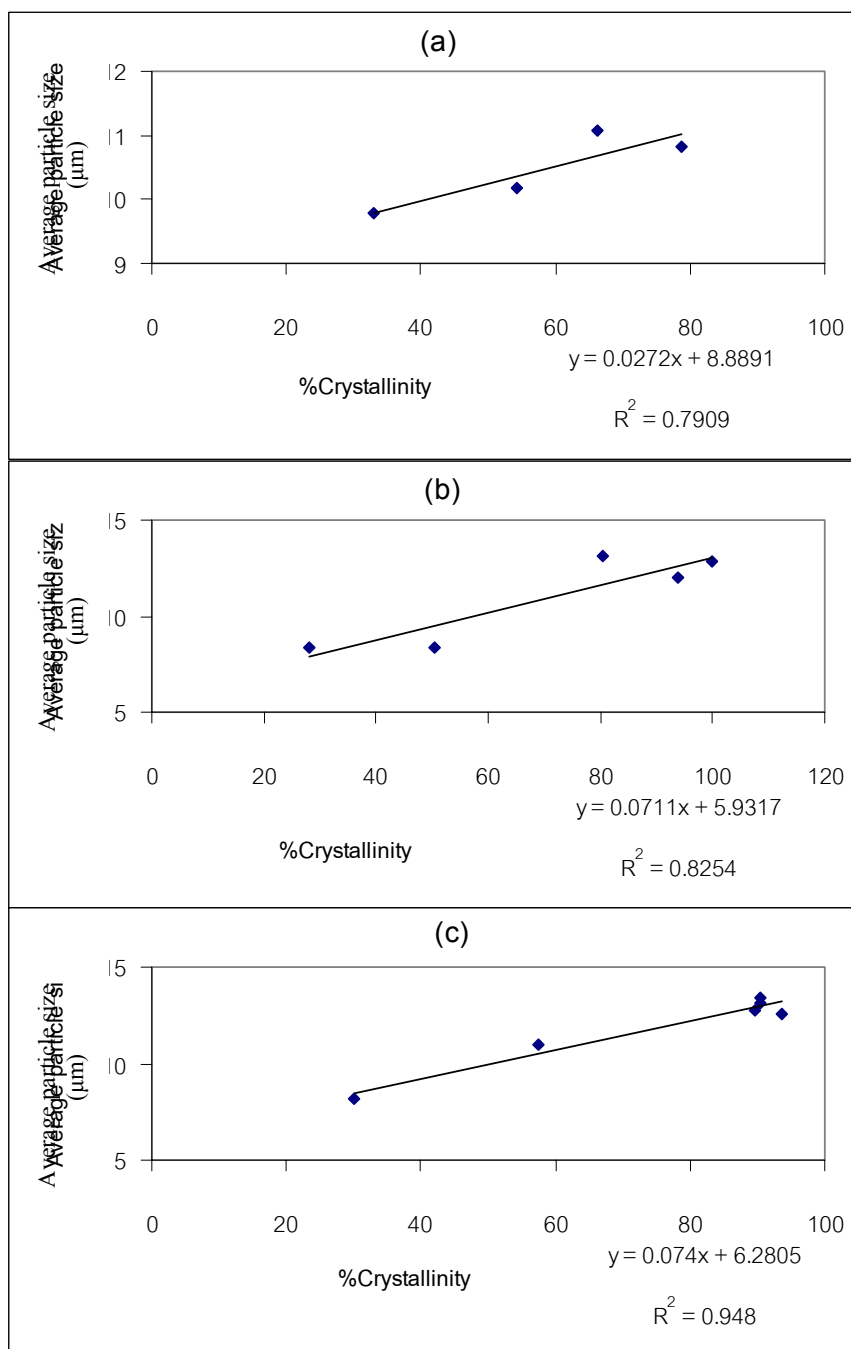


**Figure 3.25** Zeolite X crystal growth with metakaolin activated at 900°C, 7.5% NaOH, 10% Na<sub>2</sub>SiO<sub>3</sub>, aged 3 days at different reaction temperatures on the syntheses (a) 80°C, (b) 90°C, (c) 100°C.

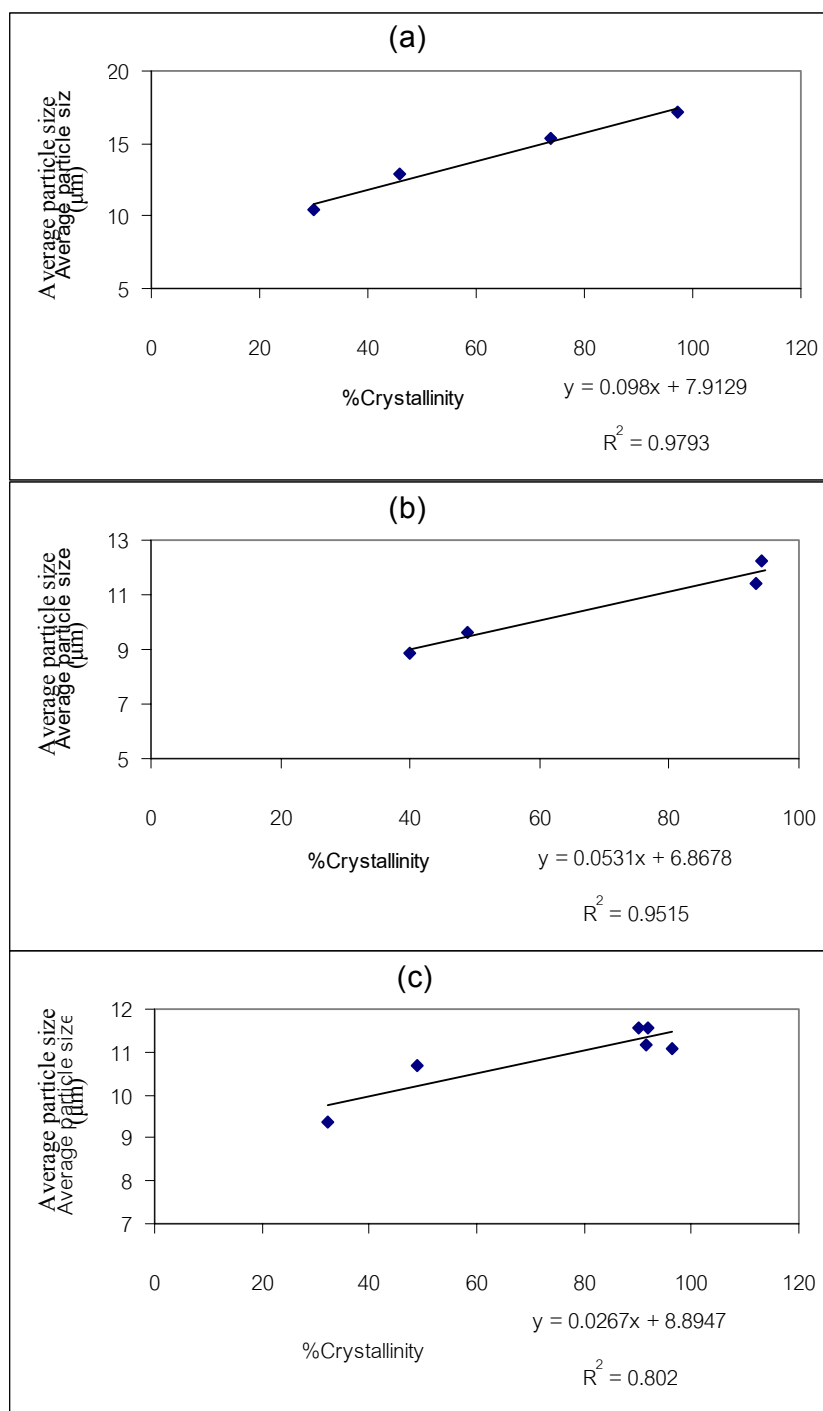


**Figure 3.26** Zeolite X crystal growth with metakaolin activated at 900°C, 7.5% NaOH, 10% Na<sub>2</sub>SiO<sub>3</sub>, reaction temperature 90°C at different ageing times of reaction mixture on the syntheses (a) aged 1 day, (b) aged 3 days, (c) aged 5 days.

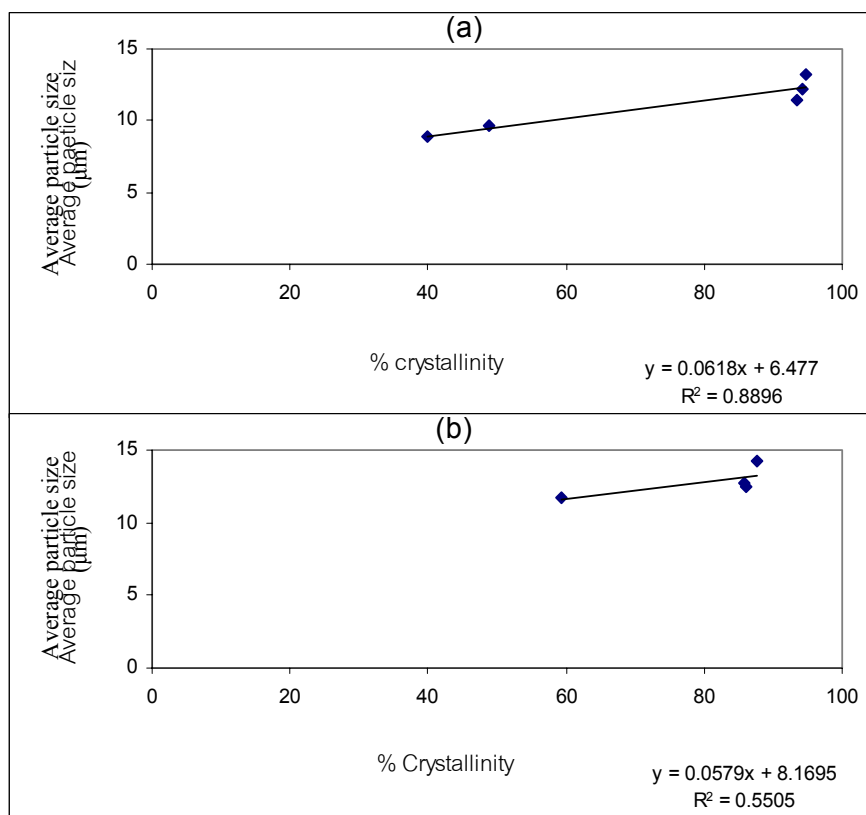


**Figure 3.27** Zeolite X crystal growth with metakaolin activated at  $900^\circ\text{C}$ , 10%  $\text{Na}_2\text{SiO}_3$ , aged 3 days at different NaOH concentrations on the syntheses (a) 7.5% NaOH, (b) 10% NaOH.

**Table 3.5** The particle size distribution coefficients obtained from the slope of the plot between mean particle size and % crystallinity depending on various parameters in experiment.

	Ageing time			Reaction temperature			Alkaline concentration	
	1 day	3 days	5 days	$80^\circ\text{C}$	$90^\circ\text{C}$	$100^\circ\text{C}$	7.5%NaOH	10%NaOH
Slope	0.098	0.053	0.027	0.027	0.071	0.074	0.062	0.058

### 3.6 Chemical composition diagram

Zeolite synthesis behavior is complicated by a delicate interplay of composition, temperature and time factors. Several different zeolite phases can be crystallized from  $\text{Na}_2\text{O-SiO}_2\text{-Al}_2\text{O}_3\text{-H}_2\text{O}$  system in a batch reactor and it is wellknown that the crystallized products are sensitively dependent on the total batch composition and other initial and boundary conditions of the reaction system (Breck, 1974., and Barrer., 1982). The effect of the total batch composition on the nature of zeolite products is usually presented in the form of a crystallization diagram. These diagrams show welldefined distinct regions in the composition space where different zeolite products appear under the specified reaction condition (Šefčík, J., and McCormick, A. V., 1999).

An attempt of this part is only to show the appearance region of pure zeolite phase synthesized from the starting material like Narathiwat kaolin, as a plot of a triangular phase diagram. The chemical compositions ( $\text{Na}_2\text{O-SiO}_2\text{-Al}_2\text{O}_3$ ) of reaction mixtures with various degrees of NaOH and  $\text{Na}_2\text{SiO}_3$  contents were calculated as mole fraction. The result is shown in Figure 3.28 with the data for zeolite X and sodalite obtained from this study and zeolite A from Janjira's work (2002). It indicates that the composition ranges for zeolite X is shorter than zeolite A and these composition ranges can be used to synthesize zeolite X or zeolite A for the  $\text{Na}_2\text{O-SiO}_2\text{-Al}_2\text{O}_3\text{-H}_2\text{O}$  system. When the reaction mixture contains  $\text{Al}_2\text{O}_3$  with a mole fraction less than 0.08 and  $\text{Na}_2\text{O}$  not more than 0.70, a pure phase of zeolite X should be obtained. In addition, at very high alkaline concentration ( $\text{Na}_2\text{O}>0.7$ ) the product will be sodalite for all the ratios of Si/Al.

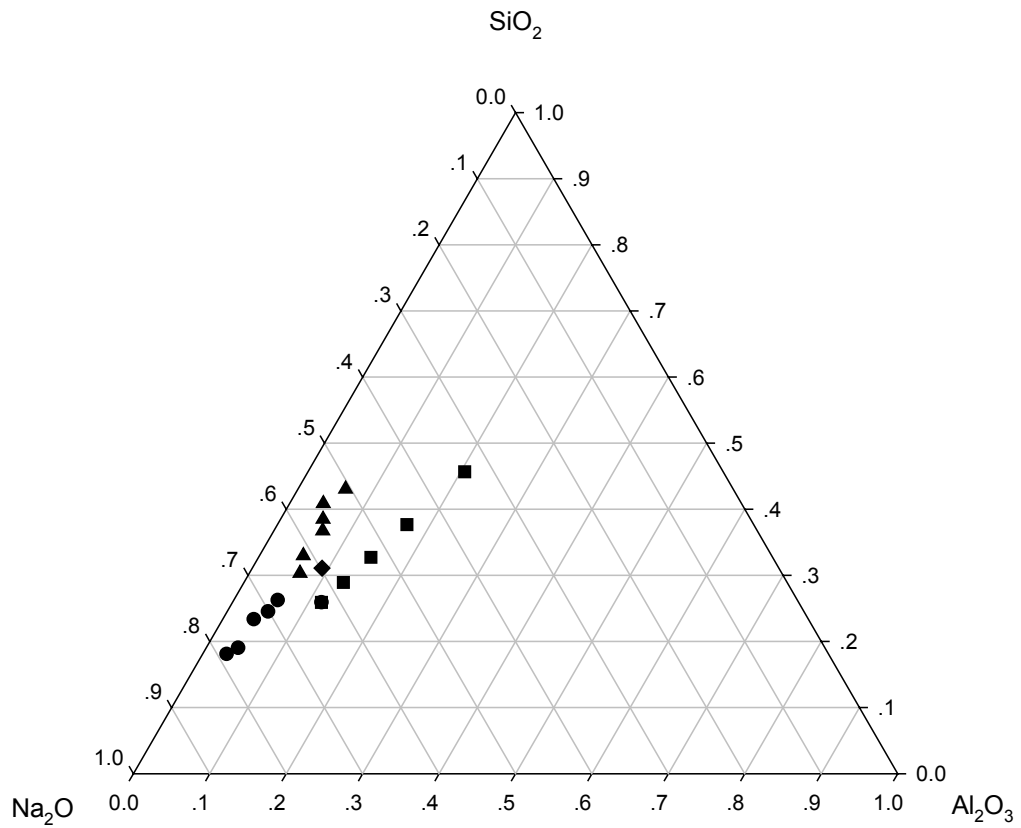


**Figure 3.28** Ternary chemical composition diagram  $\text{SiO}_2\text{-Al}_2\text{O}_3\text{-Na}_2\text{O}$  defining specific crystallization domains from Narathiwat kaolin activated at  $900^\circ\text{C}$  and the reaction temperature  $90^\circ\text{C}$ . ( $\blacktriangle$ ) zeolite X, ( $\blacksquare$ ) zeolite NaA, ( $\bullet$ ) sodalite, ( $\blacklozenge$ ) zeolite X+A.

## **Chapter IV**

### **Conclusion**

The results obtained in this study can be summarized as follows.

The Narathiwat kaolin under investigation is found to be an excellent material for the synthesis of zeolite X because of its high content of kaolinite mineral. The hydrothermal transformation of metakaolin into zeolite X depends on the metakaolinization temperature, the quantity of added silica, NaOH concentration, the reaction temperature and the ageing time for zeolitisation. The optimum condition to get the pure phase zeolite X with good crystallinity has been found to be metakaolinisation of the clay at 900°C for 1 h, 10%w/v sodium silicate, 7.5%w/v NaOH, an ageing of reactants for 3 days at 30°C and heating at  $90\pm 2^\circ\text{C}$  for 24 h under an autogeneous pressure. When only metakaolin (without addition of silica) was used in the reaction, the solid phase product was only zeolite A. While the synthesis of zeolite X at 100°C also produced the phase of zeolite P<sub>1</sub>.

The influence of the studied parameters on the particle size distributions hints that the mean particle size gradually increases with the increasing reaction temperature and the increasing in degree of crystallinity. However, it seems gradually to decrease with an increase in ageing time and an increase in the alkaline concentration.

The order of zeolite X crystallization process and nucleation with respect to concentration of alkali and silicate were found to be 3 and 4.5 in NaOH, -1/2 and -1

in  $\text{Na}_2\text{SiO}_3$  respectively. This implies that the higher alkaline concentration is, the higher rate of transformation will be observed. On the other hand, the rate of zeolite X formation decreases with an increase in the concentration of  $\text{Na}_2\text{SiO}_3$ .

The apparent activation energy is found to be 12.5 kcal/mol for zeolite X crystallization process and 38 kcal/mol for nucleation. This indicates that the energy barrier of the building zeolite X nuclei process is very high when compared with the growth process.

The transformation kinetics can be fitted on an Avrami's equation with a time exponent about 4 for the reaction temperatures 80-90°C and 2 for 100°C. It means that the three dimensional growth is combined with the first order nucleation at the reaction temperature 80°C or 90°C, while at 100°C the nucleation is zero order when combined with growth process in two dimensions.

# References

## References

- Breck, D. W., and Flanigen, E. M. (1968). *Molecular Sieves*. Chemical Industry. London. P. 47.
- Breck, D.W. (1974). **Zeolite Molecular Sieve: Structure Chemistry and Use**, John Wiley and Sons. New York.
- Barrer, R. M. (1978) **Zeolite and Clay Mineral, Sorbents and Molecular Sieves**. London: Academic Press.
- Barrer, R. M. (1982). *Hydrothermal Chemistry of Zeolites*. Academic Press, London.
- Bekkum, V.H., Jansen, J. C., and Flanigen, E. M.(1991). *Zeolites and Molecular Sieves: an Historical Perspective*. **Introduction to Zeolite Science and Practice**. 58: 13-33.
- Bougeard, D., Geidel, E., and Smirnov, K. S. (2000). Vibrational spectra and structure of kaolinite: A computer simulation study. **International zeolite Association. Elsevier. B.** 104: 9210-9217.
- Chandrasekhar, S., and Lovat, V, C., (1993). Hydrothermal reaction of kaolinite in presence of fluoride ions at pH< 10. **J. Zeolites**. 13: 534-541.
- Chandrasekhar, S., and Pramada, P. N. (1999). Investigation on the synthesis of zeolite Na-X from Kerala kaolin. **J. of Porous Mater.** 6: 283-297.
- Deng, Y., White, G. N., and Dixon, J. B.,(2002). Effect of structural stress on the intercalation rate of kaolinite. **J. Colloid and Interface Science**. 250: 379-393.
- Deepak, A., and Alan, C. (1997). The transformation of kaolin to low- silica X zeolite. **J. zeolites**. 19: 359-365.

- Demortier, A., Gobeltz, J. P., and Duhayon, C. (1999). Infrared evidence for the formation of an intermediate compound during the synthesis of zeolite Na-A from metakaolin. **J. Inorganic Materials**. 1: 129-134.
- Flanigen, E. M., Khatami, H., and Szymanski, H. A. (1971). Infrared structural studies of zeolite frameworks. **Molecular Sieve Zeolites**. 101:201-228.
- Freund, E. F. (1976). Mechanism of the crystallization of zeolite X. **J. Crystal Growth**. 34:11-23.
- Grim, R. E. (1968). **Clay Mineralogy, Structure of Clay Mineral**. New York: Mcgraw-Hill. 57-66.
- Gualtieri, A., Norby, P., and Hanson, J. (1997). Kinetics of formation of zeolite NaA from natural kaolinite. **J. Phys Chem Minerals**. 24: 191-199.
- Grizzetti, R., and Artioli, G. (2002). Kinetics of nucleation and growth of zeolite LTA from clear solution by in situ and ex situ XRPD. **Microporous Materials**. 54: 105-112.
- Howell, P. H., and Acara, N. A. (1964). US. Patent 3, 119, 660.
- Janjira, W. (2002). **Synthesis and Kinetic Study of Zeolite NaA from Thai Kaolin**. M. S. thesis, Suranaree University of Technology.
- Kacirek, H., and Lechert, H. (1976). Rate of crystallization and a model for the growth of zeolite Na-Y zeolite. **J. Phys Chem**. 80: 1291-1296.
- Kuhl, G. H. (1971). **Molecular Sieve Zeolites I**. J. Adv. Chem. Series.101 (American Chemical Society. Washington D.C). p. 63.
- Meier, W. M., and Olson, D. H. (1996). **Atlas of Zeolite Structure Types**. International zeolite Association. Elsevier. 130-189.

- Rocha, J., and Klinowski, J. (1990). Solid state NMR studies of the structure and reactivity of metakaolinite . **Angew. Chem. Int. Ed. Engl.** 29: 553-554.
- Rocha, J., Adams., J. M., and Klinowski, J.(1990). The rehydration of metakaolinite to kaolinite: **J. Solid State chem.** 89: 260-274.
- Schoeman, B.J., and Regev, O. (1996). Zeolites. 17: 447.
- Šefčík, J., and McCormick, A. V. (1999). Prediction of crystallization diagrams for synthesis of zeolites. **J. Chemical Engineering Science.** 54: 3513-3519.
- Takahashi, H., and nishimura., (1970). Rep. Int. Ind. Ser.,Univ. Tokyo. 20: 85-117.
- Thomson, R. W., and Dyer, A. (1985). Mathematical analyses of zeolite crystallization. **J. Zeolite.** 5: 202-210.
- Velde, B. (1992). **Introduction to clay minerals. Chemistry, origin, uses and environmental significance.** Chapman and Hall, London.
- Zhu, L., and Seff, K. (1999). Reinvestigation of the crystal structure of dehydrated sodium zeolite X. **J. Phys. Chem. B.**103:9512-9518.
- Zhu, L., and Seff, K. (2000). Cation crowding in zeolite. Reinvestigation of the crystal structure of dehydrated potassium-exchanged zeolite X. **J. Phys. Chem. B.**104: 8946-8951.
- Zhen, S., and Seff, K. (2000). Crystallographic study of the reaction of zinc vapor with fully Cd<sup>2+</sup>-exchanged zeolite X. **J. Phys. Chem.** 104: 9811-9816.

# **Appendices**

## **Appendix A**

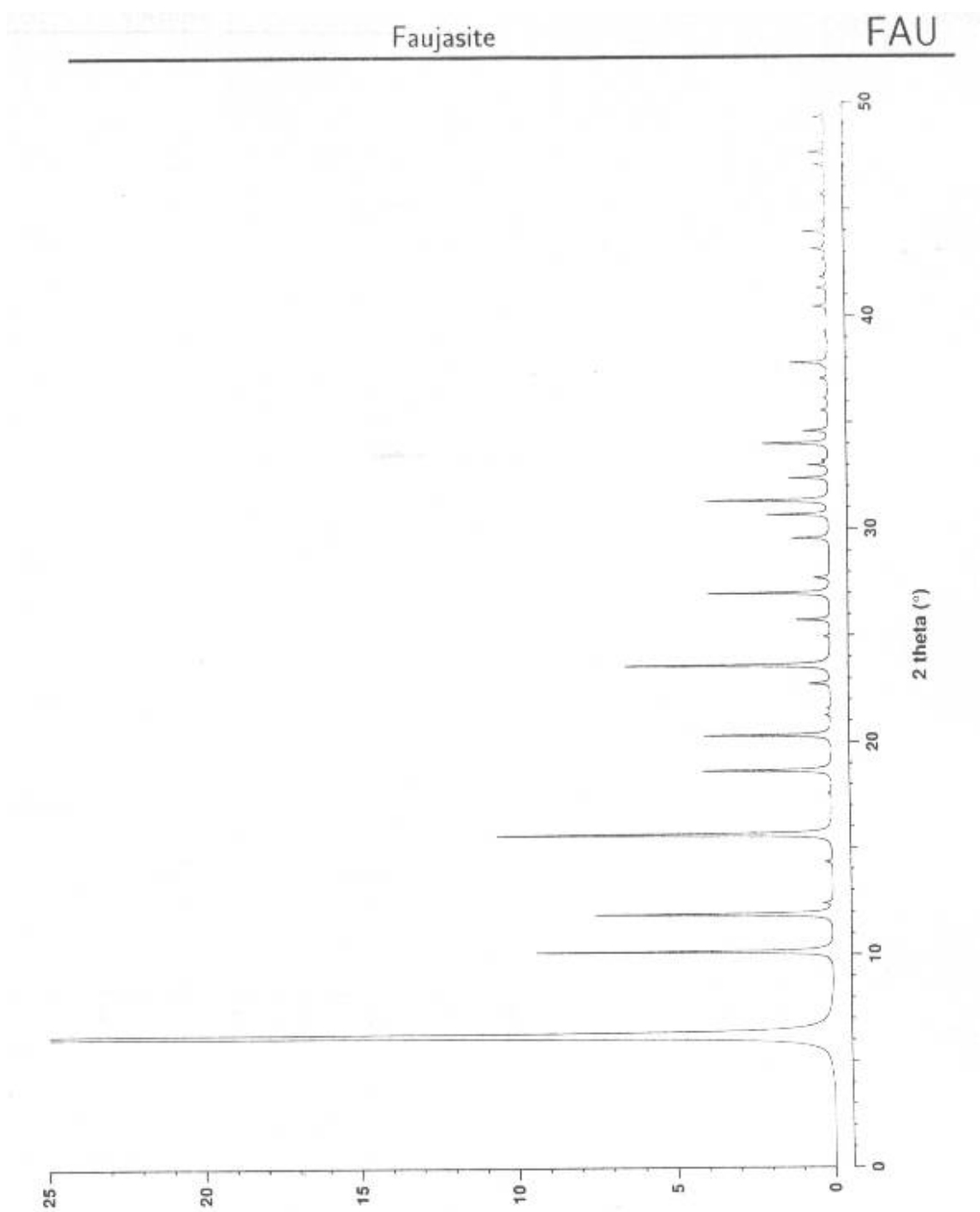
### **Simulated XRD powder patterns for zeolites**

COMPOSITION:  $(\text{Na}_{9.6}\text{Ca}_{4.8})(\text{Si}_{134.4}\text{Al}_{57.6}\text{O}_{384}) \cdot 263\text{H}_2\text{O}$   
Kaiserstuhl, Germany.

CRYSTAL DATA:  $Fd\bar{3}m$  (No. 227) origin at centre ( $\bar{3}m$ )  
 $a = 24.74 \text{ \AA}$      $b = 24.74 \text{ \AA}$      $c = 24.74 \text{ \AA}$   
 $\alpha = 90^\circ$          $\beta = 90^\circ$          $\gamma = 90^\circ$

REFERENCE: W. H. Baur,  
Am. Miner. 49, 697-704 (1964).

<i>h</i>	<i>k</i>	<i>l</i>	$2\theta$	<i>d</i>	<i>M</i>	<i>I</i> <sub>rel</sub>	<i>h</i>	<i>k</i>	<i>l</i>	$2\theta$	<i>d</i>	<i>M</i>	<i>I</i> <sub>rel</sub>	<i>h</i>	<i>k</i>	<i>l</i>	$2\theta$	<i>d</i>	<i>M</i>	<i>I</i> <sub>rel</sub>
1	1	1	6.19	14.284	8	100.0	7	3	3	29.55	3.023	24	1.2	11	1	1	40.43	2.231	24	0.1
2	2	0	10.11	8.747	12	9.4	6	6	0	30.66	2.916	12	1.3	8	8	0	41.28	2.187	12	0.3
3	1	1	11.86	7.459	24	7.5	8	2	2	30.66	2.916	24	0.7	9	7	1	41.79	2.161	48	0.1
2	2	2	12.39	7.142	8	0.3	5	5	5	31.31	2.857	8	3.5	10	6	0	42.62	2.121	24	0.1
4	0	0	14.32	6.185	6	0.2	7	5	1	31.31	2.857	48	0.4	9	7	3	43.11	2.098	48	0.2
3	3	1	15.61	5.676	24	10.7	8	4	0	32.37	2.766	24	1.2	11	3	3	43.11	2.098	24	0.3
4	2	2	17.56	5.050	24	0.1	7	5	3	32.98	2.716	48	0.5	8	8	4	43.92	2.062	24	0.6
5	1	1	18.64	4.761	24	4.1	9	1	1	32.98	2.716	24	0.2	12	0	0	43.92	2.062	6	0.1
4	4	0	20.30	4.373	12	4.1	8	4	2	33.19	2.699	48	0.2	9	7	5	45.65	1.987	48	0.1
5	3	1	21.25	4.182	48	0.2	6	6	4	33.99	2.637	24	2.1	8	8	6	47.04	1.932	24	0.2
6	2	0	22.73	3.912	24	0.7	9	3	1	34.58	2.593	48	0.8	12	4	2	47.04	1.932	48	0.2
5	3	3	23.58	3.773	24	6.5	8	4	4	35.55	2.525	24	0.2	10	8	2	47.64	1.909	48	0.6
4	4	4	24.93	3.571	8	0.2	8	6	2	37.06	2.426	48	0.2	9	7	7	49.28	1.849	24	0.2
5	5	1	25.72	3.464	24	1.1	9	5	1	37.61	2.392	48	0.1	13	3	1	49.28	1.849	48	0.2
6	4	2	26.97	3.306	48	3.9	6	6	6	37.79	2.381	8	1.1							
7	3	1	27.70	3.221	48	0.4	7	7	5	40.43	2.231	24	0.3							



FAU

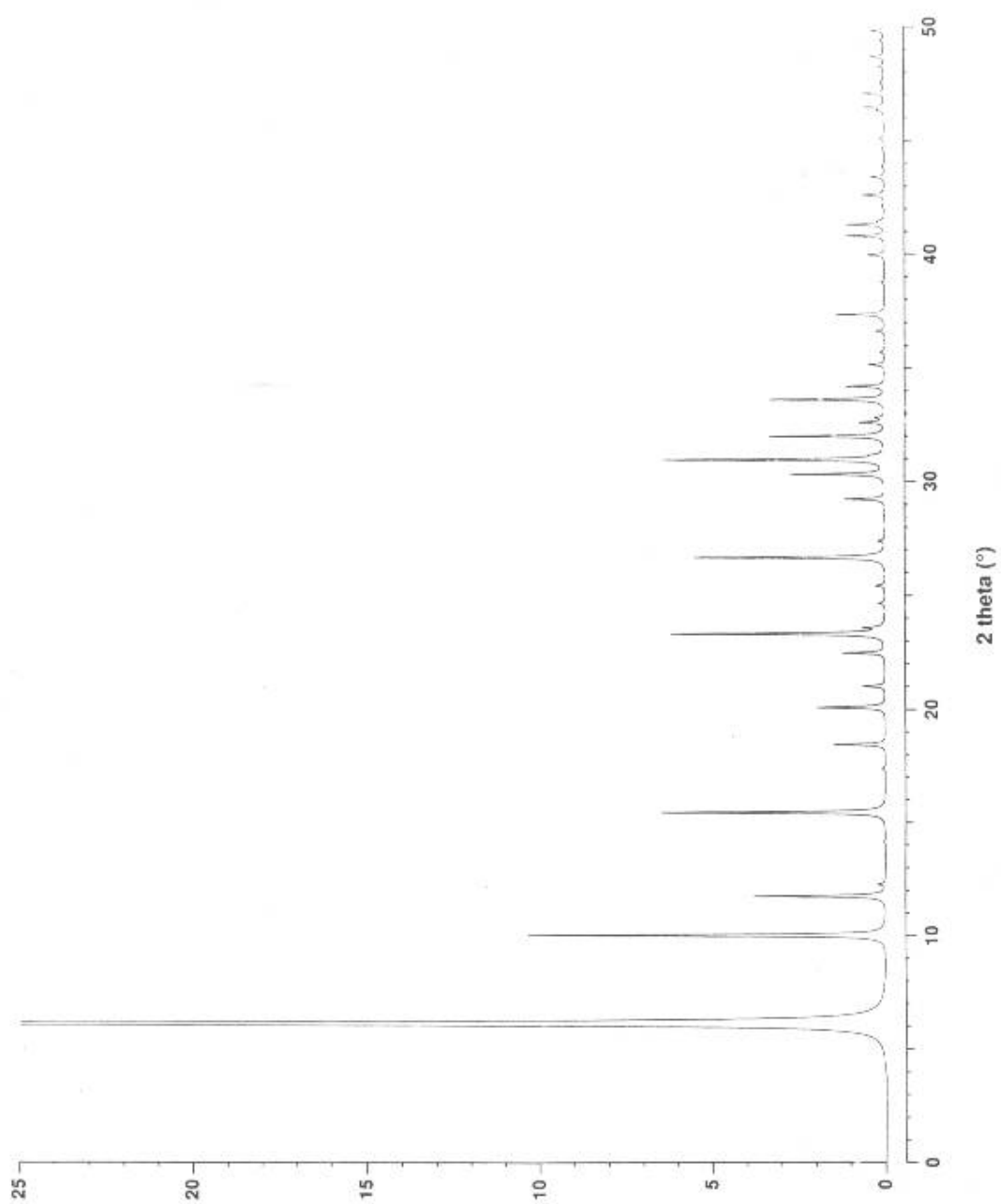
Hydrated Na-X

COMPOSITION:  $\text{Na}_{88}(\text{Si}_{104}\text{Al}_{88}\text{O}_{384}) \cdot 220\text{H}_2\text{O}$ CRYSTAL DATA:  $Fd\bar{3}$  (No. 203) origin at centre ( $\bar{3}$ ) $a = 25.028 \text{ \AA}$     $b = 25.028 \text{ \AA}$     $c = 25.028 \text{ \AA}$  $\alpha = 90^\circ$     $\beta = 90^\circ$     $\gamma = 90^\circ$ REFERENCE: D. H. Olson,  
J. Phys. Chem. 74, 2758-2764 (1970).

<i>h</i>	<i>k</i>	<i>l</i>	$2\theta$	<i>d</i>	<i>M</i>	<i>I</i> <sub>rel</sub>	<i>h</i>	<i>k</i>	<i>l</i>	$2\theta$	<i>d</i>	<i>M</i>	<i>I</i> <sub>rel</sub>	<i>h</i>	<i>k</i>	<i>l</i>	$2\theta$	<i>d</i>	<i>M</i>	<i>I</i> <sub>rel</sub>
1	1	1	6.12	14.450	8	100.0	6	6	0	30.30	2.950	12	1.0	7	7	5	39.95	2.257	24	0.3
2	2	0	10.00	8.849	12	10.4	8	2	2	30.30	2.950	24	1.7	11	1	1	39.95	2.257	24	0.2
3	1	1	11.73	7.546	24	3.8	5	5	5	30.94	2.890	8	5.7	8	8	0	40.79	2.212	12	1.1
2	2	2	12.25	7.225	8	0.2	7	1	5	30.94	2.890	24	0.4	9	1	7	41.29	2.187	24	0.2
3	3	1	15.43	5.742	24	6.5	7	5	1	30.94	2.890	24	0.4	9	5	5	41.29	2.187	24	0.1
4	2	2	17.36	5.109	24	0.1	6	6	2	31.15	2.871	24	0.2	9	7	1	41.29	2.187	24	0.2
3	3	3	18.42	4.817	8	0.3	8	0	4	31.98	2.798	12	1.6	11	1	3	41.29	2.187	24	0.3
5	1	1	18.42	4.817	24	1.3	8	4	0	31.98	2.798	12	1.8	11	3	1	41.29	2.187	24	0.3
4	4	0	20.07	4.424	12	2.0	7	3	5	32.59	2.747	24	0.1	8	8	2	41.45	2.178	24	0.1
5	3	1	21.00	4.231	24	0.6	7	5	3	32.59	2.747	24	0.4	11	3	3	42.59	2.123	24	0.6
6	0	2	22.47	3.957	12	0.2	9	1	1	32.59	2.747	24	0.1	8	8	4	43.38	2.086	24	0.3
6	2	0	22.47	3.957	12	1.1	8	2	4	32.80	2.731	24	0.1	9	9	1	46.31	1.960	24	0.2
5	3	3	23.31	3.817	24	6.2	8	4	2	32.80	2.731	24	0.1	12	2	4	46.46	1.954	24	0.2
6	2	2	23.58	3.773	24	0.5	6	6	4	33.59	2.668	24	3.4	12	4	2	46.46	1.954	24	0.3
4	4	4	24.64	3.612	8	0.2	9	1	3	34.17	2.624	24	0.6	10	2	8	47.06	1.931	24	0.2
5	5	1	25.41	3.505	24	0.2	9	3	1	34.17	2.624	24	0.5	10	8	2	47.06	1.931	24	0.4
6	2	4	26.65	3.345	24	2.4	8	4	4	35.13	2.554	24	0.5	12	4	4	48.24	1.887	24	0.2
6	4	2	26.65	3.345	24	3.2	8	2	6	36.61	2.454	24	0.1	9	7	7	48.67	1.871	24	0.2
7	3	1	27.37	3.258	24	0.1	6	6	6	37.34	2.408	8	1.2	9	9	5	49.82	1.830	24	0.2
7	3	3	29.21	3.058	24	1.2	10	2	2	37.34	2.408	24	0.2	13	3	3	49.82	1.830	24	0.1

Hydrated Na-X

FAU

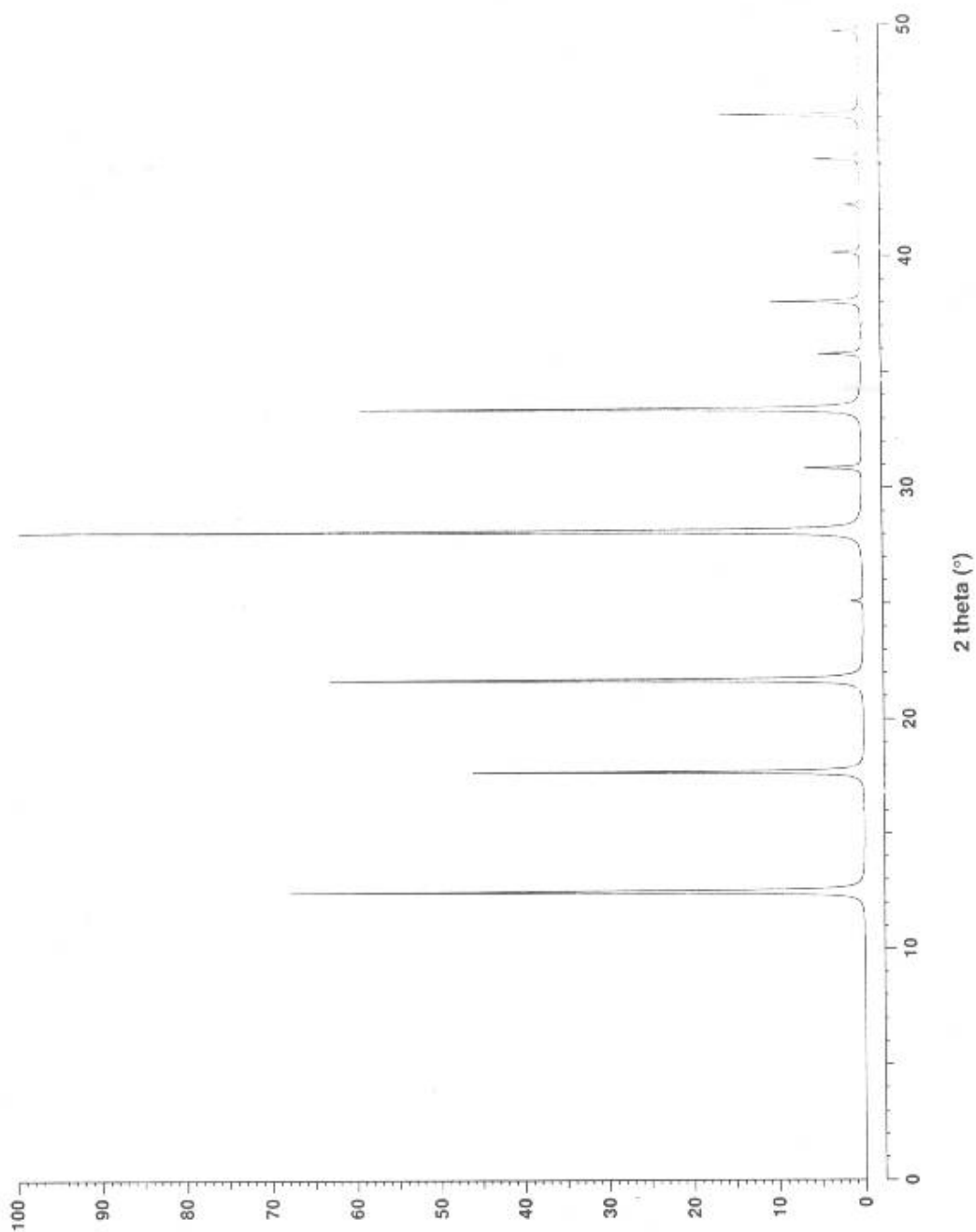


GIS

Na-P1

COMPOSITION:  $\text{Na}_6(\text{Si}_{10}\text{Al}_6\text{O}_{32}) \cdot 12\text{H}_2\text{O}$ CRYSTAL DATA:  $\bar{1}$  (No. 82) $a = 10.043 \text{ \AA}$     $b = 10.043 \text{ \AA}$     $c = 10.043 \text{ \AA}$  $\alpha = 90^\circ$     $\beta = 90^\circ$     $\gamma = 90^\circ$ REFERENCE: Ch. Baerlocher and W. M. Meier,  
Z. Kristallogr. 135, 339-354 (1972).

<i>h</i>	<i>k</i>	<i>l</i>	$2\theta$	<i>d</i>	<i>M</i>	$I_{\text{rel}}$	<i>h</i>	<i>k</i>	<i>l</i>	$2\theta$	<i>d</i>	<i>M</i>	$I_{\text{rel}}$	<i>h</i>	<i>k</i>	<i>l</i>	$2\theta$	<i>d</i>	<i>M</i>	$I_{\text{rel}}$	
1	0	1	12.46	7.101	8	92.1	2	3	1	33.38	2.684	8	11.5	2	4	2	44.18	2.050	8	0.5	
1	1	0	12.46	7.101	4	1.0	3	1	2	33.38	2.684	8	45.0	4	2	2	44.18	2.050	8	6.5	
0	0	2	17.66	5.022	2	2.7	3	2	1	33.38	2.684	8	1.2	1	0	5	46.08	1.970	8	1.6	
2	0	0	17.66	5.022	4	60.6	0	0	4	35.76	2.511	2	6.8	1	3	4	46.08	1.970	8	11.1	
1	1	2	21.67	4.100	8	66.1	1	1	4	38.01	2.367	8	1.0	1	4	3	46.08	1.970	8	0.2	
1	2	1	21.67	4.100	8	7.0	1	4	1	38.01	2.367	8	12.0	3	1	4	46.08	1.970	8	0.1	
2	1	1	21.67	4.100	8	13.3	3	0	3	38.01	2.367	8	0.4	3	4	1	46.08	1.970	8	1.8	
2	0	2	25.08	3.551	8	0.8	3	3	0	38.01	2.367	4	0.3	4	1	3	46.08	1.970	8	2.0	
2	2	0	25.08	3.551	4	1.1	4	1	1	38.01	2.367	8	0.6	4	3	1	46.08	1.970	8	0.9	
1	0	3	28.10	3.176	8	34.9	2	0	4	40.15	2.246	8	0.9	5	0	1	46.08	1.970	8	3.3	
3	0	1	28.10	3.176	8	100.0	4	0	2	40.15	2.246	8	1.4	5	1	0	46.08	1.970	4	2.2	
3	1	0	28.10	3.176	4	1.6	4	2	0	40.15	2.246	4	2.3	1	5	2	49.72	1.834	8	0.3	
2	2	2	30.84	2.899	8	9.0	2	3	3	42.20	2.141	8	0.3	2	1	5	49.72	1.834	8	0.7	
1	2	3	33.38	2.684	8	7.5	3	2	3	42.20	2.141	8	1.0	2	5	1	49.72	1.834	8	0.2	
1	3	2	33.38	2.684	8	12.7	3	3	2	42.20	2.141	8	1.0	5	1	2	49.72	1.834	8	2.9	
2	1	3	33.38	2.684	8	3.5	2	2	4	44.18	2.050	8	0.4								

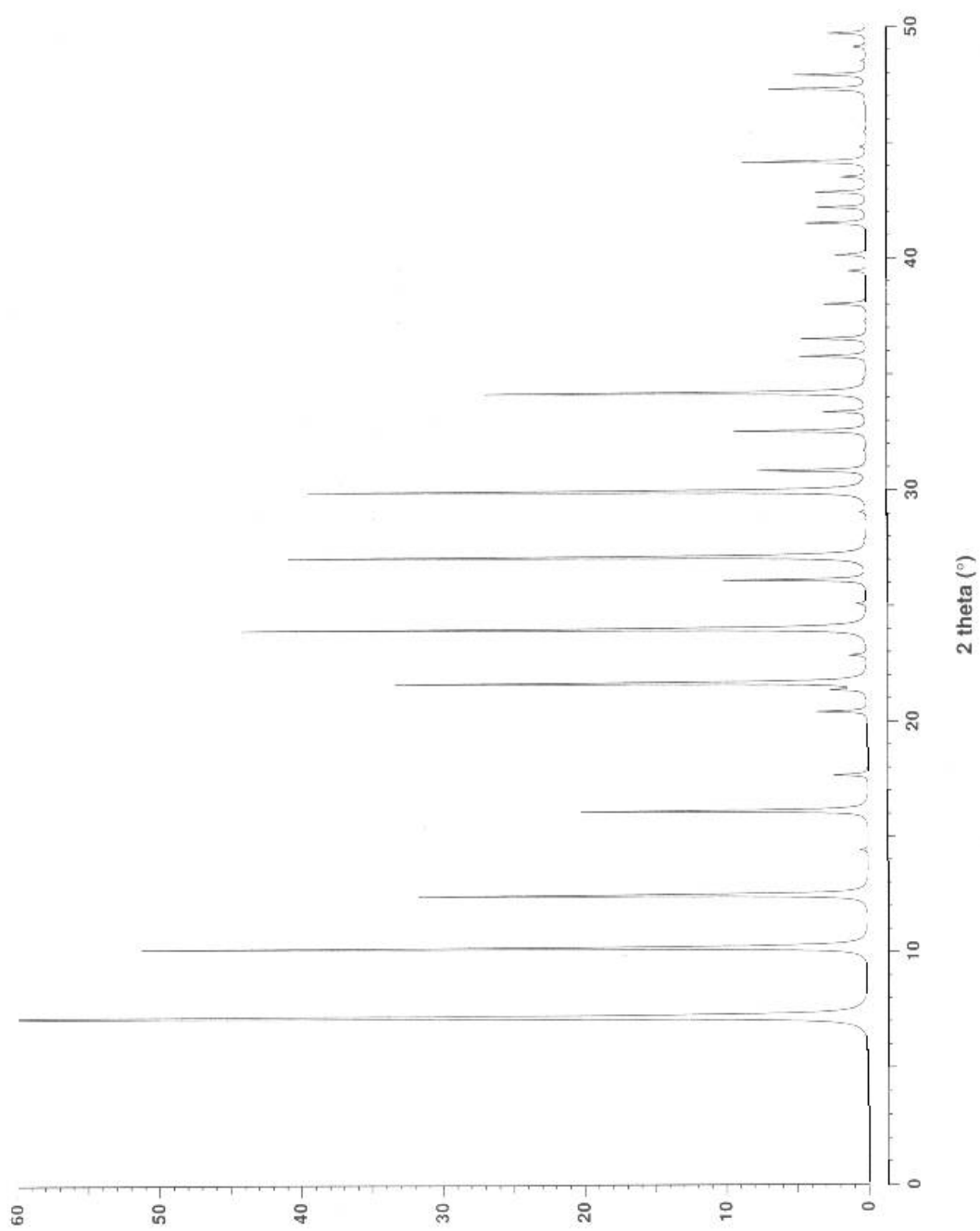


## LTA

## Hydrated Linde Type A

COMPOSITION:  $\text{Na}_{96}(\text{Si}_{96}\text{Al}_{96}\text{O}_{384}) \cdot 216\text{H}_2\text{O}$ CRYSTAL DATA:  $Fm\bar{3}c$  (No. 226) $a = 24.61 \text{ \AA}$      $b = 24.61 \text{ \AA}$      $c = 24.61 \text{ \AA}$  $\alpha = 90^\circ$      $\beta = 90^\circ$      $\gamma = 90^\circ$ REFERENCE: V. Gramlich and W. M. Meier,  
Z. Kristallogr. 133, 134-149 (1971).

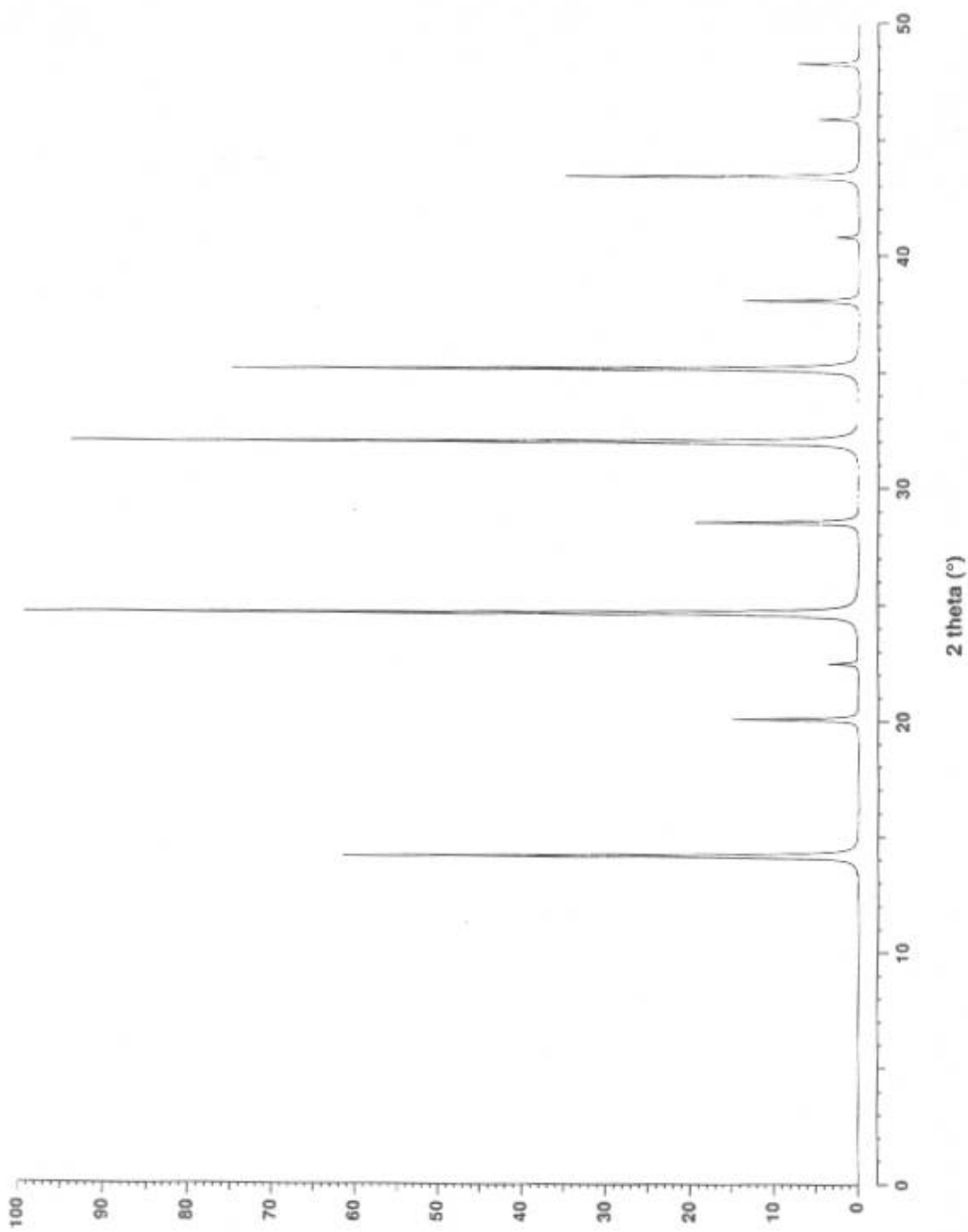
<i>h</i>	<i>k</i>	<i>l</i>	$2\theta$	<i>d</i>	<i>M</i>	<i>I</i> <sub>rel</sub>	<i>h</i>	<i>k</i>	<i>l</i>	$2\theta$	<i>d</i>	<i>M</i>	<i>I</i> <sub>rel</sub>	<i>h</i>	<i>k</i>	<i>l</i>	$2\theta$	<i>d</i>	<i>M</i>	<i>I</i> <sub>rel</sub>
2	0	0	7.18	12.305	6	100.0	6	6	0	30.83	2.900	12	2.3	8	6	6	42.85	2.110	24	2.3
2	2	0	10.17	8.701	12	51.3	8	2	2	30.83	2.900	24	5.4	10	6	0	42.85	2.110	24	1.2
2	2	2	12.46	7.104	8	31.8	6	6	2	31.70	2.823	24	0.2	10	6	2	43.51	2.080	48	1.8
4	0	0	14.40	6.153	6	0.5	8	4	0	32.54	2.752	24	9.3	8	8	4	44.16	2.051	24	0.9
4	2	0	16.11	5.503	24	20.3	8	4	2	33.37	2.685	48	3.0	12	0	0	44.16	2.051	6	7.8
4	2	2	17.65	5.024	24	2.4	6	6	4	34.18	2.623	24	27.1	12	2	0	44.80	2.023	24	0.5
4	4	0	20.41	4.350	12	3.6	9	3	1	34.77	2.580	48	0.1	12	2	2	45.44	1.996	24	0.1
5	3	1	21.36	4.160	48	2.1	8	4	4	35.75	2.512	24	4.7	12	4	0	46.69	1.946	24	0.2
4	4	2	21.67	4.102	24	22.8	8	6	0	36.51	2.461	24	0.4	8	8	6	47.30	1.922	24	4.2
6	0	0	21.67	4.102	6	10.6	10	0	0	36.51	2.461	6	4.1	10	8	0	47.30	1.922	24	2.3
6	2	0	22.85	3.891	24	1.2	10	2	0	37.26	2.413	24	0.1	12	4	2	47.30	1.922	48	0.3
6	2	2	23.99	3.710	24	44.3	6	6	6	38.00	2.368	8	1.4	10	8	2	47.91	1.899	48	5.1
4	4	4	25.07	3.552	8	0.7	10	2	2	38.00	2.368	24	1.6	10	6	6	48.51	1.877	24	0.3
6	4	0	26.11	3.413	24	10.1	8	6	4	39.43	2.285	48	1.0	12	4	4	49.11	1.855	24	0.9
6	4	2	27.11	3.289	48	41.0	10	4	0	39.43	2.285	24	0.3	10	8	4	49.70	1.834	48	1.8
8	0	0	29.03	3.076	6	0.4	10	4	2	40.14	2.247	48	2.2	12	6	0	49.70	1.834	24	0.9
6	4	4	29.94	2.984	24	19.7	8	8	0	41.51	2.175	12	4.3							
8	2	0	29.94	2.984	24	19.9	10	4	4	42.19	2.142	24	3.4							





Sodalite octahydrate

SOD



## **Appendix B**

### **XRD powder patterns of the synthesis products**

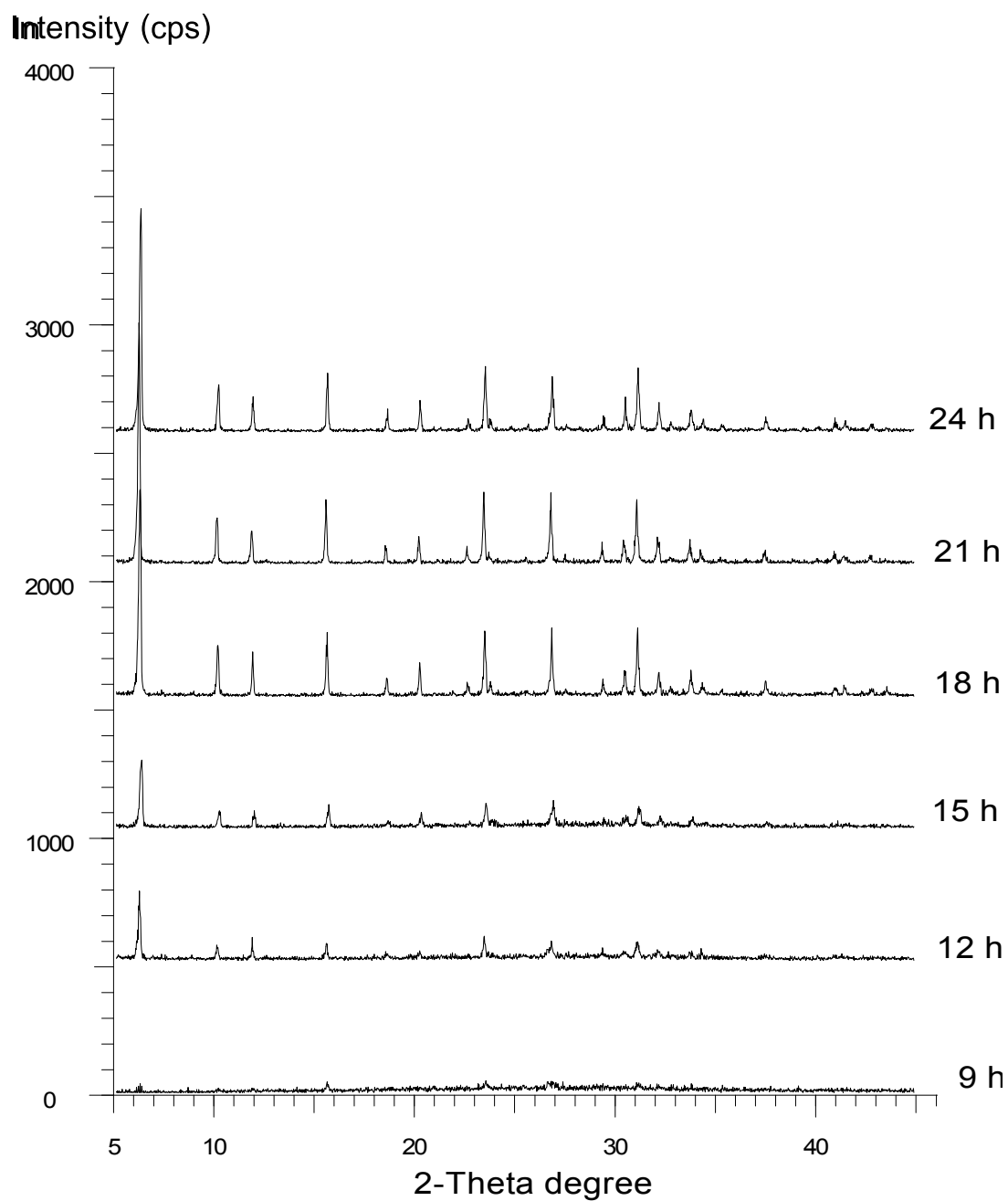


**Figure 1** XRD powder patterns of the solid phases obtained in the synthesis of kaolin activated at 900°C, 5% Na<sub>2</sub>SiO<sub>3</sub>, 7.5% NaOH, aged 3 days and reaction temperature 90°C at various times.

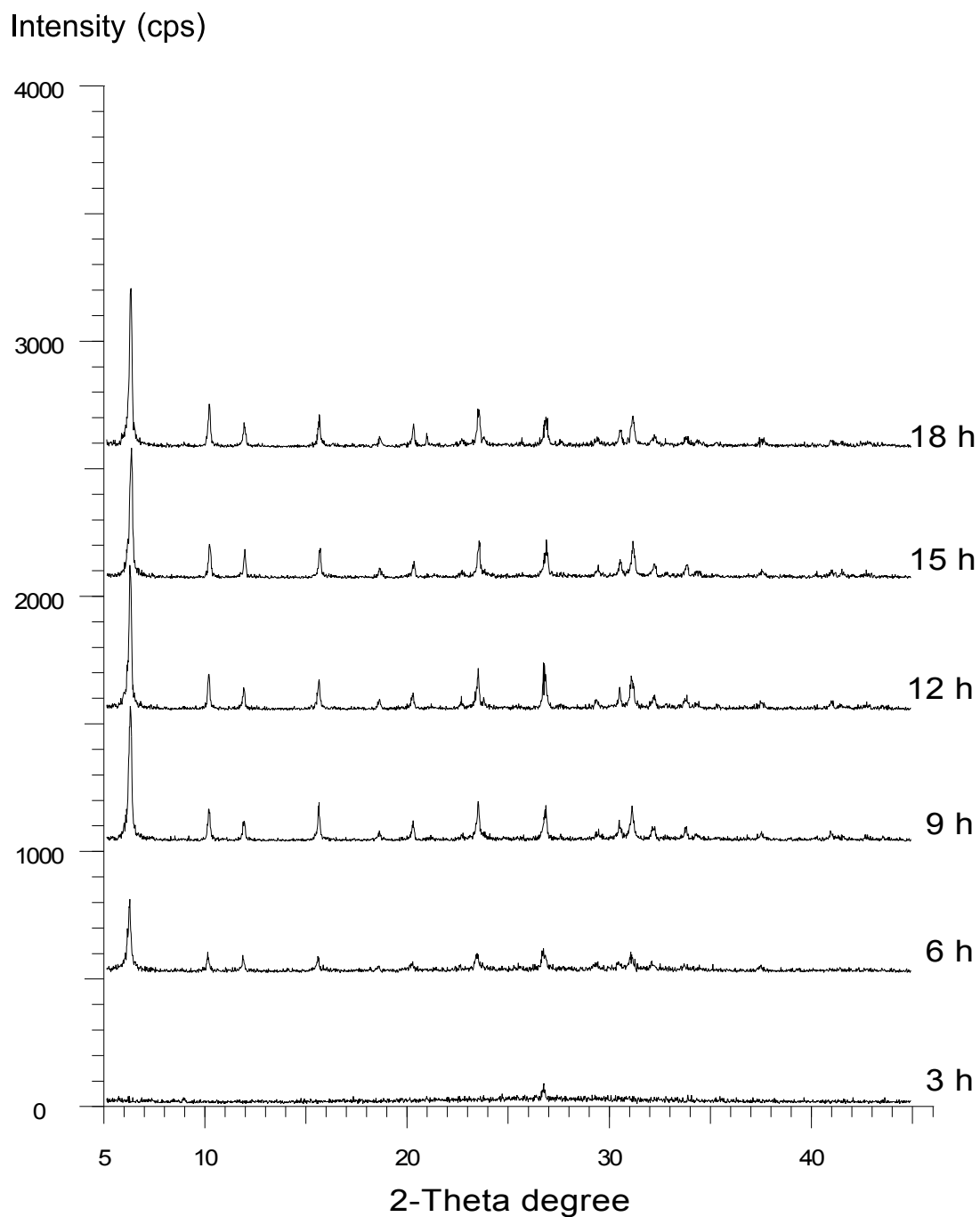


**Figure 2** XRD powder patterns of the solid phases obtained in the synthesis of kaolin activated at 900°C, 7.5% Na<sub>2</sub>SiO<sub>3</sub>, 10% NaOH, aged 3 days, and reaction temperature 90°C at various times.

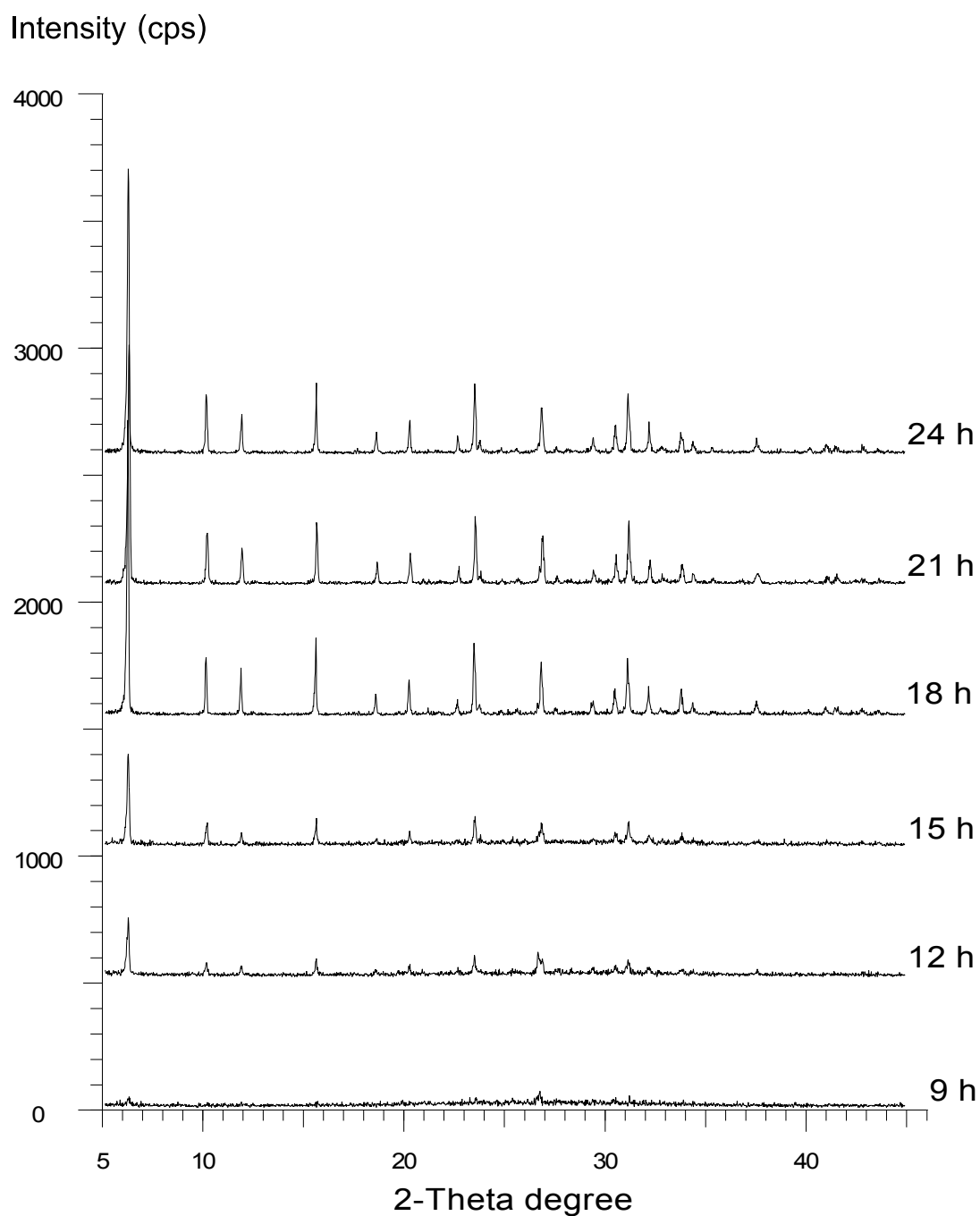


**Figure 3** XRD powder patterns of the solid phases obtained in the synthesis of kaolin activated at 900°C, 7.5% Na<sub>2</sub>SiO<sub>3</sub>, 7.5% NaOH, aged 3 days, and reaction temperature 90°C at various times.

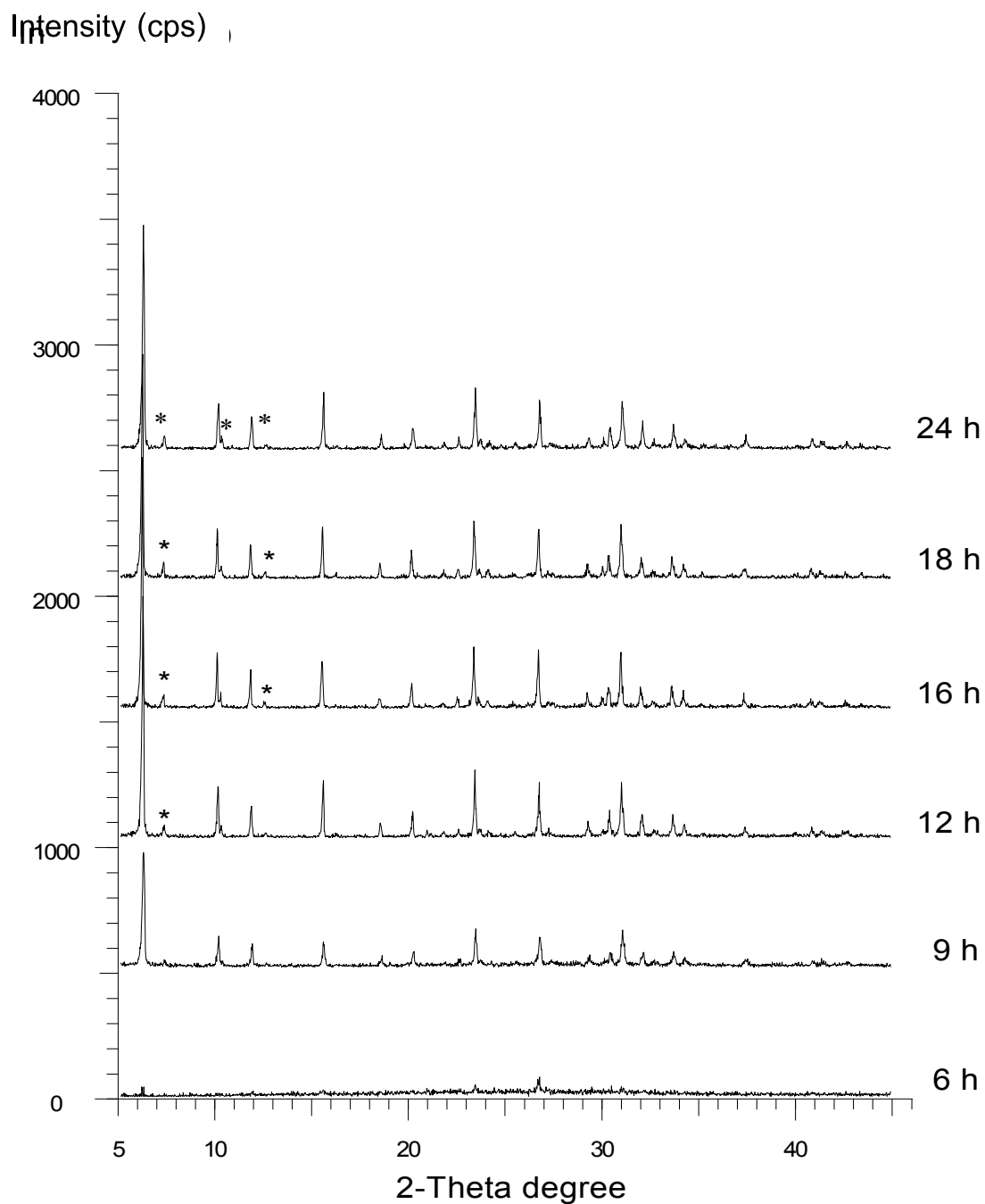


**Figure 4** XRD powder patterns of the solid phases obtained in the synthesis of kaolin activated at 900°C, 2.5% Na<sub>2</sub>SiO<sub>3</sub>, 7.5% NaOH, aged 3 days, and reaction temperature 90°C at various times.

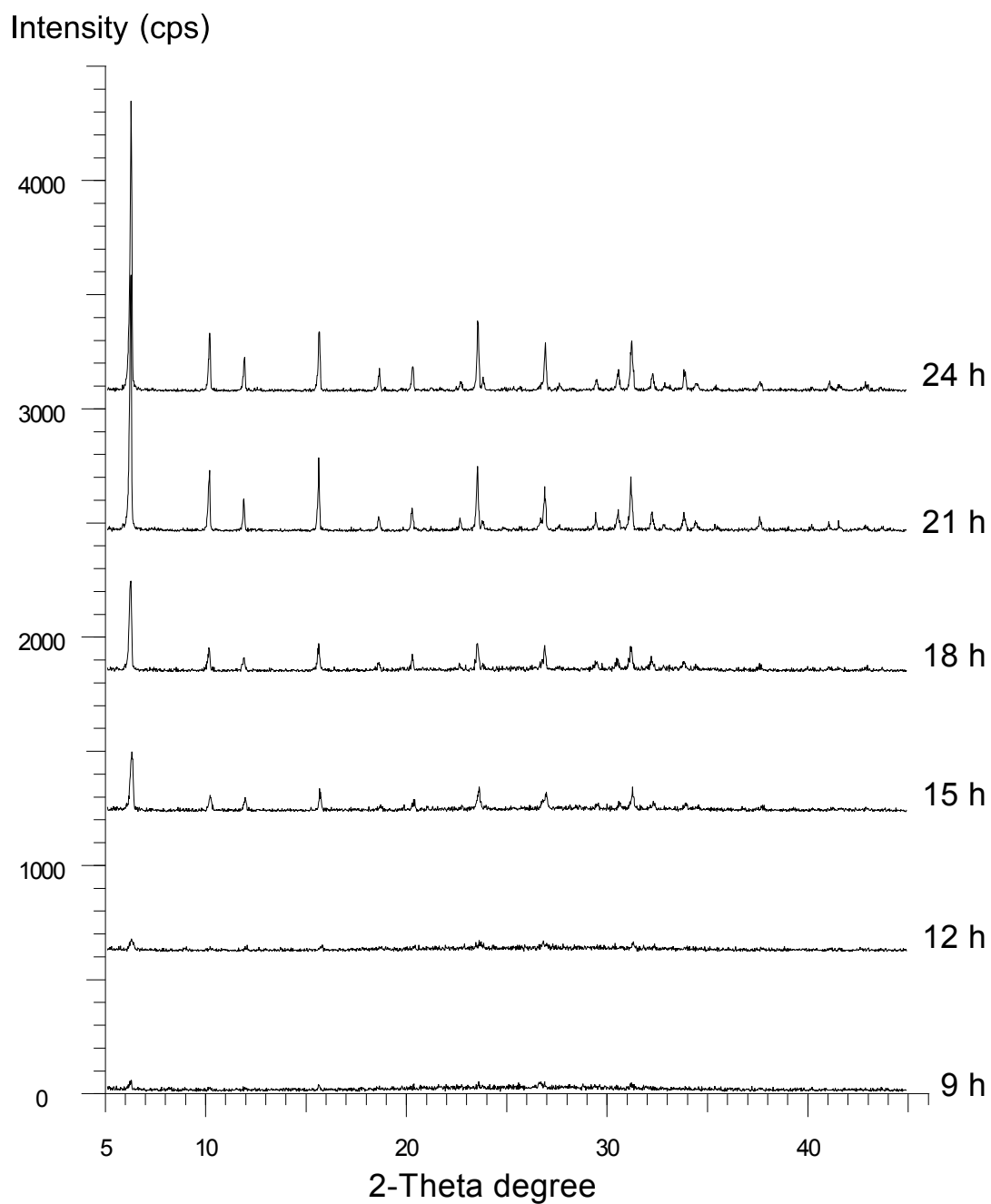


**Figure 5** XRD powder patterns of the solid phases obtained in the synthesis of kaolin activated at 900°C, 10% Na<sub>2</sub>SiO<sub>3</sub>, 7.5% NaOH, aged 3 days, and reaction temperature 90°C at various times.

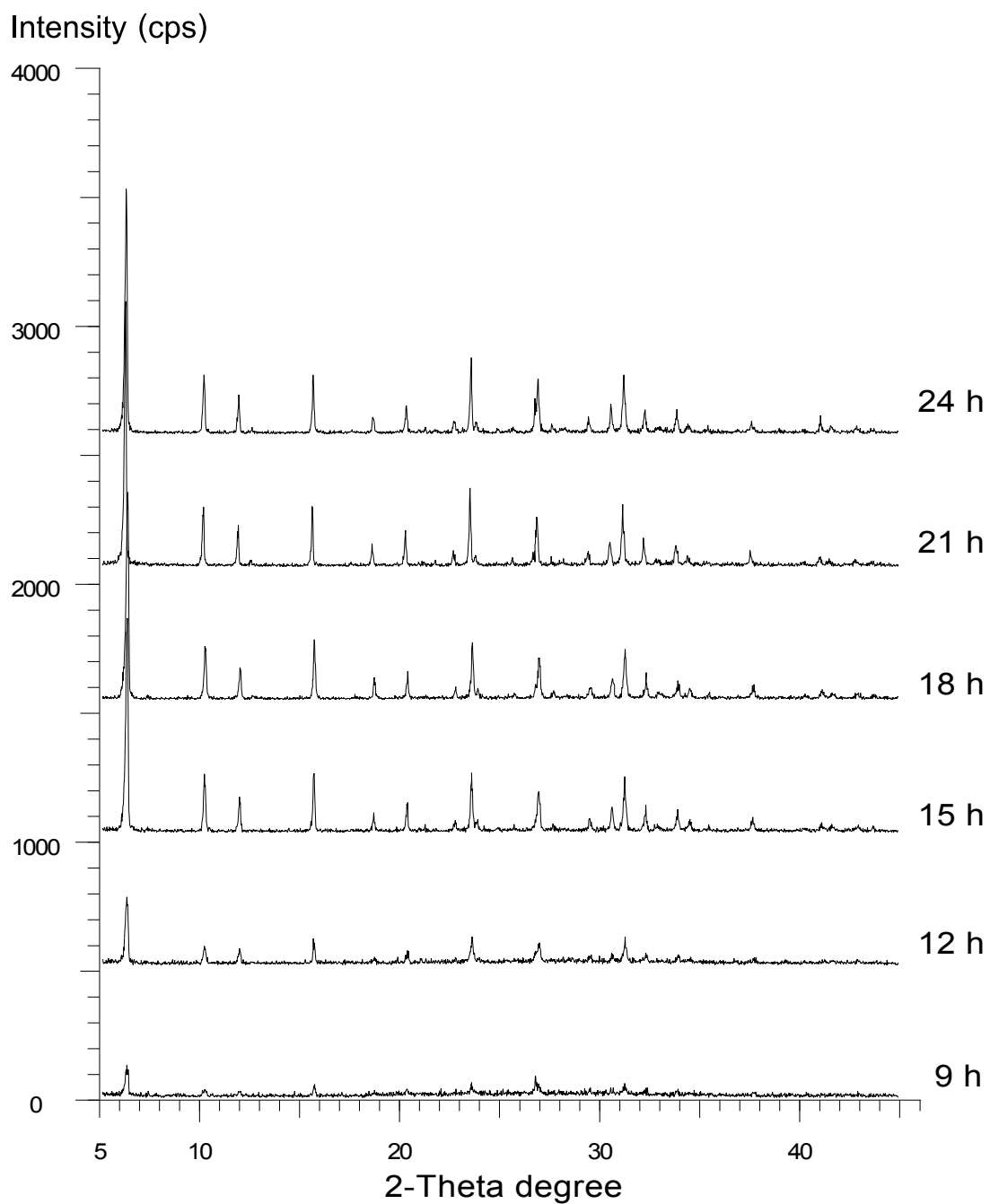


**Figure 6** XRD powder patterns of the solid phases obtained in the synthesis of kaolin activated at 900°C, 7.5% Na<sub>2</sub>SiO<sub>3</sub>, 7.5% NaOH, aged 5 days, and reaction temperature 90°C at various times.

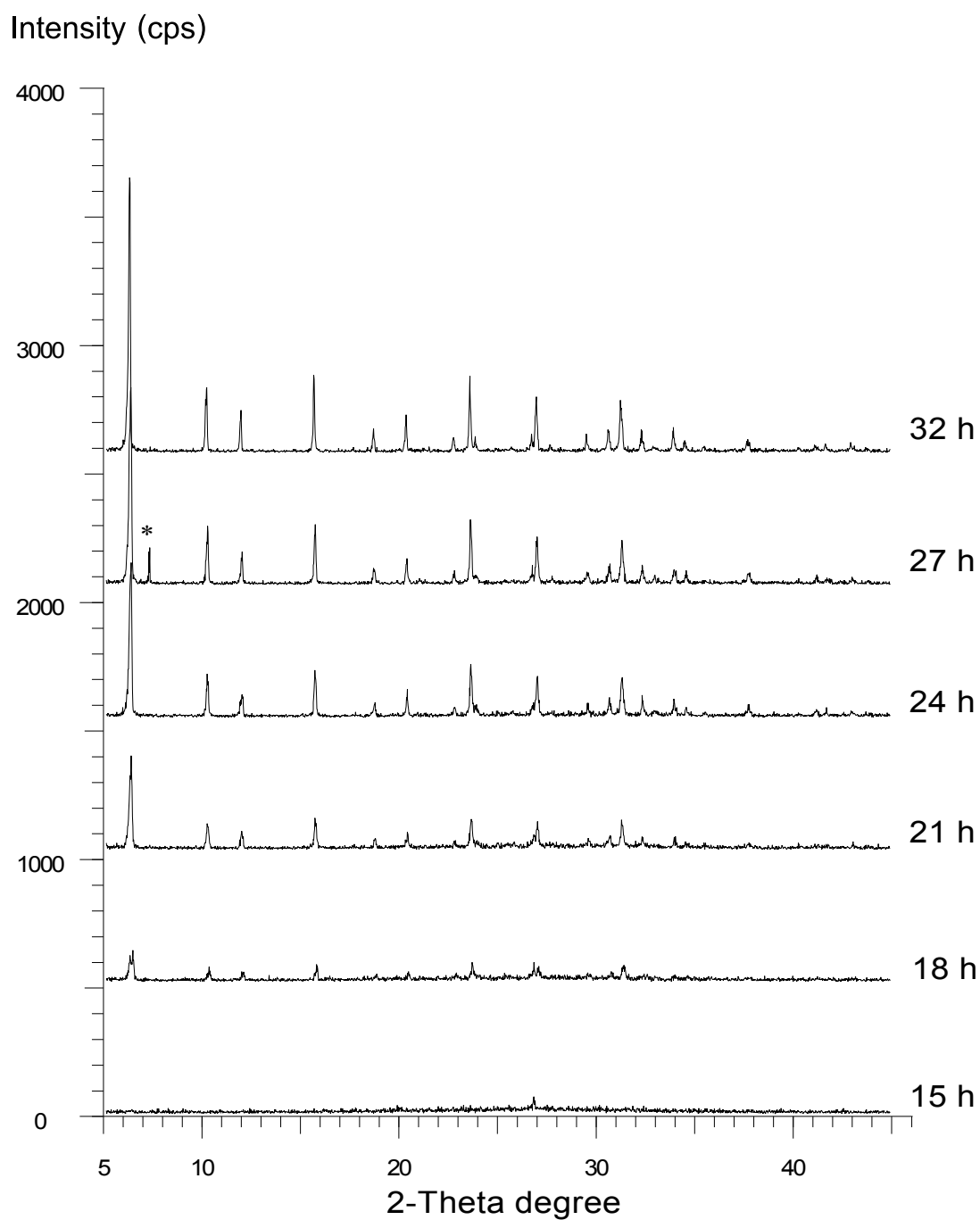


**Figure 7** XRD powder patterns of the solid phases obtained in the synthesis of kaolin activated at 900°C, 15% Na<sub>2</sub>SiO<sub>3</sub>, 7.5% NaOH, aged 3 days, and reaction temperature 90°C at various times.

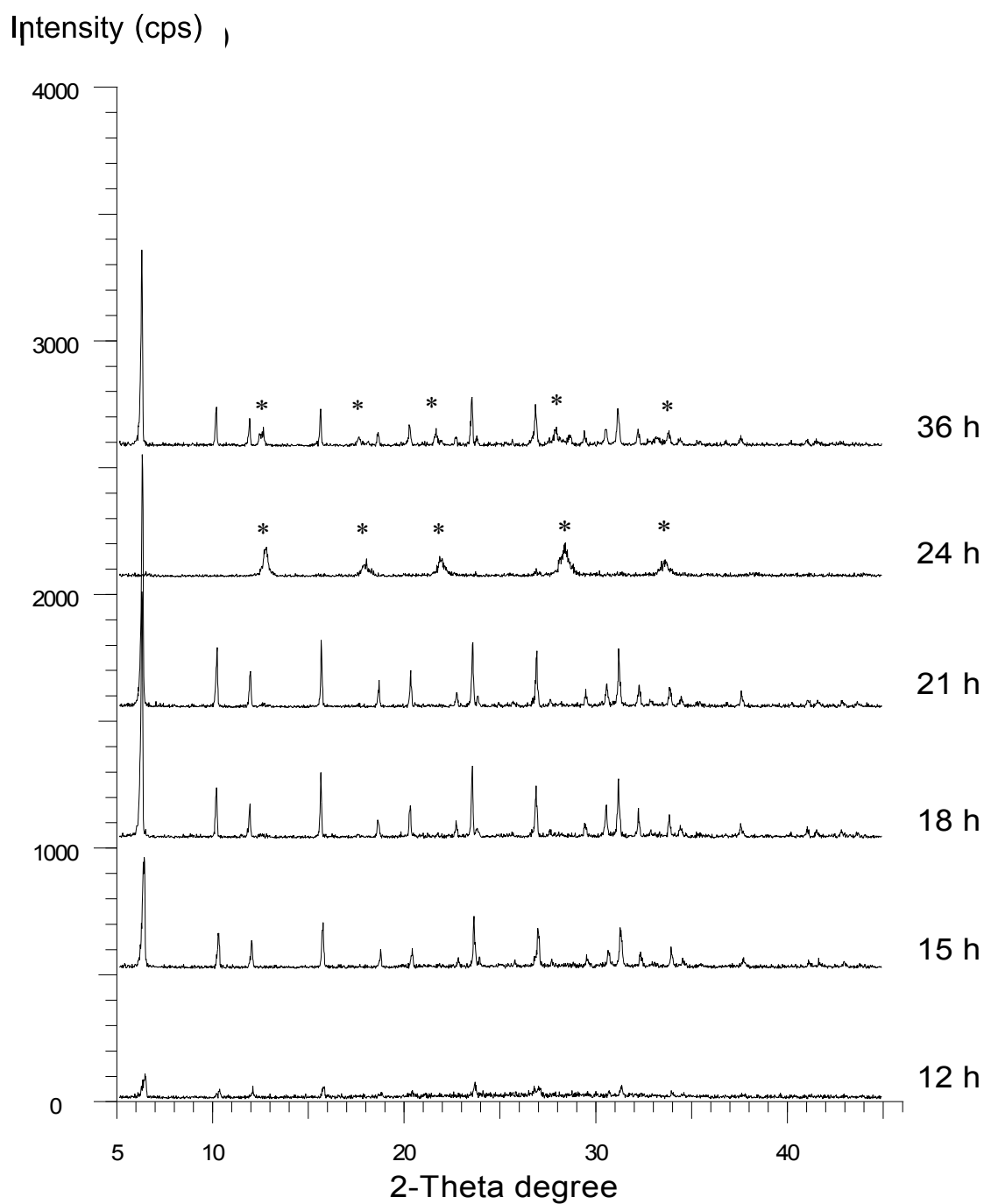


**Figure 8** XRD powder patterns of the solid phases obtained in the synthesis of kaolin activated at 900°C, 10% Na<sub>2</sub>SiO<sub>3</sub>, 7.5% NaOH, aged 1 day, and reaction temperature 100°C at various times.

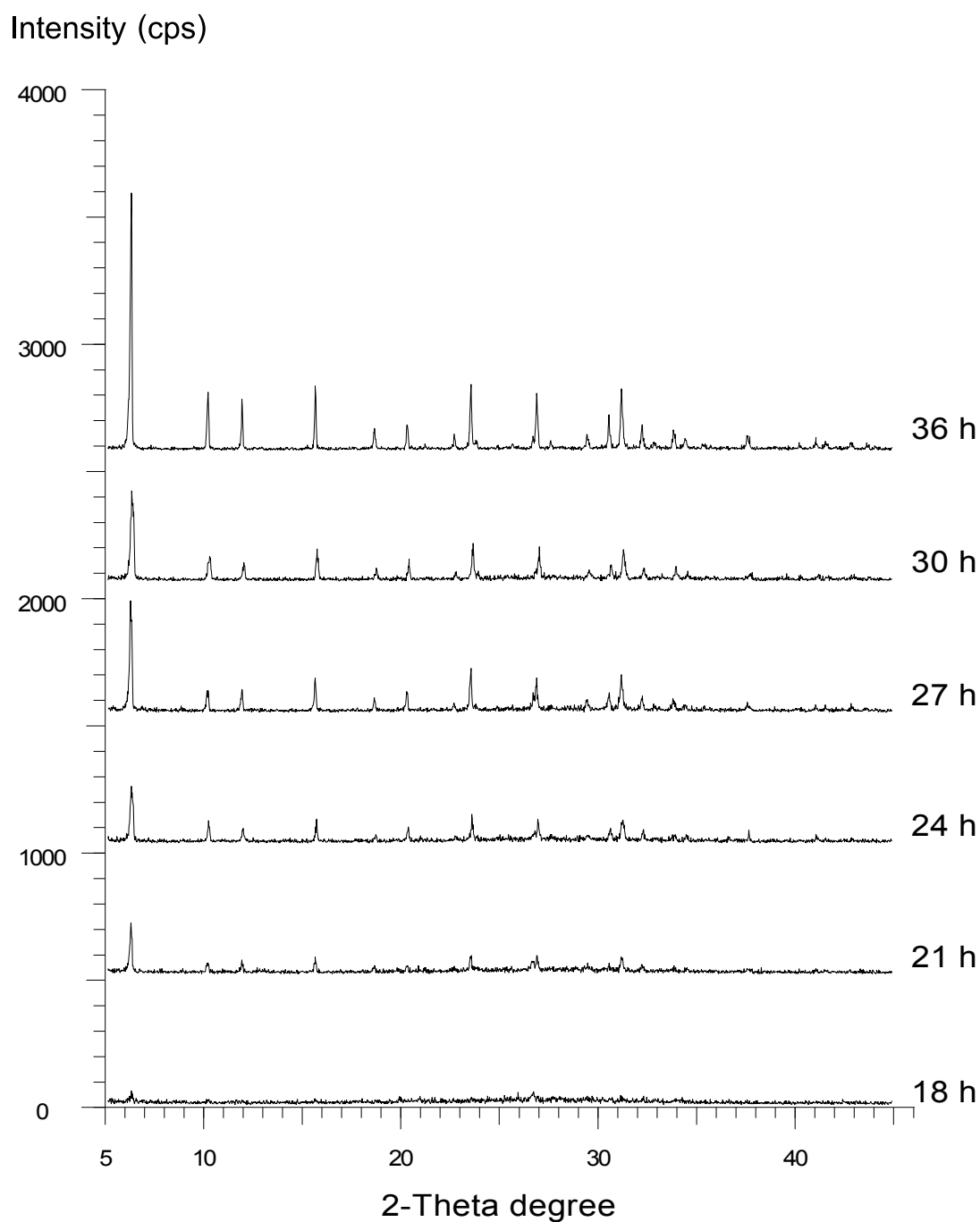


**Figure 9** XRD powder patterns of the solid phases obtained in the synthesis of kaolin activated at 900°C, 10% Na<sub>2</sub>SiO<sub>3</sub>, 7.5% NaOH, aged 1 day, and reaction temperature 90°C at various times.

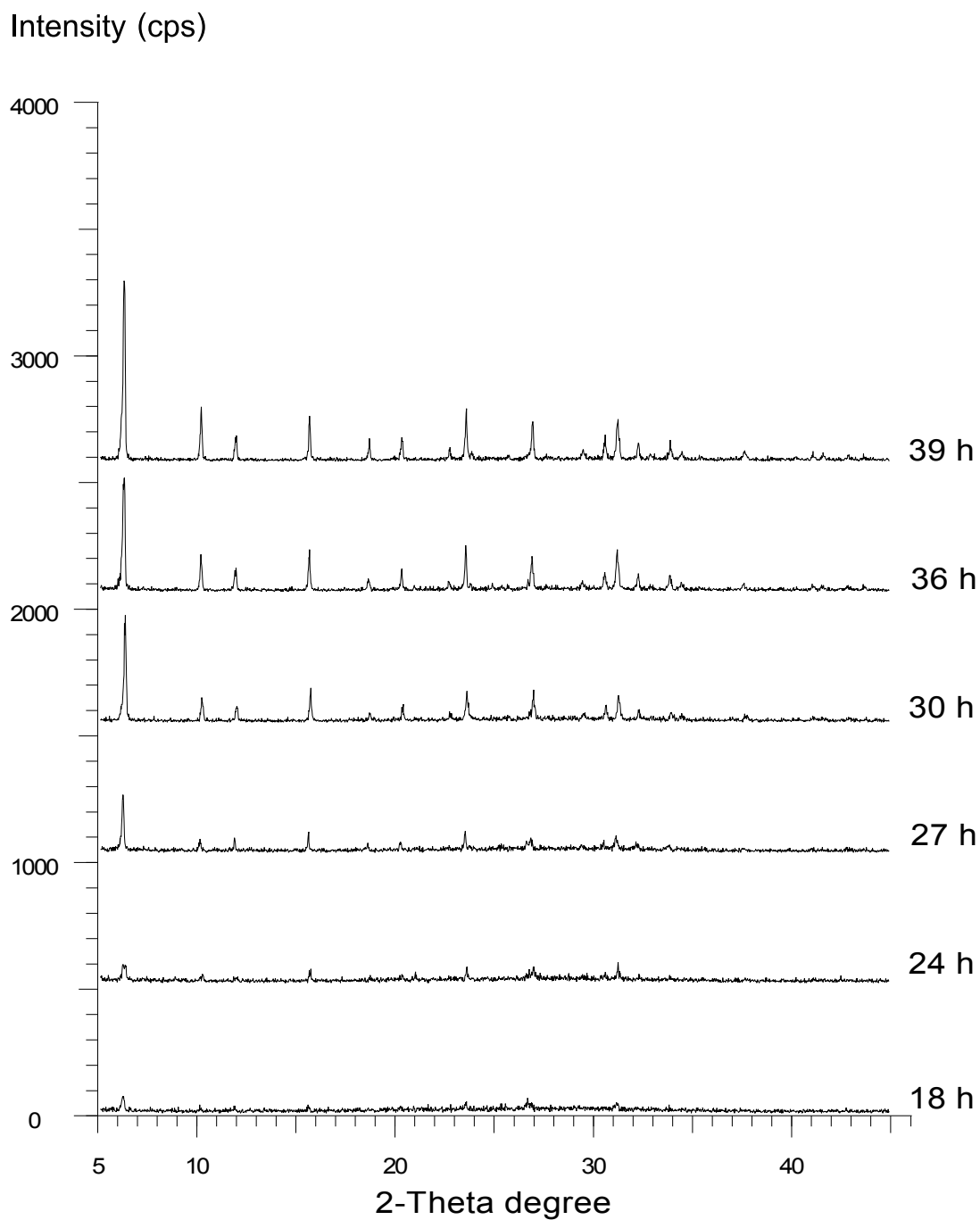


**Figure 10** XRD powder patterns of the solid phases obtained in the synthesis of kaolin activated at 900°C, 10% Na<sub>2</sub>SiO<sub>3</sub>, 7.5% NaOH, aged 3 days, and reaction temperature 80°C at various times.

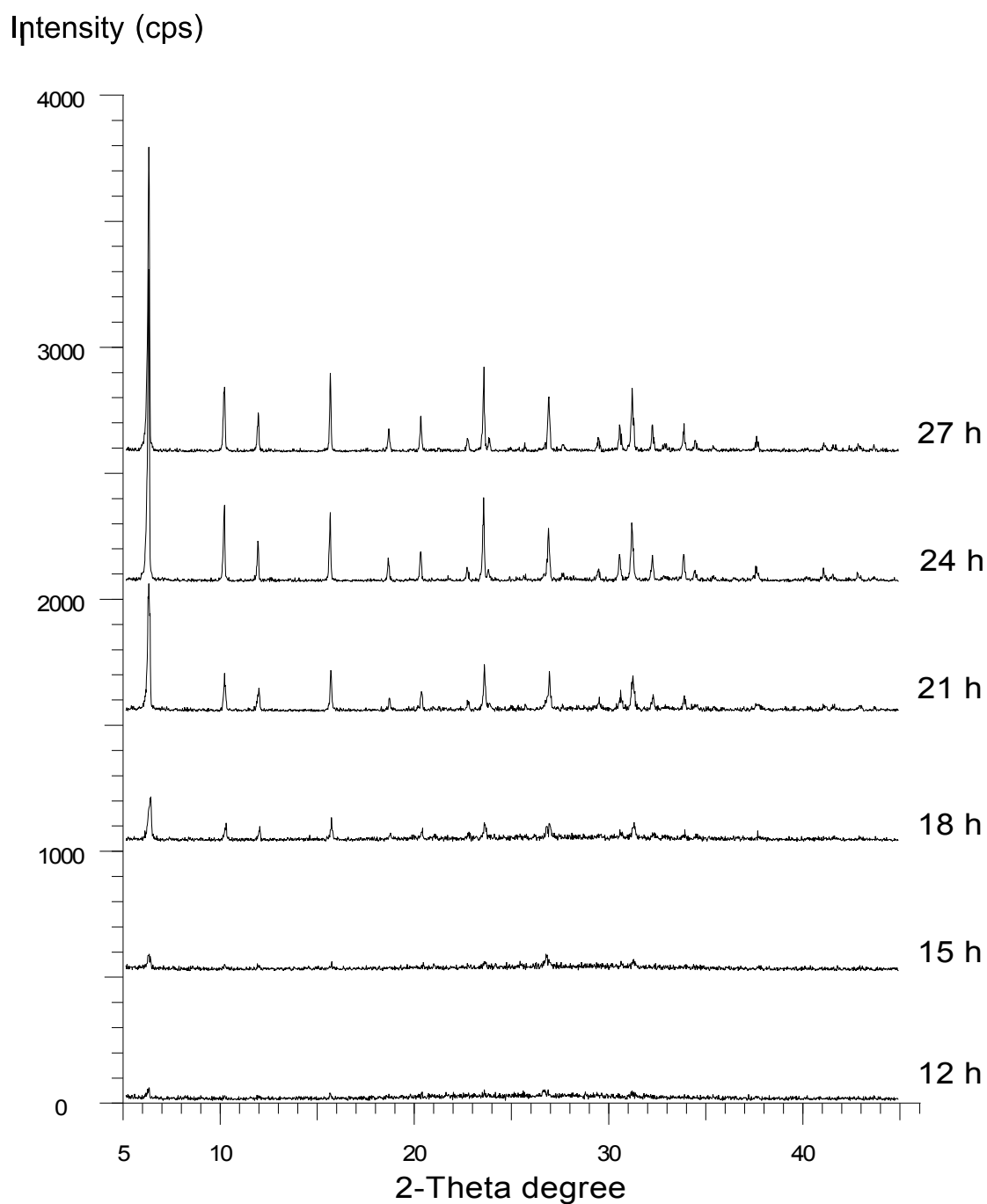


**Figure 11** XRD powder patterns of the solid phases obtained in the synthesis of kaolin activated at 800°C, 10% Na<sub>2</sub>SiO<sub>3</sub>, 7.5% NaOH, aged 3 days, and reaction temperature 90°C at various times.

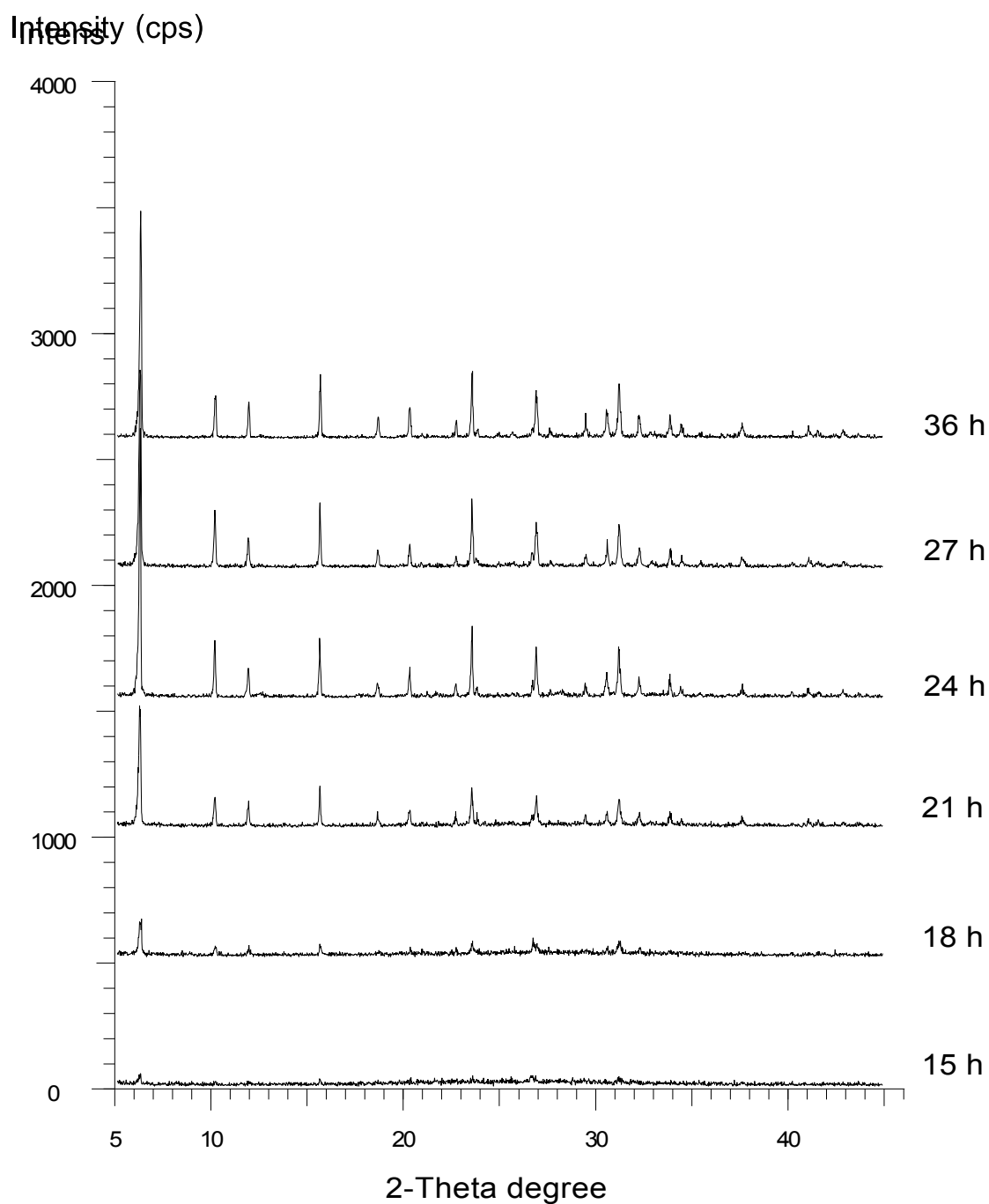


**Figure 12** XRD powder patterns of the solid phases obtained in the synthesis of kaolin activated at 700°C, 10% Na<sub>2</sub>SiO<sub>3</sub>, 7.5% NaOH, aged 3 days, and reaction temperature 90°C at various times.

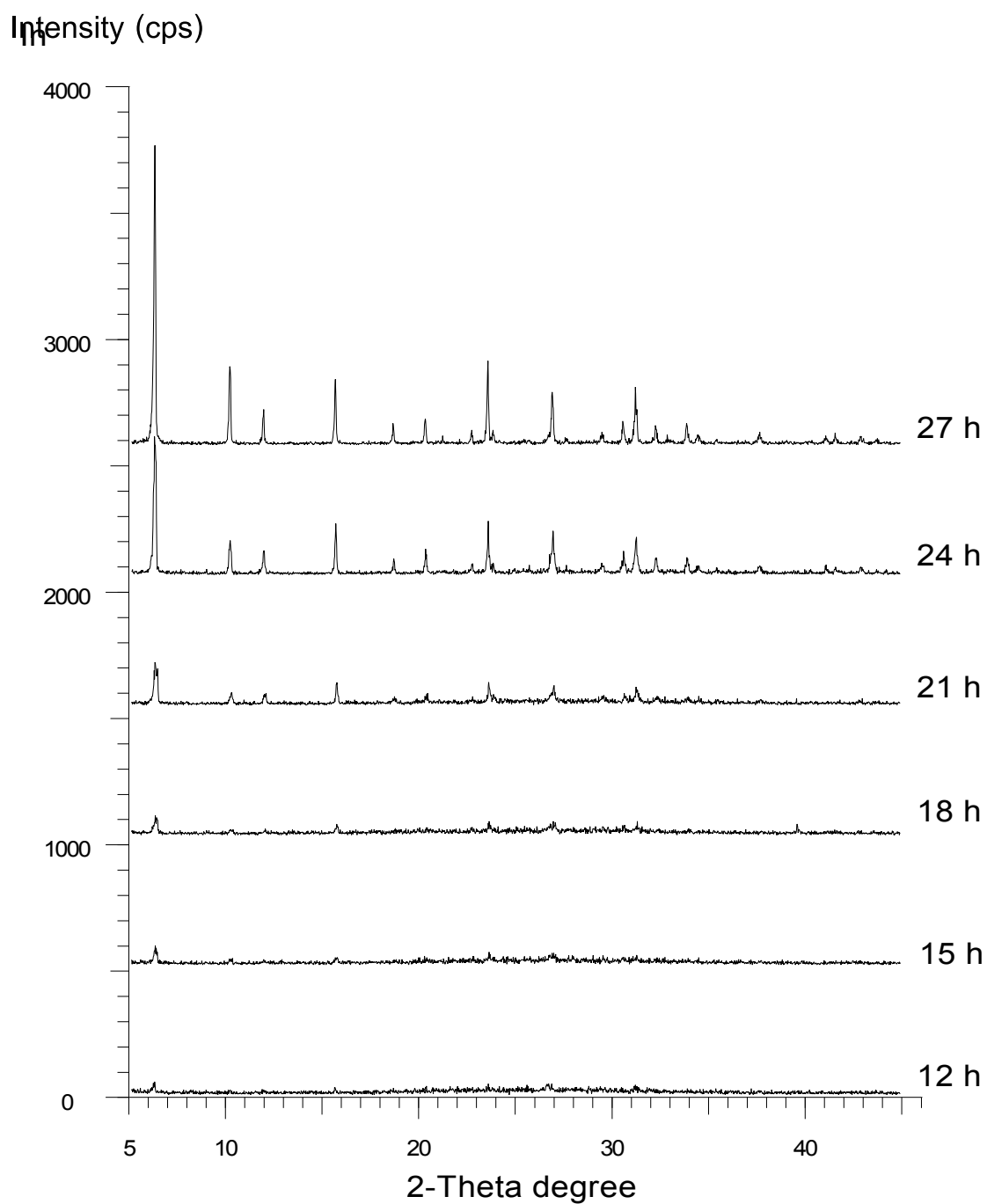


**Figure 13** XRD powder patterns of the solid phases obtained in the synthesis of kaolin activated at 900°C, 7.5% Na<sub>2</sub>SiO<sub>3</sub>, 7.5% NaOH, aged 1 day, and reaction temperature 90°C at various times.

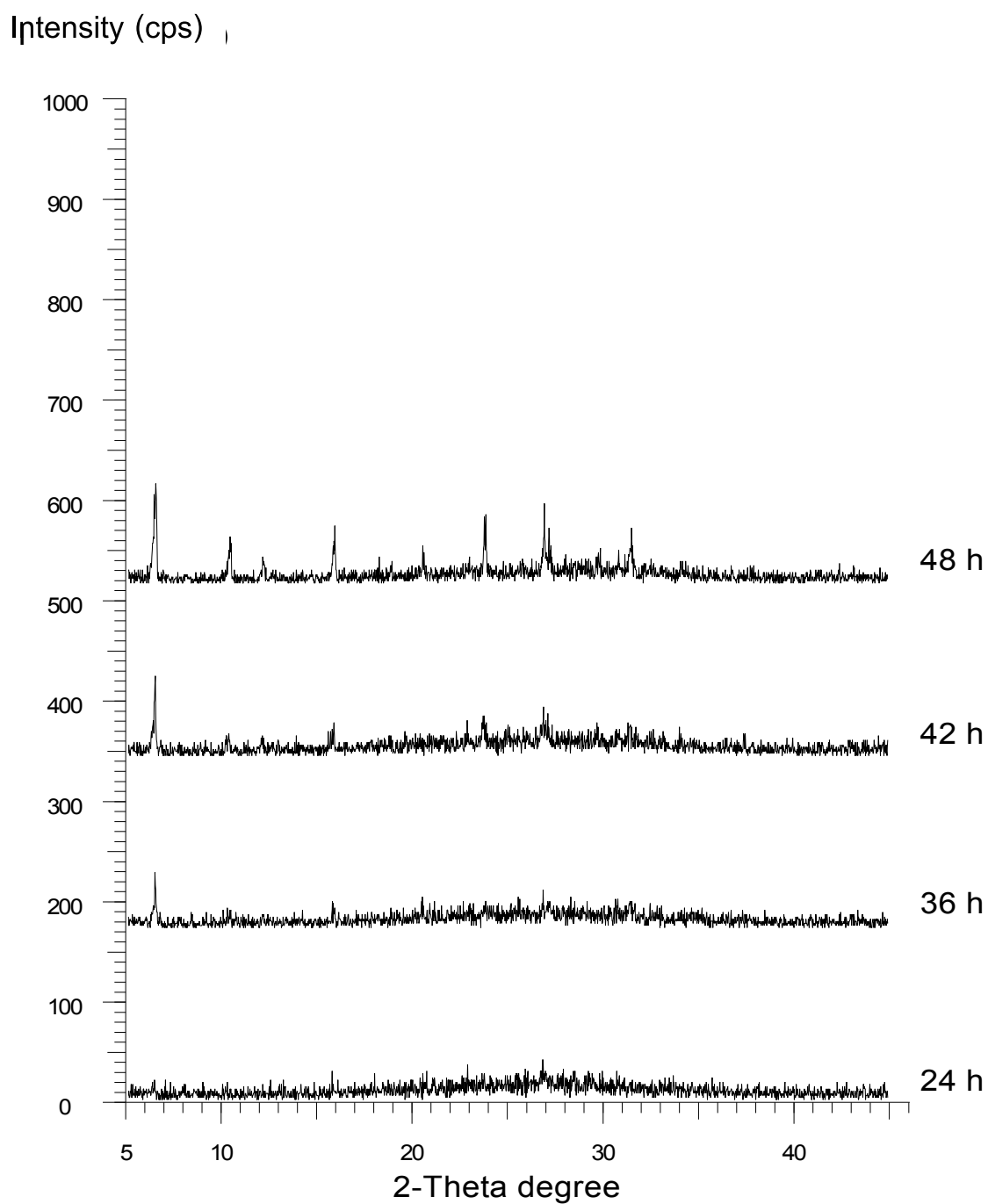


**Figure 14** XRD powder patterns of the solid phases obtained in the synthesis of kaolin activated at 900°C, 7.5% Na<sub>2</sub>SiO<sub>3</sub>, 5% NaOH, aged 1 day, and reaction temperature 90°C at various times.

## Curriculum Vitae

NAME: Saythong Thammavong

SEX: Male

NATIONALITY: Laotian

DATE OF BIRTH: May 11, 1962

MARITAL STATUS: Married

EDUCATIONAL BACKGKROUND:

1985-1989 B. Sc. Chemistry-Biology

National University of Laos

WORK EXPERIENCE

1989-1996 Lecturer in Chemistry at School for Student to Studies Abroad in  
Vientiane.

1996-2000 Lecturer in Chemistry at School of Foundation Study, National  
University of Laos.